



Critical minerals: From discovery to supply chain, program with abstracts



Ministry of
Energy, Mines and
Low Carbon Innovation

GeoFile 2021-14

**Ministry of Energy, Mines and Low Carbon Innovation
Mines, Competitiveness, and Authorizations Division
British Columbia Geological Survey**



Australian Government
Geoscience Australia



Critical Minerals: From discovery to supply chain

A virtual workshop, November 16-18, 2021, organized by the British Columbia Geological Survey, Geological Survey of Canada, United States Geological Survey, Geoscience Australia, and Geological Association of Canada-Pacific Section.

Recommended citation format for individual abstracts

Nassar, Nedal T., 2021. Characterizing and prioritizing critical mineral supply chain risks and potential abatement strategies. In: *Critical Minerals From Discovery to Supply Chain, Program with Abstracts*. British Columbia Ministry of Energy, Mines and Low Carbon Innovation, British Columbia Geological Survey GeoFile 2021-14, pp. 2-3.

Front cover: Folds in banded niobium-bearing dolomite carbonatite. Aley carbonatite complex (345 Ma), northeastern British Columbia. Photo by Duncan McLeish.

Back cover: Tantalum- and niobium -bearing dolomite carbonatite. Aligned fluorapatite megacrysts and dark ferrikatophorite prisms set in a recrystallized and oxidized brown-red ferroan dolomite groundmass. Upper Fir carbonatite complex (330 Ma), southeastern British Columbia. Photo by Alexei Rukhlov.



Ministry of
Energy, Mines and
Low Carbon Innovation



Critical minerals: From discovery to supply chain, program with abstracts

Workshop steering committee

Allen Andersen, United States Geological Survey

Evan Orovan, British Columbia Geological Survey and Centre of Ore Deposit and Earth Sciences,
University of Tasmania

Jan M. Peter, Geological Survey of Canada

Johnathan Savard, British Columbia Geological Survey and Geological Survey of Canada

George J. Simandl, British Columbia Geological Survey

Zhehan Weng, Geoscience Australia

Neil Wildgust, British Columbia Geological Survey

Ministry of Energy, Mines and Low Carbon Innovation
British Columbia Geological Survey
GeoFile 2021-14

Program

Tuesday, November 16

List of speakers

13:30 PST (21:30 GMT) **Acknowledgement of traditional lands and opening remarks**

Adrian S. Hickin, Chief Geologist and Executive Director, British Columbia Geological Survey
The Honourable Bruce Ralston, M.L.A., Minister of Energy, Mines and Low Carbon Innovation

Session 1: Critical minerals and markets

Chair: Neil Wildgust, British Columbia Geological Survey

Nedal T. Nassar (keynote), United States Geological Survey
Characterizing and prioritizing critical mineral supply chain risks and potential abatement strategies

Andrew Miller, Benchmark Mineral Intelligence Ltd.
Building a supply chain for the lithium ion economy

Andrew Heap, Geoscience Australia
Critical Minerals Mapping Initiative: Geoscience for discovery

George J. Simandl, British Columbia Geological Survey
Critical, specialty, magnet, battery, and photovoltaic materials: Key factors for responsible exploitation and development decision making

Question and answer period

16:30 PST (0:30 GMT) **Session 2: Geology of critical minerals**

Chair: Jan M. Peter, Geological Survey of Canada

Stephen E. Kesler, Department of Earth and Environmental Sciences, University of Michigan
Lithium deposits: From magmas to playas

Murray W. Hitzman, Irish Centre for Research in Applied Geosciences, University College Dublin
Geology of cobalt

Sarah-Jane Barnes, Sciences de la Terre, Université du Québec à Chicoutimi
Critical metals found in magmatic ore deposits; Ni, Cu, Co, PGE, Te, Se, Bi, and V

Anthony E. Williams-Jones, Department of Earth and Planetary Sciences, McGill University
The rare earth elements: A tale of mantle plumes, magmas, and fluids

Andrew Conly, Department of Geology, Lakehead University
The diverse nature of graphite deposits: An overview of their geological characteristics and economic considerations

Robert R. Seal II, United States Geological Survey
Mine waste as a potential source of critical minerals: The importance of understanding speciation and identifying synergies between resource recovery and environmental management

Max Frenzel, Helmholtz Institute Freiberg for Resource Technology
Geochemistry and economic geology of Ga, Ge and In: An overview

Question and answer period

Wednesday, November 17

List of speakers

13:30 PST (21:30 GMT)

Session 3: World-class critical mineral deposits

Chair: Zhehan Weng, Geoscience Australia

Hong-Rui Fan, Chinese Academy of Sciences

The giant Bayan Obo REE-Nb-Fe deposit (China): Ore genesis and resource potential

M. Christopher Jenkins, Department of Earth Sciences, Carleton University

The nature and composition of the J-M Reef, Stillwater Complex, Montana, USA

Philippe Muchez, KU Leuven, Department of Earth and Environmental Sciences

Cu-Co ore deposits in the Central African Copperbelt: Origin and transport of metals, ore mineral precipitation, and regional and stratigraphic distribution

Philip L. Verplanck, United States Geological Survey

An overview of the world-class Mount Weld rare earth element deposit

Kathryn Goodenough, British Geological Survey

African lithium pegmatites

Question and answer period

16:30 PST (0:30 GMT)

Session 4: Selected critical mineral deposits I

Chair: Evan Orován, British Columbia Geological Survey and Centre of Ore Deposit and Earth Sciences, University of Tasmania

Marcus Haynes, Geoscience Australia

The potential for critical minerals: Australia's contribution to the global supply chain

Helen Degeling, Geological Survey of Queensland

Strategic resources and the new economy: Queensland's critical mineral potential

Vladimir Lisitsin, Geological Survey of Queensland

Critical minerals in traditional deposit types in the Mount Isa region, Queensland, Australia

Carl Spandler, Department of Earth Sciences, University of Adelaide

Unconformity-related REE deposits of the Browns Range, Australia

Evan Orován, British Columbia Geological Survey and Centre of Ore Deposit and Earth Sciences, University of Tasmania

The Trial Harbour Ni skarn, Zeehan mineral field, western Tasmania

Michael G. Gadd, Geological Survey of Canada

Critical minerals in Paleozoic hyper-enriched black shales

Question and answer period

Thursday, November 18

List of speakers

13:30 PST (21:30 GMT) **Session 5: Selected critical mineral deposits II**

Chair: Allen Andersen, United States Geological Survey

Mark W. Bultman, United States Geological Survey
Potential for concealed critical mineral deposits in the northern Trans-Pecos region of West Texas and southern New Mexico from a new aeromagnetic survey

Kathryn E. Watts, United States Geological Survey
Temporal and petrogenetic links between Mesoproterozoic alkaline and carbonatite magmas at Mountain Pass, California

Frank Santaguیدا, First Cobalt Corp.
New cobalt-copper resources: New perspectives from the Iron Creek project, Idaho cobalt belt

Craig Bow, Group Ten Metals Inc.
Precious and base metal mineralization within the Peridotite zone of the Stillwater Complex, Montana, USA

Thomas R. Benson, Lithium Americas Corp.
Geology of the Thacker Pass deposit in the McDermitt Caldera, Nevada: The largest and highest grade known sedimentary lithium resource in the United States

Fiorella Sist, Controlled Thermal Resources (US) Inc.
Development of a mineralized brine resource: The Hell's Kitchen lithium and power project, Salton Sea, USA

Question and answer period

16:30 PST (0:30 GMT) **Session 6: Exploration methods and technical considerations**

Chair: George Simandl, British Columbia Geological Survey

M. Beth McClenaghan, Geological Survey of Canada
Application of indicator mineral methods to critical material exploration

René Booyesen, Helmholtz Institute Freiberg for Resource Technology
Multi-scale and multi-source remote sensing of REEs in southern Africa

Mike D. Thomas, Geological Survey of Canada
Use of geophysical methods in exploration for critical materials

Sandra Lorenz, Helmholtz Institute Freiberg for Resource Technology
Outcrop sensing for the exploration of REEs and lithium

Tassos Grammatikopoulos, SGS Canada Inc.
Integration of process mineralogy in critical element deposits

John R. Goode, J.R. Goode and Associates
Rare earth elements: Challenges facing present and potential producers

Moritz Kirsch, Helmholtz Institute Freiberg for Resource Technology
Multi-source hyperspectral imaging of drill cores for the exploration of critical minerals

Question and answer period

Closing remarks

Adrian S. Hickin, Chief Geologist and Executive Director, British Columbia Geological Survey

Abstracts

Session 1: Critical minerals and markets

Tuesday, November 16, 13:30 PST (21:30 GMT)

List of speakers

Acknowledgement of traditional lands and opening remarks

Adrian S. Hickin, Chief Geologist and Executive Director, British Columbia Geological Survey

The Honourable Bruce Ralston, M.L.A., Minister of Energy, Mines and Low Carbon Innovation

Chair: Neil Wildgust, British Columbia Geological Survey

Nedal T. Nassar (keynote), United States Geological Survey
Characterizing and prioritizing critical mineral supply chain risks and potential abatement strategies

Andrew Miller, Benchmark Mineral Intelligence Ltd.
Building a supply chain for the lithium ion economy (no abstract)

Andrew Heap, Geoscience Australia
Critical Minerals Mapping Initiative: Geoscience for discovery

George J. Simandl, British Columbia Geological Survey
Critical, specialty, magnet, battery, and photovoltaic materials: Key factors for responsible exploitation and development decision making

Question and answer period

Characterizing and prioritizing critical mineral supply chain risks and potential abatement strategies

Nedal T. Nassar^{1a}

¹ National Minerals Information Center, Mineral Resources Program, U.S. Geological Survey, Reston, VA 20191, USA

^a nnassar@usgs.gov

From the nanoscale to the global scale, mineral commodities form the foundation of every modern economy. While mineral commodity dependencies are not new, the pace at which technology has accelerated the use of certain elements of the periodic table is unprecedented. Emerging technologies including those required for renewable energy generation and storage—such as electric vehicles, solar panels, and wind turbines—are expected to require record quantities of a wide variety of mineral materials.

While poised for large surges in demand, mineral commodity supply chains have come under increasing strain over the past few years. Continuing trends—including increasingly concentrated global production, declining ore grades, and limited end-of-life recycling—have recently been coupled with heightened trade tensions, calls for resource nationalism, persistent labor strikes, and the ongoing global pandemic to bring global supply chains to a breaking point (Nassar and Fortier, 2020). Several Executive Orders and recent legislation in the United States have been passed to focus and accelerate the

Federal Government’s actions to identify and address stressors on these supply chains, which are increasingly recognized as vital to national economic and security interests.

In this presentation recent and ongoing efforts on evaluating mineral commodity supply chain risks and vulnerabilities will be discussed, including a detailed description of the risk-modeling framework utilized to quantitatively evaluate the mineral commodity supply chains that pose the greatest supply risk to the U.S. economy (Nassar et al., 2020b). Specifically, supply risk is defined as the confluence of three factors: the likelihood of a foreign supply disruption, the dependency of U.S. manufacturers on foreign supplies, and the ability of U.S. manufacturers to withstand a supply disruption. Over 50 mineral commodities—several at multiple production stages—are assessed for the years 2007 to 2018. The results for year 2018 across each of three components of supply risk—disruption potential, trade exposure, and economic vulnerability—are displayed in Fig. 1. The latest results identify gallium, niobium, cobalt, and neodymium as the mineral commodities of greatest

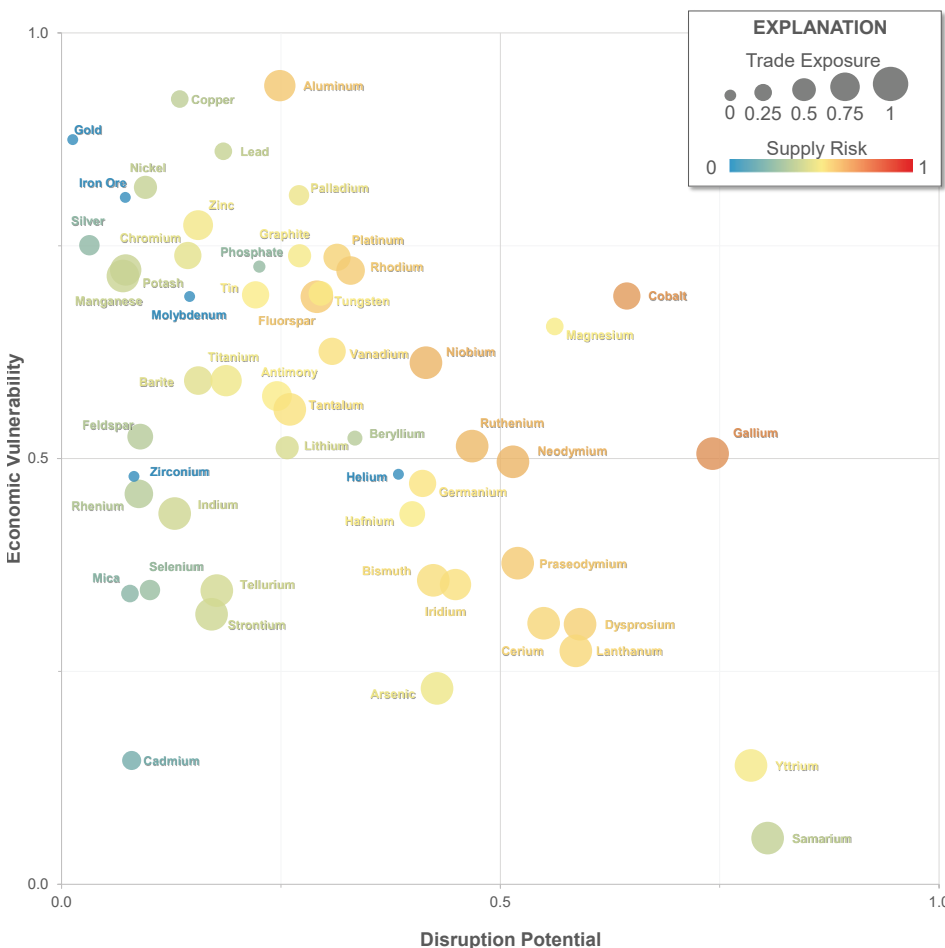


Fig.1. Assessment of mineral commodity supply risk. The graph shows the disruption potential (horizontal axis), economic vulnerability (vertical axis), trade exposure (point size), and overall supply risk (point shade) for various mineral commodities in 2018. For some commodities, indicator scores are rounded to avoid disclosing company proprietary data. From Nassar and Fortier (2021).

concern (Nassar and Fortier, 2021). These results will be used to revise and prioritize the U.S. Critical Minerals List. They also form the basis for future work, which will look to not only update the results on a regular basis but also enhance each component of the supply risk modeling framework.

The presentation will also discuss recent work on improving our understanding of U.S. import dependencies (Nassar et al., 2020a). Results from that work indicate that although the United States is highly dependent on imports from nonmarket economies for only a small subset of mineral commodities including the rare earths and several metalloids (Fig. 2), there are several factors including indirect and embedded trade flows and foreign ownership of mineral assets that may be masking the extent of these dependencies.

Once a mineral commodity supply chain is identified as high risk it is then important to determine how the risk can be reduced. The concept of supply risk abatement wedges will thus be introduced as a means by which different supply risk abatement strategies—such as substitution, increasing recycling, increasing primary production, and improving manufacturing efficiencies—can be evaluated. When coupled with demand and supply scenarios, this framework can help to

identify key gaps and opportunities at each stage of the supply chain that exist today and that may occur in the future to provide actionable recommendations to researchers and policymakers.

Nassar, N.T., and Fortier, S.M., 2020. U.S. Mineral supply chain security in the age of pandemics and trade wars. *TheScienceBreaker*, 06.

<https://doi.org/10.25250/thescbr.brk421>

Nassar, N.T., and Fortier, S.M., 2021. Methodology and technical input for the 2021 review and revision of the U.S. critical minerals list. U.S. Geological Survey Open-File Report 2021-1045, 31p.

<https://doi.org/10.3133/ofr20211045>

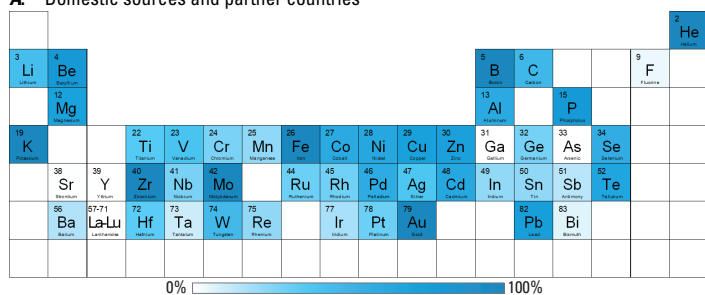
Nassar, N.T., Alonso, E., and Brainard, J., 2020a. Investigation of U.S. foreign reliance on critical minerals—U.S. Geological Survey Technical Input Document in Response to Executive Order No. 13953 Signed September 30. U.S. Geological Survey Open-File Report 2020–1127, 37p.

<https://doi.org/10.3133/ofr20201127>

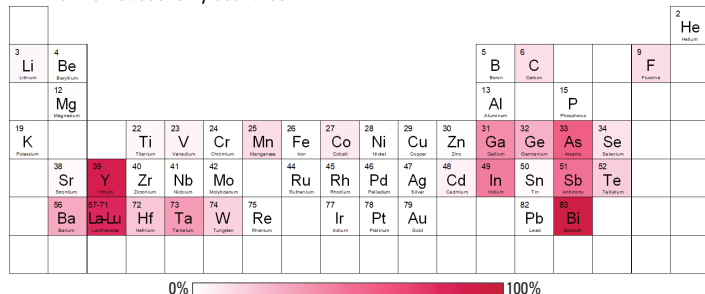
Nassar, N.T., Brainard, J., Gulley, A., Manley, R., Matos, G., Lederer, G., Bird, L.R., Pineault, D., Alonso, E., Gambogi, J., and Fortier, S.M., 2020b. Evaluating the mineral commodity supply risk of the U.S. manufacturing sector. *ScienceAdvances*, 6, eaay8647.

<https://doi.org/10.1126/sciadv.aay8647>

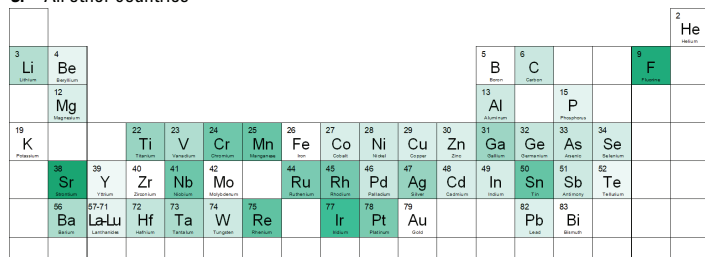
A. Domestic sources and partner countries



B. Nonmarket economy countries



C. All other countries



D. Overall

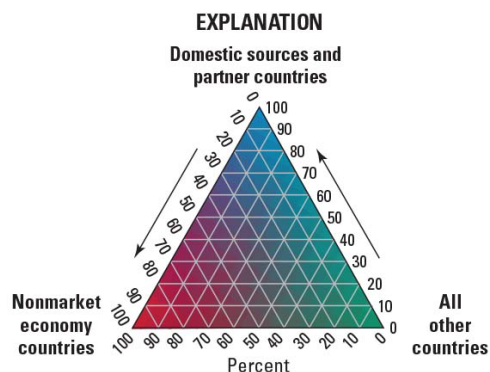
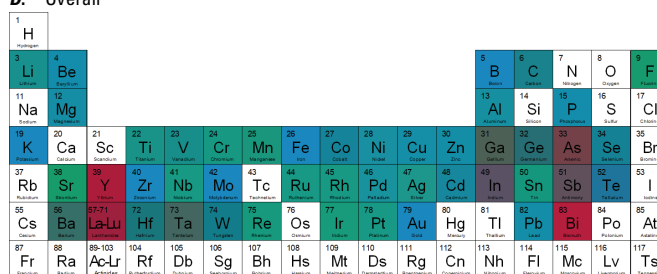


Fig. 2. Source of mineral commodities consumed in the United States. For selected elements of the periodic table, the estimated percent of 2018 U.S. consumption (in colour gradients) for the associated mineral commodities obtained from: **a)** domestic sources and partner countries, defined here as those having a security of supply agreement with the United States; **b)** nonmarket economy countries as defined by the U.S. Department of Commerce; and **c)** all other countries. **d)** Ternary diagram, based on the mix of sources. Elements not assessed are not included. Data pertain to refinery or metal production and include secondary production (old scrap recycling), where applicable and available. From Nassar et al. (2020a).

Critical Minerals Mapping Initiative: Geoscience for discovery

Andrew Heap^{1a}, Geneviève Marquis², and Tom Crafford³

¹ Geoscience Australia, Canberra ACT 2601, Australia

² Geological Survey of Canada, Ottawa, ON K1A 0E8, Canada

³ United States Geological Survey, Virginia 20192, United States

^a corresponding author: andrew.heap@ga.gov.au

Global technological advancement, fuelled by the goal of sustainable development of a growing population, has become reliant on a diverse suite of materials. Known as critical minerals, many were of little economic interest until recently and are at risk of supply. The global economy is now responding to rapidly increasing demand by securing stable long-term supply of these minerals. This pivot is an opportunity for mining nations such as Australia, Canada, and the US to do more by diversifying our resource base and adding value in the process. However, the science underpinning critical mineral discovery and development is not as well developed compared to that supporting discoveries of resources that have been mined for millennia (e.g., coal, iron, copper, zinc, and gold).

To reduce the supply risks for critical minerals, in December 2019, Geoscience Australia (GA), the Geological Survey of Canada (GSC) and the United States Geological Survey (USGS) formed the Critical Minerals Mapping Initiative (CMMI; Kelly, 2010; Emsbo et al., 2021; Kelly et al., 2021). The initiative seeks to accelerate critical minerals geoscience by advancing the understanding of critical mineral distribution, unravelling the geological controls on critical minerals, and identifying new sources of supply through mineral prospectivity mapping and

resource assessment. Here, we review the key achievements of the CMMI to date and highlight future directions.

Given many critical minerals are co- or by-products of the extraction and processing of known resources, the initial focus of the CMMI was to grow our empirical knowledge of the distribution of critical minerals in ores. In June 2021, we released the world's largest Critical Minerals in Ores (CMiO) database through a new online portal (<http://criticalminerals.org/>; Fig. 1). The dataset combines 7,311 geochemical analyses of mineralized samples from 60 countries, which represents the complete holdings in the combined databases of GA, USGS, and GSC (Champion et al., 2020). To enable mineral system assessments, where possible, analyses are attributed by deposit type using a new ore deposit classification scheme developed specifically for this purpose (Hofstra et al., 2021). This is the first classification scheme agreed to by the three CMMI partners and, we posit, marks an important milestone in standardizing mineral systems science. Ongoing efforts are expanding the dataset to increase global coverage, cover more deposit types, and improve the quality of analyses. Element relationships within the database are being explored to advance mineral systems knowledge. These advances are being used to

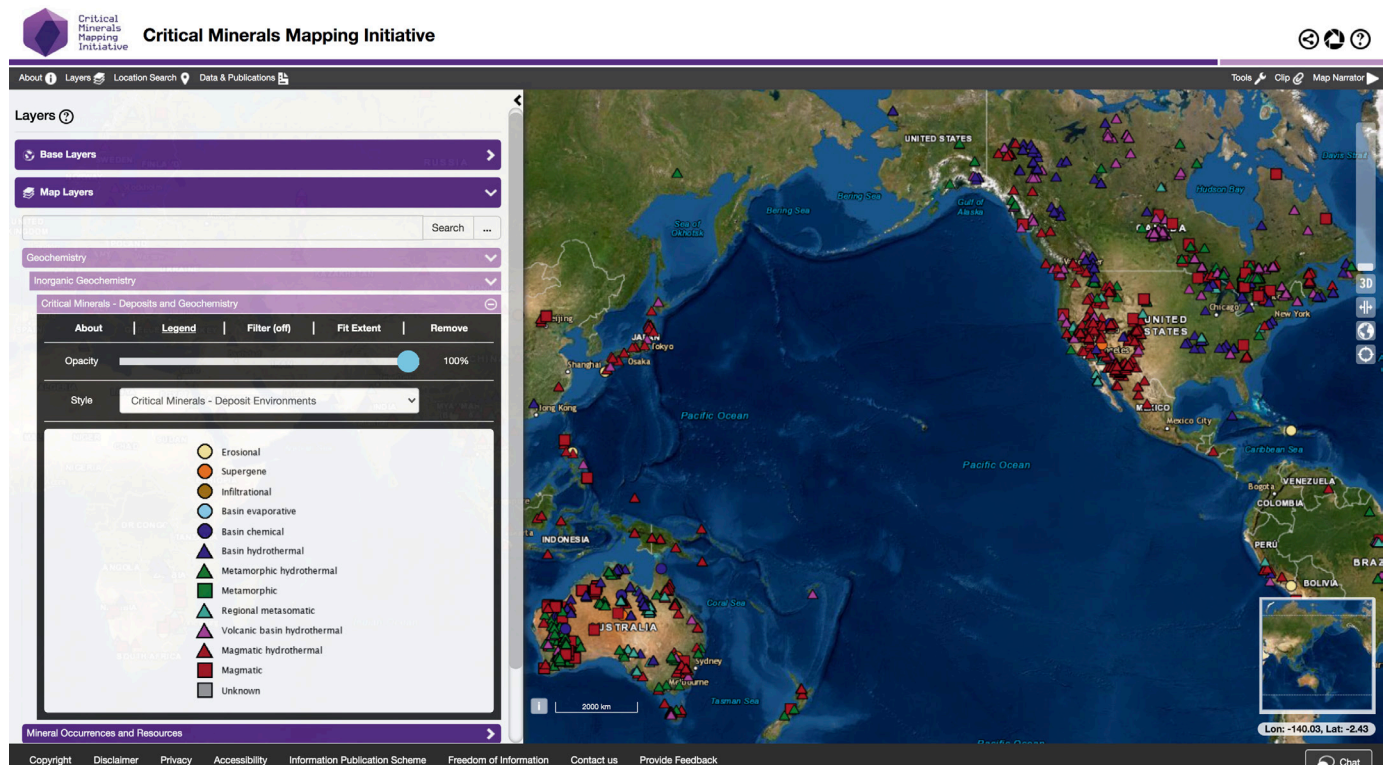


Fig. 1 Critical Mineral Mapping Initiative Portal (<http://criticalminerals.org/>) showing the Critical Minerals in Ores dataset across Asia, Australia, and North and South America attributed by deposit environments following the new mineral deposit classification by Hofstra et al. (2020).

identify new supply opportunities from sampled deposits, to infer opportunities in unsampled deposits, and to infer critical minerals in mine waste.

Building on insights from the CMiO database, the CMMI partners are also seeking to reduce the risk of exploration in new provinces by advancing mineral potential mapping to enable mineral discovery and thereby a stable pipeline of critical mineral projects. Our initial work is targeted on sediment-hosted base metal mineralization with associated critical minerals (e.g., Bi, Co, Ga, Ge, In, Sb). This is because Australia, Canada, and the US are endowed with world-class deposits of this type. Combining the expertise of the partners has allowed us to review key criteria used in the exploration for these deposits by assembling datasets spanning all three countries and analyzing them using modern spatial analytics. The results are improved machine- and knowledge-driven mineral potential models spanning two continents, Australia and North America, along with insights into the predictive power of our data coverages. Next, we intend to test the performance of our approach on different mineral system types.

Importantly, the CMMI is developing a shared foundation on which to build new knowledge of mineral systems. The search and development of critical minerals is being advanced through the mineral systems approach, which provides an holistic framework for integrating key geological processes leading to deposit formation and shaping its development. The test of our advancements will be the improved success rate of the minerals exploration industry and discovery of new deposits. We therefore make our information freely available, and the portal provides an up-to-date collation of our outputs. We engage industry at conferences and workshops organized through professional associations.

Champion, D., Raymond, O., Huston, D., Sexton, M., Bastrakov, E., van der Wielen, S., Butcher, G., Hawkins, S., Lane, J., Czarnota, K., Schroder, I., McAlpine, S., Britt, A., Lauzière, K., Lawley, C., Gadd, M., Pilote, J.-L., Haji Egeh, A., Létourneau, F., Granitto, M., Hofstra, A., Kreiner, D., Emsbo, P., Kelley, K., Wang, B., Case, G., Graham, G., and Lisitsin, V. Critical minerals in ores - web map service

<https://services.ga.gov.au/gis/critical-minerals/wms>

Emsbo, P., Lawley, C., and Czarnota, K., 2021. Geological surveys unite to improve critical mineral security *Eos*, 102.

<https://doi.org/10.1029/2021EO154252>

Hofstra, A., Lisitsin, V., Corriveau, L., Paradis, S., Peter, J., Lauzière, K., Lawley, C., Gadd, M., Pilote, J., Honsberger, I., Bastrakov, E., Champion, D., Czarnota, K., Doublier, M., Huston, D., Raymond, O., van der Wielen, S.E., Emsbo, P., Granitto, M., and Kreiner, D., 2021. Deposit classification scheme for the Critical Minerals Mapping Initiative Global Geochemical Database. U.S. Geological Survey OpenFile Report 2021-1049, 60 p.

<https://doi.org/10.3133/ofr20211049>

Kelly, K.D., 2020. International geoscience collaboration to support critical mineral discovery. U.S. Geological Survey Fact Sheet 2020-3035.

<https://doi.org/10.3133/fs20203035>

Kelley, K.D., Huston, D.L., and Peter, J.M., 2021. Toward an effective global green economy: The Critical Minerals Mapping Initiative (CMMI). *Society for Geology Applied to Mineral Deposits Newsletter*, 48, 1-5.

Critical, specialty, magnet, battery, and photovoltaic materials: Key factors for responsible exploitation and development decision making

George J. Simandl^{1,2a}, Laura Simandl³, and Suzanne Paradis⁴

¹British Columbia Geological Survey, Ministry of Energy, Mines and Low Carbon Innovation, Victoria, BC V8W 9N3, Canada

²School of Earth and Ocean Sciences, University of Victoria, Victoria, BC V8P 5C2, Canada

³RDH Building Sciences Inc., Victoria, BC V8T 1Z4, Canada

⁴Geological Survey of Canada, Sidney, BC V8L 4B2, Canada

^acorresponding author: george.simandl@gov.bc.ca

Raw materials are essential for the global economy, improving our quality of life, and the national security of industrialized countries. With positive forecasts for electric vehicle market growth, in addition to the global focus on alternative energy sources and the reduction in greenhouse gas emission, we are facing a level of change comparable to the 1766-1840 industrial revolution. Opportunities in innovation, investment, mineral exploration, and the development of new deposits and supply chains abound. However, constraints on these opportunities, and the practical ramifications of the overlap of ‘critical’, ‘specialty’, ‘battery’, ‘magnet’ and ‘photovoltaic’ materials should be recognized.

The ‘critical material’ field (Fig. 1) combines results of the criticality studies conducted by the U.S. Department of the Interior (2018) and the European Commission (2020). To reduce supply risks, governments and major corporations are encouraging the development of critical material deposits and related supply chains through economic stimuli, long-term contracts, joint ventures, and vertical integration. This represents excellent opportunities for explorationists. However,

it may result in the development of deposits that would be deemed sub-economic if the World Trade Organization’s rules were followed.

Materials, including those perceived as critical, with a global annual production of less than 200,000 tonnes are referred to as ‘specialty’. Examples are Ta (in capacitors and steel alloys), REE (e.g., Nd and Dy in high-intensity magnets), Nb, W, Be, and Sc (as alloying agents). In the long term, energy-related market growth rates for graphite, Li, Co, In, V, Ni, Ag, and Nd (Fig. 2a) appear bullish. However, to maintain objectivity, such projections must be considered in conjunction with the market projections expressed in tonnes (Fig. 2b) and the size of the current market base.

The term ‘battery material’, as used today by exploration companies, refers to Li, Co, Mn, V, Ni, and graphite, disregarding materials used in lead–acid, nickel–cadmium (NiCd), nickel–metal hydride (NiMH), and other older battery technologies still in use. The automotive industry relies mainly on Li-ion batteries where the anode consists of graphite or other carbon-based materials (\pm minor silicon). Layered LiMO₂ cathodes, where M consists of a combination of Co, Ni, Al, and/or Mn are the most popular. Non-layered cathode varieties (e.g., lithium–iron–phosphate) are less common.

In the future, stationary energy storage systems used as emergency backups, and for dealing with the intermittent nature of renewable energy sources may rival the raw materials needs of the automotive industry. However, because low-energy density is not an issue, several non-lithium systems (e.g., vanadium redox flow, lead–acid, nickel–cadmium, nickel–metal hydride, and high-temperature batteries such as sodium–sulfur and sodium–nickel–chloride) have the potential to compete with Li-ion batteries for this market segment.

Today, the term ‘magnet materials’ refers to materials used in REE (NdFeB) magnets, such as neodymium (Nd), dysprosium (Dy), and less commonly terbium (Tb), praseodymium (Pr) and Co, omitting materials used in mainstream ferrite-type magnets and niche magnet technologies such as AlNiCo magnets. REE magnets are used in motors for electric vehicles, wind turbines and a variety of portable electronic equipment. The high risk of supply disruption in the global REE market keeps governments, manufacturers, exploration companies, and investors interested in REE deposits, related supply chains, REE recycling, and intensive research for the development of substitutes for REE magnets.

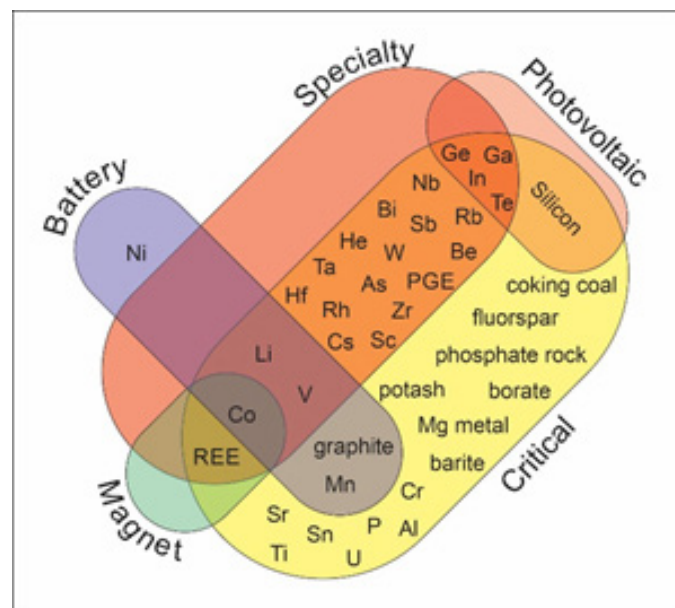


Fig. 1. Overlapping material categories. The terms ‘critical’, ‘specialty’, ‘battery’, ‘magnet’, and ‘photovoltaics’ as used by manufacturers, explorationists, environmentalists, banks, and governments (e.g., Co belongs to specialty, critical, battery, and magnet categories). From Simandl et al. (2021).

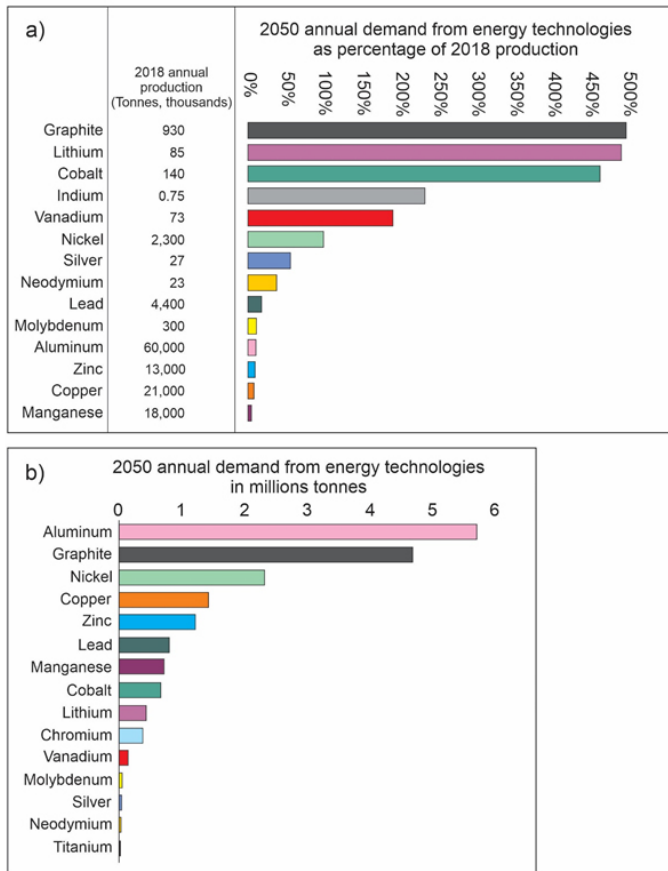


Fig. 2. Material demands based on projections for energy technologies in 2050 assuming a 2 degrees scenario as defined in the International Energy Agency (2017) report. **a)** Shown as a percentage of 2018 global production (U.S. Geological Survey, 2020). **b)** Shown in million tonnes. Modified after Hund et al. (2020).

Solar energy alone could provide enough energy to exceed the needs of the Earth’s entire human population. The main materials used in photovoltaic cells are Si, Ge, Ga, In, and Te (Fig. 1). Recent improvements in photovoltaic technology have reduced the cost of solar energy. As a result, the cumulative global capacity of photovoltaic installations reached an energy generating capacity of 518 GW in 2018 (Heath et al., 2020).

The markets for energy-related (battery, magnet, and photovoltaic) materials are expanding and represent long-term exploration and development opportunities. Projects targeting these materials are considered essential for greenhouse gas reduction, may benefit from government stimuli, and are supported by society. Fields identifying battery, magnet, photovoltaic, critical and specialty materials overlap. These overlaps represent promotional opportunities (e.g., Co-bearing deposit may be referred to as a potential source of battery, magnet, or critical materials depending on the prevailing political climate and investors’ sentiments). However, in the short term, materials within the specialty material field (Fig. 1) do not benefit from economies of scale and, unless backed by governments or manufacturers, developing deposits of these materials hinges on a variety of technical

parameters including simplicity of metallurgical processes (Simandl et al., 2021). This, and the size of the current market, must be factored into project rankings, exploration program designs, and corporate and government policies. Potential technological breakthroughs, material substitutions, geopolitical changes, new mineral discoveries, and recycling efforts must be continuously reassessed. Furthermore, to avoid misallocation of financial resources, particularly in the case of specialty materials, the current market base for a targeted commodity must be considered before designing exploration programs, ranking projects, developing new deposits and supply chains, and decision-making by government.

European Commission, 2020. Communication from the Commission to the Council, the European Parliament, the European Economic and Social Committee and the Committee of the Regions – Critical raw materials resilience: Charting a path towards greater security and sustainability. Commission of the European Communities - COM 474, 23p.

<https://op.europa.eu/en/publication-detail/-/publication/160da878-edc7-11ea-991b-01aa75ed71a1/language-en> (accessed, July 5, 2021).

Heath, G.A., Silverman, T.J., Kempe, M., Deceglie, M., Ravikumar, D., Remo, T., Cui, H., Sinha, P., Libby, C., Shaw, S., Komoto, K., Wambach, K., Butler, E., Barnes, T., and Wade, A. 2020. Research and development priorities for silicon photovoltaic module recycling to support a circular economy. *Nature Energy*, 5, 502-510.

<https://doi.org/10.1038/s41560-020-0645-2>

Hund, K., La Porta, D., Fabregas, T.P., Laing, T., and Drexhage, J., 2020. Minerals for climate action: The mineral intensity of the clean energy transition. World Bank Group. Washington, DC, 110p.

<https://pubdocs.worldbank.org/en/961711588875536384/Minerals-for-Climate-Action-The-Mineral-Intensity-of-the-Clean-Energy-Transition.pdf> (accessed July 1, 2021).

International Energy Agency, 2017. Energy technology perspectives 2017: International Energy Agency Directorate of Sustainability, Technology and Outlooks, 441 p.

https://iea.blob.core.windows.net/assets/a6587f9f-e56c-4b1d-96e4-5a4da78f12fa/Energy_Technology_Perspectives_2017-PDF.pdf (accessed May 15, 2021).

Simandl, L., Simandl, G.J., and Paradis, S., 2021. Specialty, critical, battery, magnet and photovoltaic materials: Market facts, projections and implications for exploration and development. *Geoscience Canada*, 48, 73-91.

<https://doi.org/10.12789/geocanj.2021.48.174>

U.S. Department of the Interior, 2018. Final list of critical minerals 2018. Federal Register, 83, 23296-23297. Federal Register Document Number 2018-10667.

<https://www.govinfo.gov/content/pkg/FR-2018-05-18/pdf/2018-10667.pdf> (accessed July 10, 2021).

U.S. Geological Survey, 2020. Mineral commodity summaries 2020: U.S. Geological Survey, 200 p.

<https://doi.org/10.3133/mcs2020>

Session 2: Geology of critical minerals

Tuesday, November 16, 16:30 PST (0:30 GMT)

List of speakers

Chair: Jan M. Peter, Geological Survey of Canada

Stephen E. Kesler, Department of Earth and Environmental Sciences, University of Michigan
Lithium deposits: From magmas to playas

Murray W. Hitzman, Irish Centre for Research in Applied Geosciences, University College Dublin
Geology of cobalt

Sarah-Jane Barnes, Sciences de la Terre, Université du Québec à Chicoutimi
Critical metals found in magmatic ore deposits; Ni, Cu, Co, PGE, Te, Se, Bi, and V

Anthony E. Williams-Jones, Department of Earth and Planetary Sciences, McGill University
The rare earth elements: A tale of mantle plumes, magmas, and fluids

Andrew Conly, Department of Geology, Lakehead University
The diverse nature of graphite deposits: An overview of their geological characteristics and economic considerations

Robert R. Seal II, United States Geological Survey
Mine waste as a potential source of critical minerals: The importance of understanding speciation and identifying synergies between resource recovery and environmental management

Max Frenzel, Helmholtz Institute Freiberg for Resource Technology
Geochemistry and economic geology of Ga, Ge and In: An overview

Question and answer period

Lithium deposits: From magmas to playas

Stephen E. Kesler^{1a} and Adam C. Simon¹

¹Department of Earth and Environmental Sciences, University of Michigan, Ann Arbor, MI 48105

^a corresponding author: skesler@umich.edu

Lithium forms economically interesting concentrations in a wide variety of geologic environments that fall along a spectrum from igneous rocks and their weathered products to playas. At the deepest and hottest end of this spectrum are roof zones of some peraluminous S-type granites such as the late Variscan intrusions of northern Europe. Lithium concentrations in parts of these granites in the Cinovec (Erzeberg, Germany-Czech Republic) and Cornwall (England) regions can reach 1 to 2 wt%. Complex mineralogy is an impediment to direct recovery of lithium, although various water-rock extraction methods are being considered.

Next lower in the temperature spectrum are lithium-rich pegmatites in which the most common lithium minerals are spodumene (3.73 wt% Li) and petalite (2.27 wt% Li). Processing to release lithium from these minerals involves heating to at least 700°C and acid leaching. Important present and past producers include Greenbushes (Australia), Jiajika (China), Kings Mountain (USA) and Tanco (Canada). Pegmatites commonly form clusters or groups, some of which are associated with a parent igneous intrusion that is usually peraluminous, S-type granite. In most pegmatite fields with a recognizable parent intrusion, lithium-rich pegmatites are farther from the source intrusion than barren pegmatites and are considerably less numerous. Pegmatite formation temperatures of 450°C or less provide further support for this distal relation. Most individual lithium pegmatites form lenses only a few 10s of m wide and 100s of m long, although a few are an order of magnitude larger. Pegmatite grain sizes vary from extremely coarse (m) to fine (mm) scale, and compositional zoning is common, both bulk and individual mineral. Lithium contents of different pegmatite zones vary considerably. For example, at Tanco, two zones making up ~14% of the total pegmatite contain almost all recoverable lithium, whereas at Kings Mountain, pegmatite bodies show little variation in grain size or lithium content. Unzoned pegmatites are generally finer grained than their zoned cousins, a feature that has not been completely explained. Most lithium pegmatites average less than 1 wt% Li and contain 0.1 to 1 Mt Li, although Jiajika and Greenbushes are considerably larger and preliminary estimates suggest a higher average grade for Plumbago (Fig. 1).

Lithium is also enriched in some clays and other diagenetic and low-temperature, hydrothermal minerals, hosted largely by altered rhyolitic volcanic rocks and tuffaceous sediments. The mineral host for lithium in these deposits ranges from polyolithionite, hectorite and tainiolite, in which lithium is in the crystal structure, to other smectite, illite and zeolite-type minerals with adsorbed or exchangeable lithium. Jadarite, the principal ore mineral at the Jadar deposit (Serbia), also contains boron, which is commonly enriched in these deposits. Recovery of lithium from most of these mineral settings requires heating and acid leaching, usually to temperatures of a few 100°C, considerably less than for pegmatite minerals.

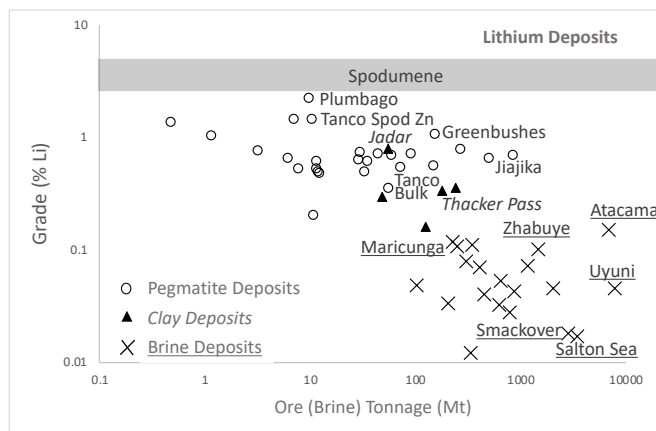


Fig. 1. Grade-tonnage relations for the three main types of lithium deposits (including the bulk and lithium-rich parts of the Tanco pegmatite). Tonnage of brine deposits represents only the mass of the brine and does not include enclosing rocks. Shaded zone, which shows the range of Li content of spodumene, provides an upper limit on the possible grade of pegmatite deposits.

Many of these deposits are closely associated with rhyolite calderas, commonly as tuffs, moat sediments, or adjacent lakes. Lithium in most of the deposits was probably introduced by circulating fluids during late stages of caldera or related volcanic evolution, although at least some of the host rocks might have been enriched in lithium originally. Most lithium-clay deposits average less than 0.35 wt% Li and contain 0.2 to 0.8 Mt Li, although Jadar averages 0.78 wt% Li.

Lithium-rich brines and other waters are found in oil fields (Smackover), geothermal zones (Salton Sea) and especially playas. Processing of brines to recover lithium originally involved sequential precipitation through evaporation, although newer methods involving absorbents, ion exchange, nanofiltration, and solvent extraction are being applied. Complications can be caused by other dissolved elements such as magnesium, which varies in concentration with the abundance of mafic rocks in the drainage area. The largest and highest-grade lithium-bearing brine deposits are found in playas that occupy closed basins where evaporative concentration of incoming waters has been enhanced by long-term, continuous subsidence, usually of tectonic origin. The most important of these closed basins are in the Andean Plateau of South America (northwest Argentina, northern Chile and southwestern Bolivia) where the basins are known as salars, and the Qaidam Basin of China. Rhyolitic magmas and rocks, including tuffs and other sediments, are the source of lithium in almost all of these deposits. In the Andean Plateau, rhyolites of the La Pacana caldera, including the Atana ignimbrite (490 ppm Li), contained enormous amounts of lithium, much of which was released into the Atacama basin by meteoric water leaching. In

salars with a less arid history, like Uyuni and Olaroz-Cauchari, brine is hosted by porosity in siliciclastic sediment that is interlayered with evaporites, whereas in regions with a more arid history (e.g., Atacama), brines are halite saturated and are hosted largely by porosity in a central layer or nucleus of halite. Most brine deposits average about 100 to 1500 mg/L Li, with significant internal variation, and contain considerably less than 1 Mt Li, although Atacama, Uyuni and Zhabuye are larger. Recovery of brines (and therefore lithium) from these deposits is complicated by the dynamic nature of the brine and compartmentalization of reservoirs, and can be lower than for rock-hosted deposits.

Central to estimates of global lithium resources is the question of whether current lithium resources are associated with unusually lithium-rich rocks. The best information comes from South America where the lithium salar region overlaps the Central Volcanic Belt (CVB). The CVB has higher lithium concentrations than other parts of the Andean volcanic belt and it overlies the thickest crust, reflecting a global correlation between lithium concentrations in felsic magmas and coeval crustal thickness. However, Paleozoic basement rocks in the CVB are enriched in lithium and appear to have been assimilated by the CVB volcanic magmas, leaving open the question of how many stages are required to make a truly good lithium-rich province.

Geology of cobalt

Murray W. Hitzman^{1a} and Peter C. Lightfoot²

¹ Irish Centre for Research in Applied Geosciences, University College Dublin, Belfield, Dublin 4, Ireland

² Department of Earth Sciences, University of Western Ontario, London, ON N6A 3K7, Canada

^a corresponding author: murray.hitzman@icrag-centre.org

Cobalt has historically been produced as a by-product of copper or nickel mining but increasing demand due to battery production is placing attention on developing new deposit models. Just over 60% of the world's cobalt comes from the Central African Copperbelt where carrollite and the weathering product heterogenite are the primary cobalt mineral species. Cobalt is not known to be a major constituent of any other major sedimentary rock-hosted stratiform copper districts, most of which produce copper and silver. Interestingly, the deposits in the Copperbelt are almost all uniformly low in silver. Although hydrothermal nickel deposits are also present in some portions of the Copperbelt, these deposits do not contain significant cobalt, and the cobalt-rich Copperbelt deposits do not contain nickel. The reason for the Copperbelt's enrichment in cobalt and paucity of silver is an active area of research. It is likely that the cobalt in the Copperbelt was ultimately sourced from mafic/ultramafic rocks in the basement or basal rift fill of the basin.

Magmatic sulphide ore deposits are typically endowed with cobalt as a by-product element recovered to nickel concentrates in the form of cobalt-bearing pentlandite. The contact- and offset-related Sudbury ore deposits have an average Ni/Co ratio of 25 with higher Ni/Co in Footwall-style deposit (42-145) where Co-poor millerite is the principal nickel-bearing sulphide. Ultramafic-related ore deposits like Thompson also exhibit a range in Ni/Co ratios; disseminated sulphides and breccia ores like those found at Birchtree have Ni/Co~25 whereas the metasediment-hosted Thompson deposit sulphides have much higher and more variable Ni/Co (40-120). The range in Ni/Co at Voisey's Bay is quite narrow, but there are systematic differences between the Ovoid (15) and the Eastern Deeps (18). Differences in Ni/Co ratio within and between magmatic sulphide ore deposits are partially explained by variations in the metal ratios in the parental magma, partitioning, and magma/sulphide ratio, but the proportion of flame-granular pentlandite, and the processes of sulphide fractionation are also key controls. Magmatic sulphide ore deposits typically have cobalt grades in the range 0.08-0.28% Co, but by-product production of cobalt from these types of deposit is well in excess of 1 million tonnes.

Nickel laterite ore deposits break out into saprolites and limonites with a global average Ni/Co~23. The proportion of Co relative to nickel is much higher in laterite deposits that contain Co-rich asbolane. Laterites developed in humid climates like Sorowako and New Caledonia are characterised by saprolites with Ni/Co~30 and more Co-rich limonite with Ni/Co~12. Laterites developed in dry climates like Western Australia have saprolites with Ni/Co~20, nontronite clays with Ni/Co~15, and limonite with Ni/Co~6. The diversity in ratio is largely a direct consequence of the processes of enrichment/

depletion occurring in the laterite profile as a function of the weathering process. The global resource base of laterite in Indonesia, New Caledonia, and the Philippines accounts for the bulk of the higher-grade deposits that are developed at surface and processed by a wide range of metallurgical methods that produce either cobalt metal or cobalt-bearing nickel pig iron.

Cobalt is the primary metal produced from the Bou Azzer copper-gold deposit in Morocco, where cobalt was most probably derived from an immediately adjacent ultramafic rock mass by hydrothermal fluids apparently sourced from later intermediate intrusive rocks. Historically, cobalt was produced from high-grade, low-tonnage, five-element (Ag-Ni-Co-As-Bi) hydrothermal vein deposits with little evidence of a connection to igneous activity. Significant amounts of cobalt are known to reside in cobaltiferous pyrite in Besshi-type volcanogenic massive sulphide deposits and some stratiform metasedimentary rock-hosted deposits such as those in the Blackbird district (USA) and Finland. Significant, but relatively low grade and metallurgically complex, cobalt resources occur in submarine Fe-Mn crusts and nodules.

Critical metals found in magmatic ore deposits: Ni, Cu, Co, PGE, Te, Se, Bi, and V

Sarah-Jane Barnes^{1a}

¹ Université du Québec à Chicoutimi, Chicoutimi, QC G7H 2B1, Canada

^a sjbarnes@uqac.ca

The switch in distribution and generation of power from largely fossil-fuel based to renewables will increase the demand for many metals (Ni, Cu, Co, PGE, V, Te, Se and Bi) found in ore deposits associated with mafic and ultramafic rocks. Most of these elements are derived from the mantle where concentrations for Ni, V and Co are at the 1000 to 100 ppm levels and at the 1 to 10 ppb level for most of the other elements. In ore deposits, Ni and V are at the percent level and Pt and Pd are at the 10 ppm level. The processes leading to an ore deposit must thus concentrate Ni and V by factors of 10 to 100 and by 1000 or more for Pt and Pd. A sufficiently high degree of partial melting of the mantle to dissolve all the sulphides in the mantle (~20%) will release all the Pd, Pt, Te, Se, Bi, and Sb to the melt resulting in an increase in the concentration of these elements by a factor of 5. However, Ni and V are not released as efficiently. This is because there are minerals that remain in the mantle, olivine in the case of Ni and Co and pyroxene and in the case of V, that retain these elements, and thus the process of partial melting does not enrich Ni or Co in the magma and V is only slightly enriched. Nonetheless, a higher degree of partial melting leads to less pyroxene retained in the source and thus higher V values and a high temperature lowers the partition coefficient of Ni into olivine resulting in magmas that are richer in Ni. Thus, the first requirement to form an ore deposit is a high degree of partial melting. In addition, in order for the deposit to be of sufficient size to be exploitable, a large volume of magma is necessary. Magmas favourable for transporting metals from the mantle to the crust are thus komatiites and picrites, and terranes with a large volume of these magmas should be the target of exploration programs.

Once the magma is emplaced into the crust, it must become saturated with a collector phase. In the case of chalcophile elements this is a sulphide liquid. In the case of V this is Fe-oxide (magnetite). To bring about saturation of the magma in a sulphide, liquid S has to be added to the magma as primary magmas are not sulphide saturated. The most common source of S is S-rich sediments, added to the magma as xenoliths and which are then dissolved into the magma and the sulphides within them are mixed into the magma. Bismuth, As, Sb may also be added with the S. The sulphides are generally not rich enough to form an ore deposit because sulphides in sediments do not contain high levels of Ni or PGE. The sulphide droplets must equilibrate with a large volume of magma so that the metals in the mafic magma can partition into the sulphide droplets. A dynamic environment is required for this, and transport of the sulphide droplets facilitates this. In an exploration program the presence of metal-poor sulphides is not necessarily a negative sign. It indicates that the net must be cast wider to search for transported sulphides.

The metal-rich sulphides must eventually be collected in sufficient quantity to be exploitable. This requires a structural

trap, somewhere where the magma flow slows, for example where a magma conduit abruptly widens. The slowing of the magma flow results in the dense sulphide droplets separating and collecting at the place where the conduit widens. The first mineral to crystallize from the sulphide liquid is monosulphide solid solution (MSS). At lower temperatures MSS exsolves or reacts to form pyrrhotite and pentlandite. Nickel and Co are moderately compatible with MSS and the massive ore found at most Ni deposits is MSS cumulate. However, most chalcophile elements are not compatible with MSS and the fractionated sulphide liquid is rich in Cu, Pd, Pt, Te, Sb and Bi. This liquid does not solidify until ~850 °C and thus it can be present as Cu-Pd-Pt-Te-Bi-Sb rich veins around the intrusions. Exploration programs should evaluate the possibility of Cu-Pd-Pt rich ore in the country rocks around any intrusion. Another target is the country rocks if the body that has been deformed is massive ore that has been decoupled from the intrusion along thrust planes.

Nickel deposits are generally sulphide-rich, containing at least 10 modal% sulphides. Platinum-group element deposits generally contain 1 modal% or less sulphides. The composition of the sulphide liquid in PGE deposits is generally similar to that of Ni deposits. However, the sulphide liquid appears to have been much richer in PGE and Te than in the Ni deposits. The partition coefficients for PGE and Te into sulphide liquid are much higher than those of Cu and Ni and hence, if the sulphide liquid reacts with sufficient magma, the sulphide can become enriched in PGE relative to Cu and Ni. The low sulphide content of the PGE deposits makes exploration challenging. However, if sulphide-rich rocks are present at the margins of an intrusion it is worth sampling the intrusion in detail to see whether upgraded sulphides are present within the intrusion.

The collector mineral for V is magnetite. Magnetite crystallizes from fractionated mafic magmas and is found as layers towards the top of layered intrusions. In order that the magnetite be rich in V, the magma should not have crystallized clinopyroxene before magnetite as this would deplete the magma in V. Also, the oxidation state of the magma is critical. V³⁺ has a much higher partition coefficient into magnetite than V⁴⁺ or V⁵⁺, therefore the magma should not be oxidized. On the other hand, if the oxidation state is too low then ilmenite will crystallize in place of magnetite.

The rare earth elements: A tale of mantle plumes, magmas, and fluids

A.E. Williams-Jones^{1a} and O.V. Vasyukova¹

¹ Department of Earth and Planetary Sciences, McGill University, Montreal, QC H3A 0E8, Canada

^a corresponding author: anthony.williams-jones@mcgill.ca

The rare earth elements (REE), like so many metals, are concentrated in the upper crust by magmas that form as a result of the partial melting of the upper mantle. Except for scandium, the REE are incompatible elements and, consequently, reach their highest concentrations in magmas that are the products of very low degrees of partial melting, i.e., carbonatitic and peralkaline silicate magmas. Although scandium, like the other REE, has a charge of +3 (Ce and Eu also commonly have +4 and +2 charges, respectively), because of its small ionic radius, which is intermediate to that of Mg^{2+} and Fe^{2+} , it is a compatible element. As a result, it is released only after higher degrees of partial melting. In principle, the magmas transporting the REE can occur in any tectonic environment with a path to the mantle. They are emplaced mainly in continental rifts after decompression-induced partial melting (mantle upwelling) or partial melting of mantle plumes, but also occur in subduction settings due to hydration melting of the metasomatized mantle wedge. Whereas both the silicate and carbonatite magmas are preferentially enriched in the light REE (La to Gd) relative to the heavy REE (HREE), carbonatite magmas contain a higher proportion of the light REE (LREE) due to their greater incompatibility and the generation of carbonatite magmas at lower degrees of partial melting. In some cases, carbonatites are the products of silicate-carbonate immiscibility and their greater enrichment in the LREE is due to the preferential partitioning of the LREE into the carbonatite magma. After emplacement, fractional crystallization (in the case of the silicate magmas) may concentrate the REE, except scandium, in the residual liquid to form NYF pegmatites (e.g., Strange Lake, Québec). In silica-undersaturated layered igneous complexes, the end-product of fractional crystallisation may be REE-enrichment to form a eudialyte syenite (e.g., the Nechalacho layered suite, Northwest Territories). Silicate-fluoride liquid immiscibility may further concentrate the REE by partitioning them into the fluoride liquid (e.g., Strange Lake). Scandium concentrates in early crystallizing minerals, notably, clinopyroxene (e.g., the Crater Lake syenite, Québec).

Although initial REE enrichment is due to magmatic processes, in most cases the REE have been mobilised to economic concentrations by hydrothermal fluids and, in some cases, the deposits are almost exclusively hydrothermal in origin. Indeed, hydrothermal fluids have remobilized the REE in most deposits hosted by silicate igneous rocks and, in most carbonatite-hosted REE-deposits, the REE minerals are hydrothermal. In the hard-soft-acid-base classification, the REE are hard acids and in aqueous fluids are predicted to form strong complexes with hard bases such as F^- , SO_4^{2-} , CO_3^{2-} , PO_4^{3-} and OH^- . They also form stable, albeit weaker, complexes with Cl^- , a borderline base. Because fluorite is an important gangue mineral in many REE deposits and fluorocarbonate minerals, especially bastnäsite $[REE(CO_3)F]$, are the main ores of many REE deposits, it was long thought that the REE are

transported mainly as fluoride complexes. We now realise that this is mostly not the case because HF is a weak acid, limiting the availability of F^- , and REE activity is buffered to very low levels by $REEF_3$ (fluocerite). Instead, at low to intermediate pH, the REE are transported predominantly as chloride complexes and, importantly, the stability of these complexes increases with decreasing atomic number of the lanthanides, promoting fractionation of the REE. The REE may also be transported as sulphate complexes. Significantly, CO_3^{2-} forms relatively weak complexes with the REE at elevated temperature (they are strong at ambient temperature) and, like F^- , is more important as a depositional ligand, particularly for fluorocarbonate minerals. The same is true of PO_4^{3-} , which deposits monazite ($LREEPO_4$) and xenotime ($HREEPO_4$).

Hydrothermal REE mineral deposition occurs either within the igneous host or distal to it. The giant Bayan Obo REE deposit (China) may be an example of the latter, although there is debate over whether the dolomite host is sedimentary (diagenetic) or a carbonatite. Deposition of the REE minerals in both settings is thought to be the result of fluid-rock interaction, with the rock supplying the ligand (e.g., fluorapatite supplying the PO_4^{3-} for monazite and xenotime deposition) or buffering the pH to a higher value. As the stability of the chloride complexes decreases with increasing atomic number of the lanthanides, interaction of the REE-bearing fluid with rocks of differential pH buffering capacity can lead to fractionation of the REE. This appears to have been the case for Lofdal (Namibia) and Browns Range (Australia), where quartzo-feldspathic host rocks with very low pH buffering capacity deposited REE minerals having the highest recorded proportion of HREE to LREE (> 80% HREE) of any notable REE deposit. In contrast to the other REE, scandium does not generally concentrate hydrothermally to economic levels in REE minerals. Instead, it concentrates by substituting for Mg/Fe in clinopyroxene and amphibole as in the Bayan Obo deposit, which is responsible for ~ 90% of global scandium production. There, scandium occurs in metasomatic aegirine in ores that contain the other REE as bastnäsite and subordinate monazite.

The REE are also concentrated by aqueous processes at ambient temperature to form regolith-hosted ion adsorption deposits in tropical/equatorial climates. These deposits are currently the main source of the HREE globally and form as the result of the weathering of A-type granites, e.g., the giant Zudong deposit (China). There, hydrothermal alteration of the source granite produced several REE minerals that are enriched in the HREE, notably synchysite-(Y), which are unstable in the humus-modified meteoric water. These waters dissolve the REE as bi-carbonate complexes and transport them down the soil profile, where they adsorb onto the surfaces of clay minerals in response to the increase in pH that accompanies fluid-rock/soil interaction. Halloysite is the principal host to the REE because of its high specific surface area and very high

cation exchange capacity. Scandium concentrates in lateritic soil profiles that develop over ultramafic igneous rocks. In this setting, the scandium is released from clinopyroxene (the main primary host of Sc) and transported down the profile, where it adsorbs onto goethite to form potentially economic deposits.

The diverse nature of graphite deposits: An overview of their geological characteristics and economic considerations

Andrew Conly^{1a} and Sevgi Gökşen¹

¹ Department of Geology, Lakehead University, Thunder Bay, ON P7B 5E1, Canada

^a corresponding author: andrew.conly@lakeheadu.ca

Graphite is one of two commonly known natural allotropes of pure carbon, with diamond being the other. It typically occurs as black crystal flakes and masses common to metamorphic rocks, but also occurs in igneous rocks and meteorites. Unlike diamond, graphite has properties akin to both metallic and non-metallic minerals, including chemical inertness, thermal stability, high electrical conductivity, and lubricity. Consequently, graphite has been widely used for a range of industrial applications (i.e., electronics, lubricants, metallurgy, and steelmaking). However, emerging technology uses in energy systems (e.g., fuel cells, Li-ion batteries) and lightweight high-strength composites (e.g., aerospace) have increased the demand for the mineral. Because of this growing demand and global supply challenges, graphite has been deemed by many nations as both a critical and strategic mineral commodity.

Traditionally, graphite deposits have been classified for commercial purposes into flake, microcrystalline (also erroneously referred to as amorphous) and lump and chip (also referred to as vein or hydrothermal) categories. Although this classification scheme is functional for commercial purposes, it does have limitations in terms of geoscience application because: 1) it essentially is based on graphite flake size, with few considerations of other geologic features or graphite properties; 2) lump/chip/vein/hydrothermal is the only end-member that somewhat characterizes deposit morphology; and 3) it does not take into consideration the diversity in geological attributes and deposit formation processes.

As an alternative to the commercial classification scheme, a two-tiered genetic classification is becoming more widely used. Although we prefer the two-tiered system, we acknowledge that it is inherently genetic and not based strictly on objectively observable or quantifiable criteria. This classification scheme also fails to take into consideration flake size, which is a key parameter in determining the commodity value (see below). Under the two-tier scheme, graphite deposits are categorized as either metamorphic or fluid-derived. Metamorphic deposits are the products of regional and contact metamorphism of a carbonaceous sedimentary protolith (e.g., black shales, hydrocarbons, coal). These deposits commonly occur as tabular, lensoidal or podiform bodies in schists and gneisses, but to a lesser extent occur in quartzite and marble. Fluid-derived deposits are the products of graphite precipitating from CO₂-CH₄-H₂O fluids, and can be subdivided into: 1) granulite-hosted, where graphite is derived from decarbonization reactions, in response to high-grade regional or contact metamorphism; and 2) igneous-hosted graphite that forms due to fluid-melt immiscibility, resulting in the generation of carbon-rich aqueous fluids. Fluid-derived deposits are more varied in morphology and their location is strongly influenced by geological structural features. Morphologically, fluid-derived deposits may occur as open space fill features (veins

and breccias), disseminated crystals and crystal aggregates and wall-rock replacement. Because these deposits form from carbonaceous aqueous fluids, the graphite typically occurs in conjunction with other hydrothermal alteration products. Many fluid-derived deposits yield massive accumulations of relatively coarsely crystalline graphite, but the inherent crystal/flake size of graphite in these deposits is highly variable.

Similar to many critical and strategic metals, graphite is not traded on any commodity exchange, but is sold through direct and private agreements between the producer and end-user. In part, this trading is governed by the end uses (both traditional industrial uses and emerging applications) and processing methods that are commonly based on proprietary technology. Though commodity pricing of graphite may be somewhat enigmatic, the primary value-determining parameters are crystallinity, flake size, and carbon content. Crystallinity, which constitutes both the relative proportion of hexagonal (desired) to rhombohedral (not desired) graphite, the d-spacing, and the distance along the c-crystallographic axis between parallel-stacked, planar lattice (graphene) sheets (which is inversely related to temperature of crystallization). This parameter is determined using powder X-ray diffractometry and Raman spectroscopy. Flake size refers to the linear dimensions of graphite crystal aggregates after mineral beneficiation, and rarely does it correspond to the in-situ size of discrete graphite crystallites within the orebody. Producers commonly can generate an array of flake sizes (several nm to >850 µm). However, most produced flake sizes range between 150 µm and 850 µm (medium to 'super jumbo'), with the highest prices commanded by graphite in the 300 µm to 850 µm ('jumbo-super jumbo') range. Flake sizes <150 µm are inherent to the microcrystalline class of deposits but can also be an intended (or unintended) product of mineral processing. Carbon content is a measure of the impurities contained within the product graphite and does not correspond to the carbon content of the deposit. The carbon content of product graphite is typically determined using an array of bulk sampling methods, because coarser mineral inclusions and interstitial phases commonly account for the contamination. However, for applications that require very high purities (>99.99%), assessment of impurities is aided by transmission electron-microscopy-energy dispersive spectroscopy, because impurities can occur on the nanoscale as they can be distributed between graphene layers.

The commodity value of graphite is mutually proportional to higher degrees of crystallinity, larger flake sizes, and high carbon contents/low levels of impurities. The value of graphite is based on the processed material and not the necessarily the inherent qualities of the in-ground graphite. Therefore, graphite suppliers can modify their products to meet an end-user's requirements and offer an array of graphite products at different pricing levels. However, for higher-end and emerging uses (i.e.,

energy applications), assessing the value of a graphite deposit is more challenging because an array of mineral properties, specific to end-use intentions, must be evaluated. Such properties include: density, porosity, Brunauer–Emmett–Teller (BET) surface area, electrical resistivity, thermal expansion and conductivity, compressive-flexural-tensile strength, and modulus of elasticity. Consequently, the assessment of the value of a geologic reserve or resource of graphite is an exercise in the challenging integration of standard resource parameters, grade and tonnage, along with evaluation of mineral properties needed to determine commodity pricing. In this regard, graphite shares certain similarities in its economic evaluation with the other highly sought-after carbon allotrope, diamond, because the economic value of both minerals is dependent on intrinsic and produced quality parameters, some of which are enigmatic.

Mine waste as a potential source of critical minerals: The importance of understanding speciation and identifying synergies between resource recovery and environmental management

Robert R. Seal II^{1a}, Nadine M. Piatak¹, Sarah Jane O. White¹, and Sarah M. Hayes¹

¹ U.S. Geological Survey, Reston, VA 20192, USA

^a corresponding author: rseal@usgs.gov

Mine waste holds significant potential as a source of critical mineral commodities. However, the successful development of these resources from waste materials will require a better understanding of: 1) how waste varies by deposit type for primary, co-product, and by-product resources; 2) the importance of mineral speciation and how it changes due to weathering and mineral processing; and 3) the ability to combine recovery and environmental management approaches for active, inactive, or abandoned mines. Many mineral commodities now deemed “critical” had limited uses just a few decades ago, which destined them to mine wastes. The challenges in developing these potential resources vary depending on whether the commodity is predominantly recovered as a primary commodity (for example, antimony (Sb), lithium (Li), rare earth elements (REEs), tungsten (W)), as a co-product commodity (for example, cobalt (Co), platinum-group metals (PGMs)), or as a by-product commodity (for example, gallium (Ga), germanium (Ge), rhenium (Re), selenium (Se), tellurium (Te)). In addition, the recovery potential also depends on whether recovery is sought at active mines, inactive mines, or abandoned mines. Active mines have the advantage of existing operating infrastructures. At abandoned mines, the recovery of critical minerals and other commodities could help offset the costs of remediation without the requirement of providing a profit. In any case, a multi-pronged approach is necessary to identify viable opportunities for the recovery of critical minerals from mine waste.

A suite of nearly 100 mill tailings samples from over 20 different mineral deposit types has been assembled to evaluate the potential for critical mineral, base metal, and precious metal recovery. Differences among primary, co-product and by-product commodities influence critical mineral concentrations. Not surprisingly, waste from primary commodity deposits contain the highest concentrations of those elements. For example, tailings from Sb deposits have the highest Sb concentrations (reaching 0.3 %), tailings from REE deposit types have the highest concentrations of REEs (locally exceeding 1%), and tailings from uranium (U) deposit types have the highest U concentrations (reaching 0.1%). Deposit type also clearly influences abundances for co-product and by-product critical minerals. The highest W concentrations are found in tailings from orogenic gold deposits and from porphyry Cu deposits, reflecting the common occurrence of scheelite as an accessory mineral in the former and the granophile nature of the latter. Likewise, Te concentrations

are highest in tailings from porphyry Cu deposits – an important current source of Te – and from gold deposits. Germanium concentrations are strongly associated with zinc (Zn) deposits with tailings from Mississippi Valley type deposits having the highest concentrations among Zn deposit types. Nickel (Ni) and Co have the highest concentrations in tailings from mafic magmatic deposits, although tailings from some volcanogenic massive sulphide deposits and porphyry Cu deposits also have elevated concentrations of these elements.

A mass-balance approach allows for a better understanding of the deportment of critical minerals and other commodities in concentrates and tailings during ore processing. At an active porphyry Cu mine, roughly half of the Au, silver (Ag), Zn, PGMs, Se, and Sb in the ore is lost to tailings. Approximately two-thirds of the Te and In and most of the Co, Ge, Ga and REEs also reside in the tailings. The chalcophile nature of Au, Ag and many of the by-product critical mineral commodities suggests that they may be associated with pyrite, an hypothesis supported by ongoing mineralogical studies. By understanding the deportment of critical mineral and other commodities, specific concentrate or waste streams could be targeted for critical mineral, base- and precious-metal recovery.

Solid-phase speciation of critical minerals is important for evaluating their recovery potential from mine waste. In porphyry Cu deposits, the Te in the tailings may either substitute into the pyrite lattice or occur as telluride or sulfosalt inclusions in pyrite. In Mississippi Valley type deposits, Ge occurs in solid solution in sphalerite, but substitutional mechanisms are complex, commonly involving multiple valence states of germanium (Ge⁴⁺ and Ge²⁺) and coupled substitutions with elements such as Cu. In addition, any attempt to reprocess mine waste for recovery of critical minerals or other commodities must account for changes to the hosts of these elements due to weathering. For example, in the Tri-state district (northeastern Oklahoma, USA), sphalerite was the original Ge host, but weathering of the waste piles produced the Zn silicate hemimorphite as a secondary phase, which now hosts a majority of the Ge in wastes sampled.

Waste streams at abandoned, inactive, and active mines should be re-evaluated to identify additional value from non-traditional sources. The most tenable scenarios will likely combine resource recovery with improved environmental management practices. Such approaches will enhance the remediation of abandoned mines and improve the sustainability of active mines. For example,

critical minerals commonly associated with mafic and ultramafic host rocks include PGMs, Ni, and Co. The mill tailings and other mine wastes from these ores are dominated by olivine, pyroxene, and calcic plagioclase, which are prime targets for mineral carbonation (carbon sequestration). Therefore, the waste may be an important source of carbon credits that could lead to carbon-neutral mining operations. The importance of pyrite as a host of Au and a variety of critical mineral commodities (such as Te, Se, Co, and Ni, either as inclusions or in solid solution) highlights the potential of recovering a pyrite concentrate to improve Au and critical mineral recovery while simultaneously enhancing long-term management of acid-rock drainage risks. The increasingly common practice of producing a pyrite concentrate to better manage acid-drainage risks in a smaller volume of material will lessen long-term environmental management costs and may also be an important step toward recovering valuable resources.

Geochemistry and economic geology of Ga, Ge and In: An overview

Max Frenzel^{1a}

¹ Helmholtz-Zentrum Dresden-Rossendorf, Institute Freiberg for Resource Technology, Freiberg, Germany

^a m.frenzel@hzdr.de

As essential raw materials in the electronics, information technology, and renewable energy sectors, Ga, Ge, and In are included in most recent lists of critical raw materials. Whereas all three elements are mostly extracted as by-products from bauxite (Ga) and base-metal sulphide deposits (Ga, Ge, In), Ge is also extracted as a main product from certain coals. Despite their growing economic importance, no up-to-date synthesis is available on the geochemistry of the three elements and how this impacts their economic geology and extraction. The present contribution addresses this gap by reviewing an extensive collection of geochemical data from various sources and collating the results into an updated global overview. In particular, the behaviors of Ga, Ge and In during the most important elemental re-distribution processes in the continental crust are examined, and an assessment is made of how these processes may lead to enrichments suitable for economic extraction. Because active exploration for these elements has been the exception rather than the rule, this exercise may yield new insights into favourable environments that have so far been overlooked.

The following four families of processes were evaluated in detail: mantle melting and magmatic differentiation; hydrothermal leaching and precipitation; and continental

weathering and coal formation. For instance, Figure 1 shows the distribution of Ga across different types of broadly subduction-related volcanic rocks. In general, Ga, Ge, and In show a strong coherence with Al, Fe^{III}, and to a lesser degree Si, in the investigated processes, meaning that significant absolute enrichments (i.e., by a factor >10 in solid materials) are rare, even in favorable environments. Only three processes result in appreciable degrees of enrichment relative to Al, Fe^{III} and Si. First, the leaching of crustal materials by aqueous hydrothermal fluids generally produces >100-fold enrichments of the three elements relative to Al, Fe^{III} and Si in the fluids. However, precipitation processes appear to be relatively inefficient, resulting in absolute enrichments in hydrothermal base-metal ores of typically less than 10-fold for Ga, less than 100-fold for Ge and less than 1000-fold for In compared to crustal concentration levels. These maximum enrichments are reached in different environments: for instance, low-temperature (< 200°C) Pb-Zn deposits are particularly favorable for high Ga and Ge concentrations (cf. Fig. 2). Second, the mobilization of Ga, Ge, and In during weathering and their subsequent incorporation into plant matter produce enrichments in organic sediments and coal. All three elements are more mobile than Al and Fe, but less mobile than Si during continental weathering.

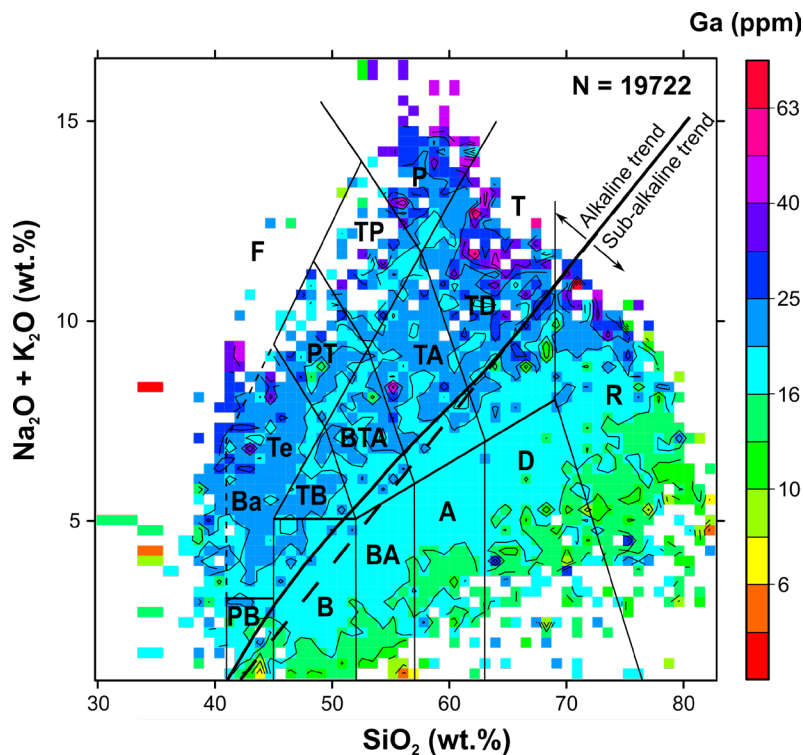


Fig. 1: Variation of mean Ga concentrations across different types of volcanic rock from subduction-related settings. Note increase in mean concentration from bottom right to top left, as well as on the upper edges of the phonolite (P) and trachyte (T) fields. Also note that the scale is logarithmic and that the geometric mean was used in the compilation of the figure. Data from the GEOROC database (Sarbas and Nohl, 2009).

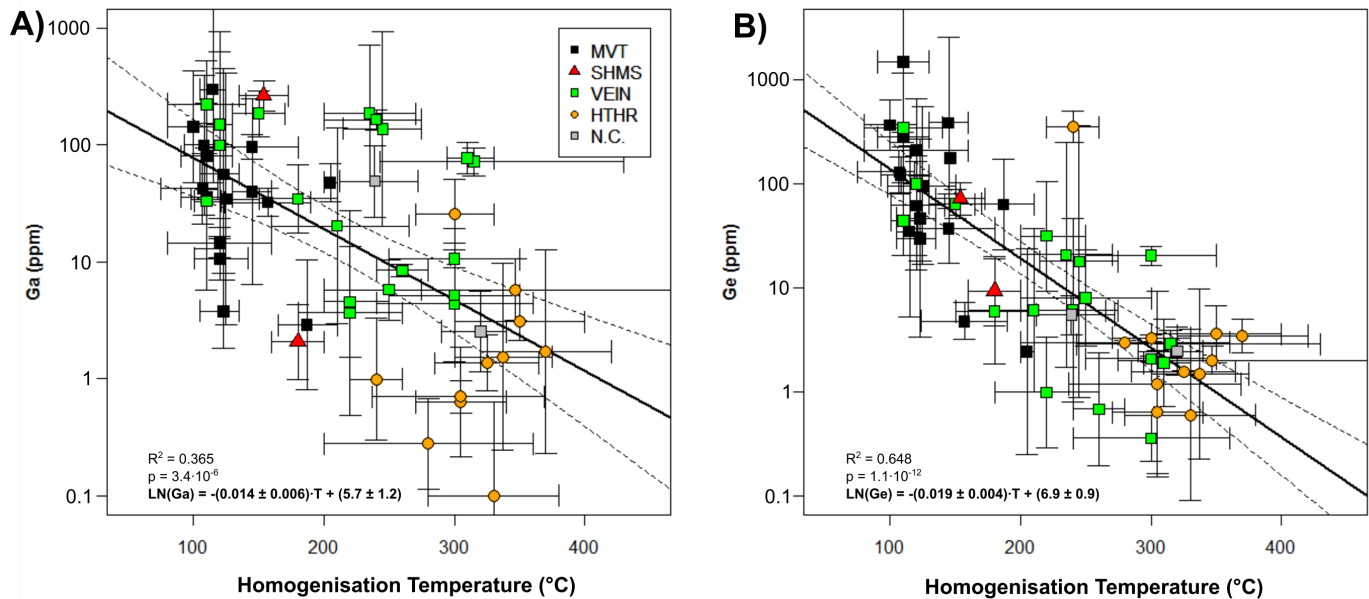


Fig. 2: Variation of Ga and Ge concentrations with fluid inclusion homogenization temperatures (broadly representative of formation temperatures) for sphalerites from various types of Pb-Zn sulphide deposits. Each symbol represents the geometric mean for a deposit, with the error bars representing 95% confidence intervals. Reproduced from Frenzel et al. (2016). Deposit types: MVT= Mississippi Valley type; SHMS=sediment-hosted massive sulphide; VEIN=vein-type; HTHR=high-temperature hydrothermal replacement (skarn and manto deposits); N.C.=not classified.

However, Ge is the most enriched in surface waters, generally by a factor 10-20 relative to Al and Fe. The resorption of Ga, Ge, In, Al and Fe by plant matter in the approximate ratios in which they occur in surface waters, as well as an apparent discrimination against Si during this process, cause the observed enrichments in organic-rich sediments and coal. The mean absolute enrichment achieved by this process is on the order of 10-fold for Ge (in ash), and less for Ga (and probably In) compared to crustal concentration levels. Third, the low-degree melting of the mantle and/or crust to produce exotic magmas such as carbonatite, kimberlite, and pantellerite, can result in enrichments by a factor of 2-10 relative to Al, Fe^{III}, and Si for all three elements. However, absolute enrichment factors generally range between 2 and 3.

Clearly, the absolute enrichments of Ga, Ge, and In achieved in these processes are small when compared to the average enrichments of factor ~1,000 attained by many other metals (e.g., Ag, Cd, Cu, Pb, and Zn) occurring at similar concentration levels in the crust, and which are typically enriched in hydrothermal or magmatic mineral deposits. Only indium comes close to such values in a small number of cases. This lack of an efficient widely available enrichment process, in combination with relatively low crustal abundances, is the main reason why these elements are relatively dispersed and do not generally form their own mineral deposits. In fact, even the concentration levels sufficient for by-product extraction (10s of g/t in ore) are only reached in certain environments.

Nevertheless, certain suitable combinations of the above processes lead to the rare occurrence of considerably larger enrichments. First, the weathering of suitable base-metal sulphide deposits may result in high concentrations of Ga, Ge, and/or In in the residual Fe-oxide-rich materials. The Apex mine in Utah is an excellent example, being the only deposit ever considered as a Ga-Ge-mine, with whole-ore

concentrations of 320 g/t Ga and 640 g/t Ge, mostly hosted in Fe^{III}-bearing minerals. For indium, no comparable occurrence has yet been described. Second, the hydrothermal overprinting of coal deposits, or coal formation in geothermally active areas, can produce extremely enriched coals, with Ge concentrations exceeding 100 g/t in the coal. Various deposits of this type exist in Russia and China. Some of the Chinese deposits are actively mined for Ge. Third, the lateritic weathering of certain alkaline or peralkaline rocks should produce enriched laterite materials. Such deposits would be particularly amenable to Ga production. However, no such Ga-rich occurrence has yet been described.

The current supply situation for all three elements is such that their extraction as by-products should be sufficient to meet demand for the foreseeable future. However, if new deposits are sought from which any of the three elements can be produced as main products, then exploration efforts should focus on combinations of favourable environments for their enrichment, such as those described above. In addition, the collection of further geochemical data on different types of hydrothermal mineralization, which have not been widely analyzed for these elements so far, may lead to the discovery of further promising targets.

Frenzel M., Hirsch T., and Gutzmer J., 2016. Gallium, germanium, indium and other trace and minor elements in sphalerite as a function of deposit type – A meta-analysis. *Ore Geology Reviews*, 76, 52-78.
 Sarbas B., and Nohl U., 2009. The GEOROC database – A decade of “online geochemistry”. *Geochimica et Cosmochimica Acta Supplement*, 73 (13), A1158.

Session 3: World-class critical mineral deposits

Wednesday November 17, 13:30 PST (21:30 GMT)

List of speakers

Chair: Zhehan Weng, Geoscience Australia

Hong-Rui Fan, Chinese Academy of Sciences
The giant Bayan Obo REE-Nb-Fe deposit (China): Ore genesis and resource potential

M. Christopher Jenkins, Department of Earth Sciences, Carleton University
The nature and composition of the J-M Reef, Stillwater Complex, Montana, USA

Philippe Muchez, KU Leuven, Department of Earth and Environmental Sciences
Cu-Co ore deposits in the Central African Copperbelt: Origin and transport of metals, ore mineral precipitation, and regional and stratigraphic distribution

Philip L. Verplanck, United States Geological Survey
An overview of the world-class Mount Weld rare earth element deposit

Kathryn Goodenough, British Geological Survey
African lithium pegmatites

Question and answer period

The giant Bayan Obo REE-Nb-Fe deposit (China): Ore genesis and resource potential

Hong-Rui Fan^{1,2}, Kui-Fang Yang^{1,2}, Xiao-Chun Li², Hai-Dong She^{1,2}

¹Key Laboratory of Mineral Resources, Institute of Geology and Geophysics, Chinese Academy of Sciences, Beijing 100029, China

²College of Earth Science, University of Chinese Academy of Sciences, Beijing 100049, China

^a corresponding author: fanhr@mail.iggcas.ac.cn

Bayan Obo is the largest rare earth element (REE) and the second largest niobium deposit in the world. It is also a large iron ore deposit. More than 80% of the REE resources in China are in the Bayan Obo region. REE reserves are 57.4 million metric tonnes (Mt) with an average grade of 6% RE₂O₃. Niobium reserves are estimated at 2.2 Mt with an average grade of 0.13% Nb₂O₅, and total Fe reserves are at least 1500 Mt with an average grade of 35%. The ores are rich in light rare earth elements (LREE), mostly Ce, La and Nd, which occupy >90% LREE. Since the discovery of REE minerals in 1935, many studies have been undertaken on the geology, mineralogy, geochronology, and geochemistry of the region. However, owing to complicated element and mineral compositions and a complex history, the origin of the deposit, potential sources, and the mechanism of REE enrichment still remain subjects of intense debate.

The Bayan Obo deposit is ca. 90 km south of the China-Mongolia border, at the northern margin of the North China Craton (NCC), bordering the Central Asian Orogenic Belt to the north. Gently folded low-grade metasedimentary units of the Bayan Obo Group (Mesoproterozoic) are distributed from south to north, and the deposit is in massive dolomites in the core of a syncline. North of the ore body, a complete Bayan Obo Group section is separated from Paleoproterozoic basement rocks along an angular unconformity. The Bayan Obo Group records rift sedimentation during breakup of the NCC in the Mesoproterozoic. The ore-hosting dolomites extend laterally for 18 km and across strike for 2 km. The origin of the ore-hosting dolomites is still disputed, with both sedimentary and carbonatite-related alternatives being proposed.

Basement rocks at Bayan Obo consist of Neoproterozoic mylonitic granite-gneiss (2588±15Ma), Paleoproterozoic syenite and granodiorite (2018±15Ma), and biotite granite-gneiss and garnet-bearing granite-gneiss (~1890 Ma). Dioritic-granitic plutons, composed of gabbro, gabbroic diorite, granitic diorite, adamellite, and biotite granite, are distributed south and east of the Bayan Obo mine. Recent geochronologic data indicate that these plutons were emplaced in a narrow time interval (263-281 Ma) consistent with subduction during closure of the Paleo-Asian Ocean; REE mineralization at Bayan Obo has no direct relationship to these late Paleozoic intrusions. Nearly 100 carbonatite dikes cut the basement rocks and/or the Bayan Obo Group. The dikes are typically 0.5 to 2.0 m wide, 10 to 200 m long, and strike northeast or northwest. Some dikes have metasomatized the country rocks, producing fenites characterized by sodic amphiboles and albite. The dikes contain mainly dolomite and calcite, with subordinate apatite, monazite, barite, bastnäsite, and magnetite. The dikes are divided into three types that correspond to different evolutionary stages: dolomite, co-existing dolomite-calcite, and calcite. The REE contents in the different carbonatite

dikes vary from ca. 0.02 to ca. 20 wt%; the calcite-type dikes have higher REE contents. Geochemical data show that Sr and LREE contents increase from dolomite type, through calcite-dolomite type, to calcite type, possibly reflecting a fractional crystallization trend.

The mine consists of three major ore bodies: East, Main and West. Relative to the West orebody, the East and Main orebodies form larger lenses, underwent more intense fluoritization and fenitization and contain more abundant REE and Nb. Fluorite appears in the fenitized dolomite, and riebeckite and phlogopite are in overlying K-rich slates. The REE ores are of four types: riebeckite, aegirine, massive, and banded. The principal REE minerals are bastnäsite-(Ce) and monazite-(Ce), which are accompanied by REE and Nb minerals, such as huanghoite, aeschynite-(Ce), fergusonite, and columbite. The iron minerals are magnetite and hematite. The main gangue minerals include fluorite, barite, alkali amphibole, apatite, quartz, and aegirine. Based on ore occurrences and crosscutting relations, three important REE mineralizing episodes are recognized. The first episode displays disseminated mineralization and contains monazite associated with ferroan dolomite, ankerite, and magnetite that is concentrated along fractures and grain boundaries in the relatively unaltered and massive dolomite. The second or main episode is banded and/or massive mineralization, which shows a generalized paragenetic sequence of strongly banded REE and Fe ores showing alteration to aegirine, fluorite, and minor alkali amphibole. The third episode cuts the banded and massive ores and consists of aegirine-rich veins containing coarser crystal fluorite, huanghoite, albite, calcite, biotite, and/or pyrite.

Elemental geochemistry, and C, O, and Mg isotopic geochemistry reveal that the ore-hosting dolomites are strongly enriched in LREEs, Ba, Th, Nb, Pb, and Sr, and have very different (PAAS)-normalized REE patterns, showing that the ore-hosting dolomite was mainly derived from the mantle (Yang et al., 2011, 2019). The ore-hosting dolomite consists of coarse-grained and fine-grained varieties. In the coarse-grained variety, euhedral-subhedral dolomite is associated with evenly distributed fine-grained apatite, magnetite, and monazite. Field observations in the northern part of the Main Orebody reveal that the coarse-grained dolomite intruded into Bayan Obo Group quartz sandstone as apophyses. The major and trace element contents of the coarse-grained dolomite are very similar to the calcite-dolomite carbonatite dikes. They display overlap within the magnesio-carbonatite region on the CaO-MgO-(FeO+Fe₂O₃+MnO) classification diagram and show similar REE contents and distribution patterns on a chondrite-normalized abundance diagram (Yang et al., 2019). The field relationships and geochemical similarities indicate that the coarse-grained dolomite is likely an early phase of a calcite-dolomite carbonatite stock. The fine-grained

(0.05-0.1 mm) dolomites consist predominantly of dolomite or ankerite and constitute the main part of the deposit. The major, trace element, and REE characteristics of these fine-grained dolomites differ from the coarse-grained variety. Fine-grained dolomite samples display major element compositions comparable to that of the dolomite carbonatite dikes. All the samples fall in the field of dolomite carbonatite dikes on the CaO-MgO-(FeO+Fe₂O₃+MnO) classification diagram. However, the REE content and distribution patterns of the fine-grained dolomite samples are similar to those of the calcite carbonatite dykes. The REE content in the dolomite carbonatite dikes is relatively low relative to the extreme accumulation in the calcite carbonatite dikes. REE minerals in the fine-grained dolomite occur as ribbons or aggregates and REE minerals are distributed around dolomite phenocrysts in the fine-grained dolomite. These observations lead us to interpret that the fine-grained dolomite represents an early-stage large-scale dolomite carbonatite pluton, and that the coarse-grained dolomite represents superposed REE mineralization that was derived from a later calcite carbonatite magma.

In the last two decades, numerous geochronologic studies have been carried out on different materials using a variety (U-Th-Pb, Sm-Nd, Rb-Sr, K-Ar, Ar-Ar, Re-Os, and La-Ba) of methods of varying precision (e.g., Nakai et al., 1989; Chao et al., 1997; Zhang et al., 2003; Campbell et al., 2014; Zhu et

al., 2015). These studies have led to three main opinions on mineralization ages: Mesoproterozoic (ca. 1.4-1.3 Ga); early Paleozoic (ca. 500-400 Ma); and two-stage (Mesoproterozoic and early Paleozoic). Work on banded ores by Campbell et al. (2014) revealed zircons with Mesoproterozoic (1325 ± 60 Ma) cores and Caledonian (455.6 ± 28.27 Ma) alteration rims and, in a review of Sm-Nd isotopic measurements, Zhu et al. (2015) concluded that early Paleozoic ages record thermal disturbance and do not imply additional mineralization events. Zhu et al. (2015) proposed that the earliest REE mineralization event was at 1286 ± 27 Ma using a Sm-Nd isochron of coarse-grained dolomite and nearby carbonatite dikes, and that a significant thermal event at ca. 400 Ma resulted in the formation of late-stage veins with coarse crystals of REE minerals.

Several possible sources of ore-forming fluids have been proposed for the Bayan Obo deposit, including deep-source fluids, anorogenic magmas, magmatic and metamorphic fluids, mantle fluids, and carbonatite magma/fluids. The oxygen, carbon, strontium, and niobium isotope composition of the carbonatites, dolomites, and obviously sedimentary limestones are taken to indicate that the coarse-grained dolomite was an igneous carbonatite and that the fine-grained dolomite recrystallized under the influence of mineralizing solutions that entrained groundwater. Sun et al. (2013) found that the Fe isotopic compositions of different rock types at the deposit

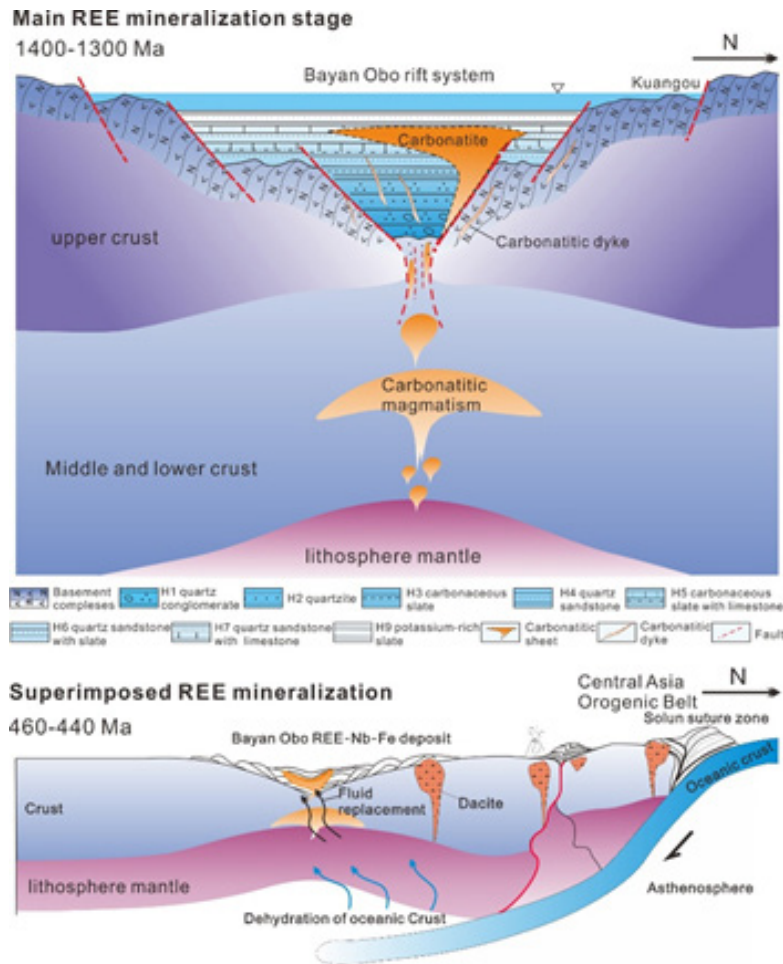


Fig 1. Two stage mineralization model for the formation of the giant Bayan Obo deposit.

differ from those of sedimentary or hydrothermal products but are consistent with a magmatic source. Fluid inclusion work on banded and vein ores at Bayan Obo (Fan et al., 2006) indicate that the original ore-forming fluids were very rich in REE, and therefore, laid a foundation to produce economic REE ores.

The Bayan Obo deposit was likely associated in space and time with large-scale carbonatitic magmatic activity (ca. 1400-1300 Ma) in response to rifting along the northern margin of the North China Craton. The depleted mantle model age (T_{DM}) from Nd isotope data on carbonatite dike and ore-hosting dolomite samples ranges from 1610 to 1790 Ma and coincides with initiation of the Bayan Obo rift (ca. 1750 Ma). During protracted extension of the Bayan Obo rift, the mantle lithosphere underwent a low degree of partial melting leading to the production of carbonatite magma at the final stage of breakup of the Columbia (Nuna) supercontinent (ca. 1400-1200 Ma). Through continuous crystal fractionation, abundant LREE accumulation occurred in the terminal calcite carbonatite magma, which was then superposed on the early dolomite carbonatite pluton, thus resulting in the formation of the giant Bayan Obo REE deposit.

The timing of the early episode of REE mineralization of the Bayan Obo deposit obtained from REE minerals and ore-hosting dolomite (ca. 1400-1300 Ma) is consistent with the reported ages of REE-rich carbonatite dikes, implying a genetic connection. Geochemical evidence from element content and Nd isotope compositions also imply that ore-hosting dolomite and the carbonatite dikes have a close relationship to magmatism. A significant thermal event at ca. 440 Ma resulted in the formation of late-stage veins with coarse crystals of REE minerals. However, the REE mineralization developed during this event resulted from remobilization of REE within the orebodies and this late mineralization appears to have made minimal contribution to the existing ore reserves. The ages of ca. 440 Ma may be related to subduction of the Paleo-Asian oceanic plate during the Silurian. In summary, the Bayan Obo giant deposit is the product of mantle-derived carbonatitic magmatism at ca. 1400 Ma, which was likely related to the breakup of Columbia. Some remobilization of REE occurred due to subduction of the Paleo-Asian plate during the Silurian, forming weak vein-like mineralization (Fig. 1).

This work is funded by the National Natural Science Foundation of China (41930430, 91962103), the Key Research Program of the Institute of Geology and Geophysics, CAS (IGGCAS-201901).

- Campbell L.S., Compston, W., Sircombe, K.N., and Wilkinson, C.C., 2014. Zircon from the East Orebody of the Bayan Obo Fe–Nb–REE deposit, China, and SHRIMP ages for carbonatite-related magmatism and REE mineralization events. *Contributions to Mineralogy and Petrology*, 168, 1041, 23p.
- Chao, E.C.T., Back, J.M., Minkin, J.A., Tatsumoto, M., Wang, J., Conrad, J.E., MaKee, E.H., Hou, Z., and Meng Q.S., 1997. The sedimentary carbonate-hosted giant Bayan Obo REE-Fe-Nb ore deposit of Inner Mongolia, China: A cornerstone example for giant polymetallic ore deposits of hydrothermal origin. *U.S. Geological Survey Bulletin* 2143, pp. 1-65.
- Fan, H.R., Hu, F.F., Yang, K.F., and Wang, K.Y., 2006. Fluid unmixing/immiscibility as an ore-forming process in the giant REE-Nb-Fe deposit, Inner Mongolian, China: evidence from fluid inclusions. *Journal of Geochemical Exploration*, 89, 104-107.

- Nakai, S., Masuda, A., and Shimizu, H., 1989. La-Ba dating and Nd and Sr isotope studies on Bayan Obo rare earth element ore deposit, Inner Mongolia, China. *Economic Geology*, 84, 2296-2299.
- Sun, J., Zhu, X., Chen, Y., and Fang, N., 2013. Iron isotopic constraints on the genesis of Bayan Obo ore deposit, Inner Mongolia, China. *Precambrian Research*, 235, 88-106.
- Yang, K.F., Fan, H.R., Santosh, M., Hu, F.F., and Wang, K.Y., 2011. Mesoproterozoic carbonatitic magmatism in the Bayan Obo deposit, Inner Mongolia, North China: Constraints for the mechanism of super accumulation of rare earth elements. *Ore Geology Reviews*, 40, 122-131.
- Yang, K.F., Fan, H.R., Pirajno, F., and Li, X.C., 2019. The Bayan Obo giant REE accumulation conundrum elucidated by intense magmatic differentiation of carbonatite. *Geology*, 47, 1198-1202.
- Zhang, Z.Q., Yuan, Z.X., Tang, S.H., Bai, G., and Wang, J.H., 2003. Age and geochemistry of the Bayan Obo ore deposit. *Geological Publishing House, Beijing*, pp 1-222 (in Chinese with English abstract).
- Zhu, X.K., Sun, J., Pan, C., 2015. Sm–Nd isotopic constraints on rare-earth mineralization in the Bayan Obo ore deposit, Inner Mongolia, China. *Ore Geology Reviews*, 64, 543-553.

The nature, composition, and origin of the J-M Reef, Stillwater Complex, Montana, USA

M. Christopher Jenkins^{1,2,a}, James E. Mungall¹, Michael L. Zientek², Gelu Costin³, Paul Holick⁴, Kevin Butak⁴, and Zhuo-sen Yao¹

¹ Mineral Deposits Laboratory, Department of Earth Sciences, Carleton University, Ottawa, ON K1S 5B6, Canada

² U.S. Geological Survey, Geology, Minerals, Energy, and Geophysics Science Center, Spokane, WA 99201, USA

³ Department of Earth, Environmental and Planetary Sciences, Rice University, Houston, TX 77005, USA

⁴ Stillwater Mine, Sibanye-Stillwater, MT 59061, USA

^a corresponding author: chris.jenkins@carleton.ca

The Stillwater Complex is a Neoproterozoic (2.71 Ga; Wall et al., 2018) layered mafic to ultramafic intrusion that hosts the world’s highest grade Pd-Pt deposit, the J-M Reef. The J-M Reef is a ~1.5 m thick stratiform layer of extremely high tenor disseminated sulphide mineralization—predominantly pyrrhotite, chalcopyrite, and pentlandite—with an average grade of between 20-25 ppm Pd + Pt. The J-M Reef is most commonly hosted in coarse-grained olivine-bearing cumulates called the Reef package in the Olivine-bearing I zone of the mafic Lower Banded series. Reef tenor sulphides can be found in all rock types of the Lower Banded series including norite, gabbro-norite, anorthosite, and not exclusively in troctolite and peridotite. Reef tenor sulphide mineralization is known to transgress silicate layering and is found as layers, pods, or large ‘ballroom’ structures in the footwall to the Reef package

(Zientek et al., 2002; Boudreau et al., 2020). The platinum group elements (PGE) in the reef are hosted in base metal sulphides (e.g., up to 5 wt % Pd in pentlandite; Godel and Barnes, 2008a) and as discrete platinum group minerals in and adjacent to base metal sulphides (Godel and Barnes, 2008b).

A database of >60,000 mineralized J-M Reef samples collected and analyzed during the past 30 years of mine development were used to examine variations in ore grade and sulphide tenor along strike and down dip in the Stillwater Mine area (Fig. 1a; Jenkins et al., 2020). Whole-rock metal concentrations were normalized to 100% sulphide and the Empirical Bayesian Kriging interpolation method was used to generate predicted values surfaces for S concentrations, sulphide tenors, and Cu/Pd ratios (Fig. 2). Most of the observed variation in sulphide tenors across the deposit is due to variations in the mass ratio

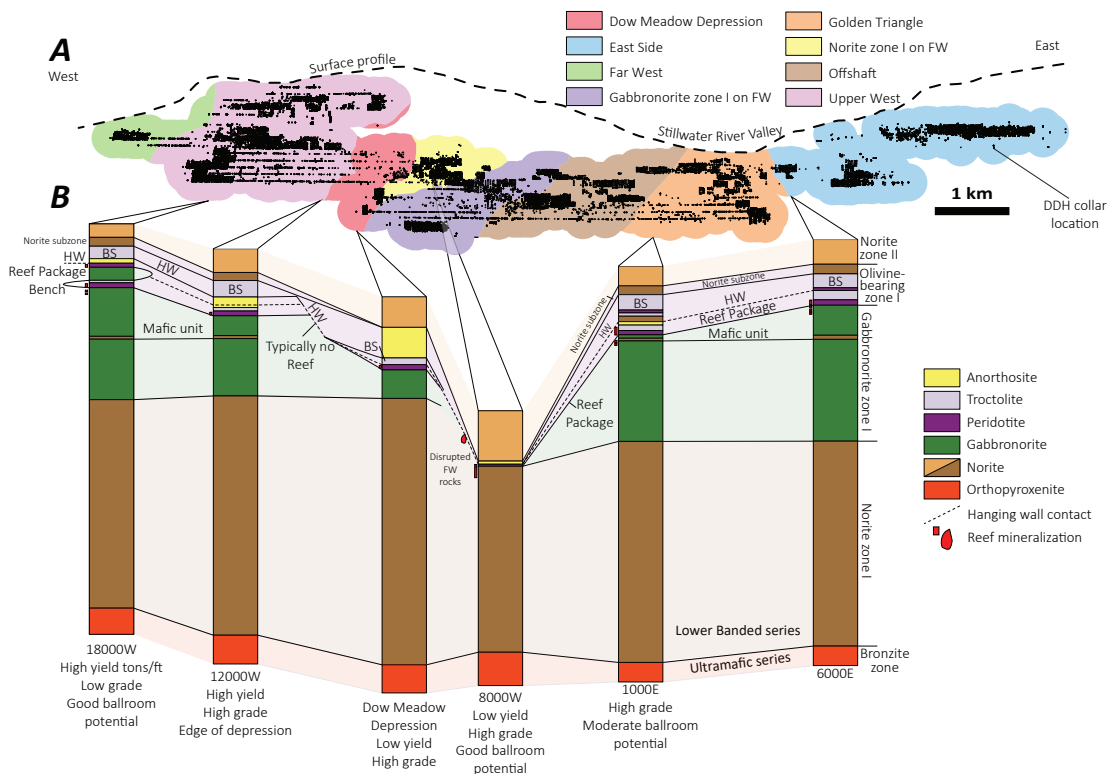


Fig. 1. a) Projected vertical section of the J-M Reef showing the location of individual drill hole collars in the Stillwater mine area. Section polygon colors correspond to mine blocks determined by geology (e.g. Norite zone I on FW) or commonly used mine geography (e.g., Golden Triangle). **b)** Stratigraphic sections showing the variation in relative layer or zone if stratigraphy was returned to horizontal across the area of the Stillwater mine. Mafic layer in Gabbro-norite Zone I was selected as datum. BS: corresponds to the “buckshot” olivine-bearing marker unit in the hanging wall to the Reef package. Modified from Jenkins et al. (2020).

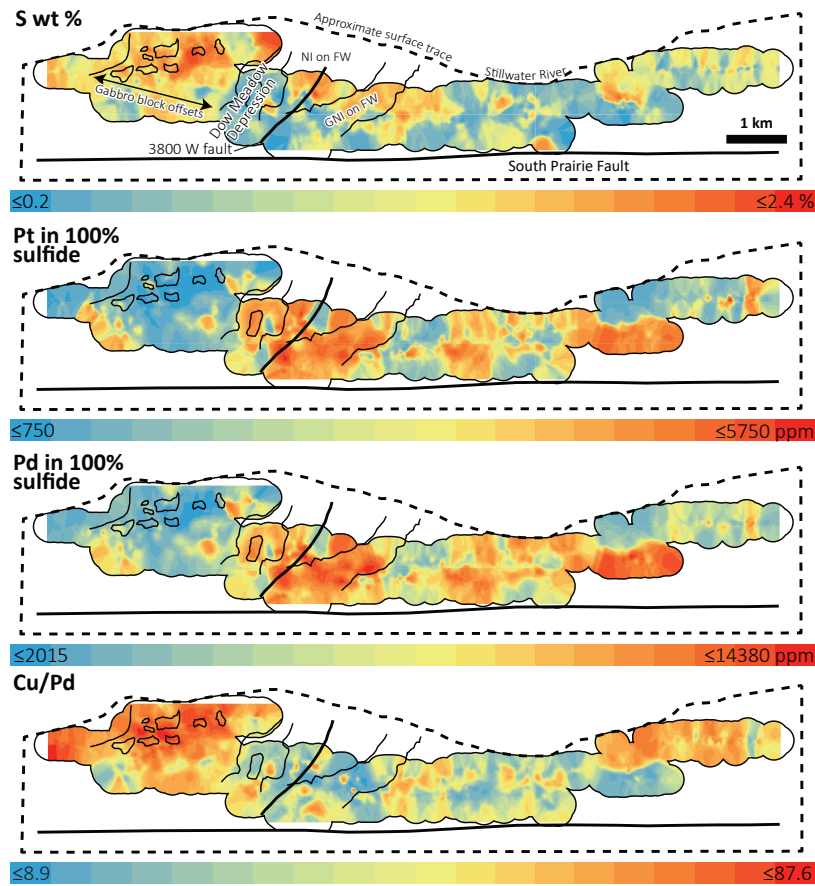


Fig. 2. Predicted value surfaces generated by Empirical Bayesian Kriging interpolation of whole-rock S and Cu/Pd and metal concentrations normalized to 100% sulphide from samples collected from the diamond drill core shown in Fig. 1. Modified from Jenkins et al. (2020).

of equilibrated silicate liquid to immiscible Fe-sulphide liquid (i.e., R factor) during the formation of the reef. Geochemical and textural evidence shows that anomalously high or low sulphide tenors are due to sampling error (e.g., the nugget effect) or variable amounts of sulfur loss due to low-temperature hydrothermal alteration of sulphide minerals.

We now ascribe the variability in R factor to variable amounts of infiltration and reaction of a hot, contaminated komatiitic liquid down into mushy gabbro cumulates that were themselves crystallized from a lower crust-contaminated komatiite liquid (Jenkins et al., submitted). The infiltration of the fresh magma upgrades resident, moderately PGE-rich sulphide liquid in the gabbro cumulates while dissolving pyroxene and feldspar and crystallizing olivine to form the olivine-bearing rocks of the Reef package. This model accounts for the unconformable relationship between the olivine-bearing rocks of the Reef package and the underlying footwall stratigraphy (Fig. 1b) and forms the reef sulphide mineralization without any external crustal sulfur, consistent with S isotopic studies of J-M Reef sulphides (e.g., Ripley et al., 2017).

Boudreau, A.E., Butak, K.C., Geraghty, E.P., Holick, P.A., and Koski, M.S., 2020. Mineral deposits of the Stillwater Complex. In: *Geology of Montana, Volume II-Special Topics*. Montana Bureau of Mines and Geology Special Publication 122, 33p.

Godel, B. and Barnes, S., 2008a. Platinum-group elements in sulfide minerals and the whole rocks of the J-M Reef (Stillwater Complex): Implication for the formation of the reef. *Chemical Geology*, 248, 272-294.

Godel, B., and Barnes, S., 2008b. Image analysis and composition of platinum-group minerals in the J-M reef, Stillwater Complex. *Economic Geology*, 103, 637-651.

Jenkins, M.C., Mungall, J.E., Zientek, M.L., Holick, P., and Butak, K., 2020. The nature and composition of the J-M Reef, Stillwater Complex, Montana, USA. *Economic Geology*, 115, 1799-1826.

Jenkins, M.C., Mungall, J.E., Zientek, M.L., Costin, G., and Yao, Z., submitted. The origin of the J-M Reef and Lower Banded series, Stillwater Complex, Montana, USA. *Precambrian Research*.

Ripley, E.M., Wernette, B.W., Ayre, A., Li, C., Smith, J.M., Underwood, B.S., and Keays, R.R., 2017. Multiple S isotope studies of the Stillwater Complex and country rocks: An assessment of the role of crustal S in the origin of PGE enrichment found in the J-M Reef and related rocks. *Geochimica et Cosmochimica Acta*, 214, 226-245.

Wall, C.J., Scoates, J.S., Weis, D., Friedman, M., Amini, M., and Meurer, W.P., 2018. Age of the Stillwater Complex: Integrating zircon geochronologic and geochemical constraints on the emplacement history and crystallization of a large, open-system layered intrusion. *Journal of Petrology*, 59, 153-190.

Zientek, M.L., Cooper, R.W.L., Corson, S.R., and Geraghty, E.P., 2002. Platinum-group element mineralization in the Stillwater Complex, Montana. In: Cabri, L.J., (Ed.), *The Geology, Geochemistry, Mineralogy and Mineral Beneficiation of Platinum Group Elements*. Canadian Institute of Mining, Metallurgy and Petroleum Special Volume 54, pp. 459-481.

Cu-Co ore deposits in the Central African Copperbelt: Origin and transport of metals, ore mineral precipitation, and regional and stratigraphic distribution

Philippe Mucchez^{1a}

¹ KU Leuven, Department of Earth and Environmental Sciences, Leuven, Belgium

^a philippe.mucchez@kuleuven.be

The Central African Copperbelt contains the largest global resource of cobalt (6 Mt) in addition to 200 Mt of copper (non-compliant estimates). Numerous studies carried out during the 20th century and in the first part of the 21st century provide clear insight in the factors controlling ore formation and the variety of ore-forming processes. The knowledge of the ore-forming processes and their complexity helps exploration and has extended the areas of interest.

Regional geological and geochemical studies have shown that likely sources of metals are both siliciclastic rocks at the base of the Katangan Supergroup and felsic basement rocks from which these siliciclastic rocks were derived (Van Wilderode et al., 2015). The large amount of cobalt, in addition to the occurrence of variable and locally significant amounts of nickel (Capistrant et al., 2015) and the presence of platinum group elements (Cailteux et al., 2005), indicate at least partly a mafic source of the metals (Annels and Simmonds, 1984). The metals were transported as chloride complexes as indicated by very high concentration in saline (up to 50 eq. wt% NaCl) mineralizing brines reported in several detailed fluid inclusion studies (e.g., El Desouky et al., 2009; Selley et al., 2018; Davey et al., 2021). These highly saline fluids originated as evaporative brines during sedimentation of the Katangan sequences. Fluids migrated upwards and laterally along structural discontinuities (faults; Lefebvre, 1989) and permeable lithologies (coarser grained siliciclastic rocks and silicified carbonate rocks). Structural control on ore deposition was demonstrated for ore deposits located in the Domes region, the External fold-and-thrust belt, and in the Kundelungu foreland (e.g., Selley

et al., 2005; Haest et al., 2007; Turlin et al., 2016). Ore precipitated from an oxidizing brine (Fig. 1) when these fluids encountered a redox gradient, typically organic-rich rocks or at a hydrocarbon trap (Hitzman et al., 2012). A major sulphur source was present in the host rocks, i.e. within pyrite (FeS₂) and anhydrite (CaSO₄). Although historically most Cu-Co ore deposits have mainly been reported from specific members in the stratigraphic column and the External fold-and-thrust belt, several recent studies have indicated that base metal ores are in the whole Lufilian arc and its foreland and at several stratigraphic levels. In addition to typical Cu-Co ore deposits in the Lower Katangan Supergroup (Roan Group), ore deposits occur in the basement, the middle Katangan Supergroup (Kamoa deposit) and in the upper Katangan (Dikulushi deposit). Therefore, exploration has not been limited to specific units in the Katangan Supergroup in the fold-and-thrust belt, but extensive and successful exploration has been extended towards the whole Lufilian arc and its foreland. In addition to this large geographical distribution, the timing of mineralization spans a broad interval from diagenesis to post-orogenic (Hitzman et al., 2012), with reported Re-Os ages spanning 150 m.y. at one deposit (Kamoto, DRC; Saintilan et al., 2018) and possibly up to 300 m.y. (Mucchez et al., 2015).

- Annels, A.E., and Simmonds, J.R., 1984. Cobalt in the Zambian Copperbelt. *Precambrian Research*, 25, 75-98.
- Cailteux, J.L.H., Kampunzu, A.B., Lerouge, C., Kaputo, A.K., and Milesi, J.P., 2005. Genesis of sediment-hosted stratiform copper-cobalt deposits, Central African Copperbelt. *Journal of African Earth Sciences*, 42, 134-158.
- Capistrant, P.L., Hitzman, M.W., Wood, D., Kelly, N.M., Williams, G., Zimba, M., Kuiper, Y., Jack, D., and Stein, H., 2015. Geology of the Enterprise hydrothermal nickel deposit, North-Western Province, Zambia. *Economic Geology*, 110, 9-38.
- Davey, J., Roberts, S., and Wilkinson, J.J., 2021. Copper- and cobalt-rich, ultrapotassic bittern brines responsible for the formation of the Nkana-Mindola deposits, Zambian Copperbelt. *Geology*, 49, 341-345.
- El Desouky, H., Mucchez, Ph., and Cailteux, J., 2009. Two Cu-Co sulfide phases and contrasting fluid systems in the Katanga Copperbelt, Democratic Republic of Congo. *Ore Geology Reviews*, 36, 315-332.
- Haest, M., Mucchez, Ph., Dewaele, S., Franey N., and Tyler, R., 2007. Structural control on the Dikulushi Cu-Ag deposit, Katanga, Democratic Republic of Congo. *Economic Geology*, 102, 1321-1333.
- Hitzman, M.W., Broughton, D., Selley, D., Woodhead, J., Wood, D., and Bull, S., 2012. The Central African Copperbelt: diverse stratigraphic, structural, and temporal settings in the world's largest sedimentary copper district. In: Hedenquist, J.W., Harris, M., and Camus, F. (Eds.) *Geology and Genesis of Major Copper Deposits and Districts of the World: A Tribute to Richard H. Sillitoe*. Society of Economic Geologists Special Publication, 16, pp. 487-514.



Fig. 1. Reddening of the siliciclastic rocks below the Cu-Co mineralized Mines Subgroup at the Luiswishi deposit (DR Congo) due to the migration of an oxidizing fluid.

- Lefebvre, J.-J., 1989. Depositional environment of copper-cobalt mineralization in the Katangan sediments of southeast Shaba, Zaire. In: Boyle, R.W., Brown, A.C., Jefferson, C.W., Jowett, E.C., and Kirkham, R.V. (Eds.), *Sediment-Hosted Stratiform Copper Deposits*. Geological Association of Canada Special Paper, 36, pp. 401-426.
- Muchez, Ph., André-Mayer, A.-S., El Desouky, H.A., and Reisberg, L., 2015. Diagenetic origin of the stratiform Cu-Co deposit at Kamoto in the Central African Copperbelt. *Mineralium Deposita*, 50, 437-447.
- Saintilan, N.J., Selby, D., Creaser, R.A., and Dewaele, S., 2018. Sulphide Re-Os geochronology links orogenesis, salt and Cu-Co ores in the Central African Copperbelt. *Scientific Reports*, 2018, 8, 14946.
- Selley, D., Broughton, D., Scott, R., Hitzman, M.W., Bull, S., Large, R., McGoldrick, P., Croaker, M., and Pollington, N., 2005. A new look at the geology of the Zambian Copperbelt. In: Hedenquist, J.W., Thompson, J.F.H., Goldfarb, R.J., Richards, J.P., (Eds.) *Economic Geology 100th Anniversary Volume*, pp. 965-1000.
- Selley, D., Scott, R., Emsbo, P., Koziy, L., Hitzman, M.W., Bull, S.W., Duffet, M., Sebanzezi, S., Halpin, J., and Broughton, D., 2018. Structural configuration of the Central African Copperbelt: Roles of evaporites in structural evolution, basin hydrology, and ore location. In: Arribas, A.M, and Mauk, J. L. (Eds.), *Metals, Minerals, and Society*. Society of Economic Geologists Special Publication, 21, pp. 115-156.
- Turlin, F., Eglinger, A., Vanderhaeghe, O., André-Mayer, A.-S., Poujol, M., Mercadier, J., and Bartlett, R., 2016. Synmetamorphic Cu remobilization during the Pan-African orogeny: microstructural, petrological and geochronological data on the kyanite-micaschists hosting the Cu(U) Lumwana deposit in the Western Zambian Copperbelt of the Lufilian belt. *Ore Geology Reviews*, 75, 52-75.
- Van Wilderode, J., Debruyne, D., Torremans, D., Elburg, M.A., Vanhaecke, F., and Muchez, Ph., 2015. Metal sources for the Nkana and Konkola stratiform Cu-Co deposits (Zambian Copperbelt): Insights from Sr and Nd isotope ratios. *Ore Geology Reviews*, 67, 127-138.

An overview of the world class Mount Weld rare earth element deposit

P.L. Verplanck,^{1a}, A. Boehlke¹, H.A. Lowers,¹ and G. Bhat,²

¹ U.S. Geological Survey, Denver, Colorado, 80215, USA

² Lynas Rare Earths Ltd., Laverton, Australia

^a corresponding author: plv@usgs.gov

The Mount Weld rare earth element (REE) deposit in Western Australia is hosted in a lateritic sequence that reflects supergene enrichment of the underlying carbonatite complex. It is one of four giant, active REE mines associated with carbonatites and is the largest REE producer outside of China. The laterite is covered by 20 to 80 m of lacustrine and alluvial sedimentary rocks such that there is no surface expression of the mineralization. The deposit was discovered by drilling a large, circular magnetic anomaly identified in a 1966 regional airborne geophysical survey undertaken by the Australian Bureau of Mineral Resources. Magnetite from the carbonatite was dated at 205 ± 10 Ma by the Re-Os method (Graham, 2004), but the age of laterization is poorly constrained.

Similar to other carbonatite-related ore deposits, ore from Mount Weld displays extreme light REE (LREE) enrichment but contains substantially higher concentrations of heavy REEs (HREEs; Fig. 1). Note that the three other carbonatite-related REE deposits mine the carbonatite body. At Mount Weld, secondary REE-bearing phosphate minerals are the primary REE-host phases in the laterite ore, with monazite as the predominant phase. Other REE-bearing phases include cerianite, churchite, florencite, and crandallite subgroup minerals. Monazite is typically fine grained and can occur as pseudomorphs after apatite and rhabdophane. Analysis of older drill core samples of the underlying carbonatite show that the carbonatite is either calcite- or dolomite-rich, with minor magnetite, apatite, olivine, biotite, pyrite, and pyrochlore. REE enrichment in the laterite is controlled by the breakdown of primary minerals, the release and transport of REEs, and the formation of secondary minerals. Profiles through the laterite show that in the REE-rich zone, apatite and primary calcite have completely broken down and dolomite decreases by approximately 60-100%, such that the loss of Ca and Mg, as well as Si and K, leads to a relative increase in the REEs. Sequestering of REEs in secondary mineral phases formed from groundwater further enhances the REE concentration. The substantial increase in HREEs compared to other carbonatites suggests that solution chemistry plays an important role in the fate and transport of the REEs.

With the projected increase in near-term demand for REEs, especially REEs used in magnets, Lynas Corporation has begun efforts to increase production. In the fall of 2020, Lynas Corp drilled 2 boreholes at the base of the current open pit and encountered fresh carbonatite containing REE fluorocarbonate minerals (parisite and bastnaesite) and monazite hosted in an ankerite-bearing carbonatite. This carbonatite unit has not been previously identified at Mount Weld. In addition to work on-site, planning for a new REE processing plant at Kalgoorlie (250 km west of the deposit) is underway, the plant will be for cracking and leaching the concentrate from the Mount Weld mine. In 2020, the U.S. Department of Defense awarded Lynas

Corp, and their partner Blue Line Corp, \$30 million towards construction of a heavy rare earth separation facility in Texas.

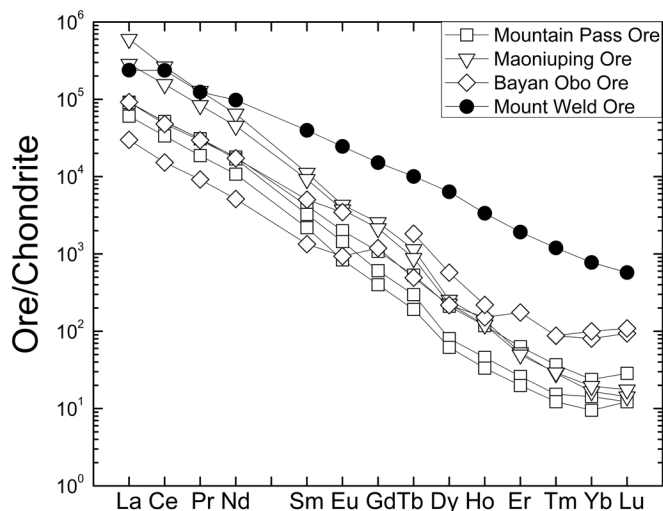


Fig. 1. Chondrite-normalized rare earth element diagram for ore samples from the four giant REE mines. Data from Verplanck et al. (2016) and Lai et al. (2012). Data normalized to chondrite values of Anders and Ebihara (1982).

Anders, E., and Ebihara, M., 1982. Solar-system abundances of the elements. *Geochimica et Cosmochimica Acta*, 46, pp. 2363-2280.

Lai, X., Yang, X., and Sun, W., 2012. Geochemical constraints on genesis of dolomite marble in the Bayan Obo REE-Nb-Fe deposit, Inner Mongolia: Implications for REE mineralization. *Journal of Asian Earth Sciences*, 64, pp. 90-102.

Verplanck, P.L., Mariano, A.N., and Mariano, A.N. Jr, 2016. Rare earth element ore geology of carbonatites. In: Verplanck, P.L., and Hitzman, M.W., (Eds.), *Rare Earth and Critical Elements in Ore Deposits*. Society of Economic Geologists Reviews in Economic Geology, 18, pp. 5-32.

African lithium pegmatites

Kathryn Goodenough¹, Richard Shaw², Paul Nex³, Eimear Deady¹ and Judith Kinnaird³

¹ British Geological Survey, Edinburgh EH14 7LT, UK

² British Geological Survey, Nicker Hill, Keyworth NG12 5GG, UK

³ University of the Witwatersrand, Johannesburg, South Africa

^a corresponding author: kmgo@bgs.ac.uk

The importance of lithium for the clean energy transition, because of its use in lithium-ion batteries for electric vehicles and energy storage, means that demand is expected to rise substantially in the coming years. Currently, lithium is mined from two types of sources: brines, in the salt lakes of the Andes; and lithium pegmatites, predominantly mined in Australia. Increasing demand for lithium is expected to drive significant growth in the number, range of deposit types and geographic diversity of producing lithium mines.

Extensive lithium pegmatites occur in many African countries (Fig.1). These pegmatites are coarse-grained, roughly tabular igneous intrusions that may be tens to hundreds of metres thick, and extend laterally for hundreds of metres to kilometres. They commonly occur in stacks or swarms, so a single deposit may contain a number of individual pegmatite bodies. Such pegmatites may be enriched in lithium, cesium, tantalum and tin (Melcher et al., 2017), and some – but not all – are distinctively zoned. They typically have complex mineralogy and textures,

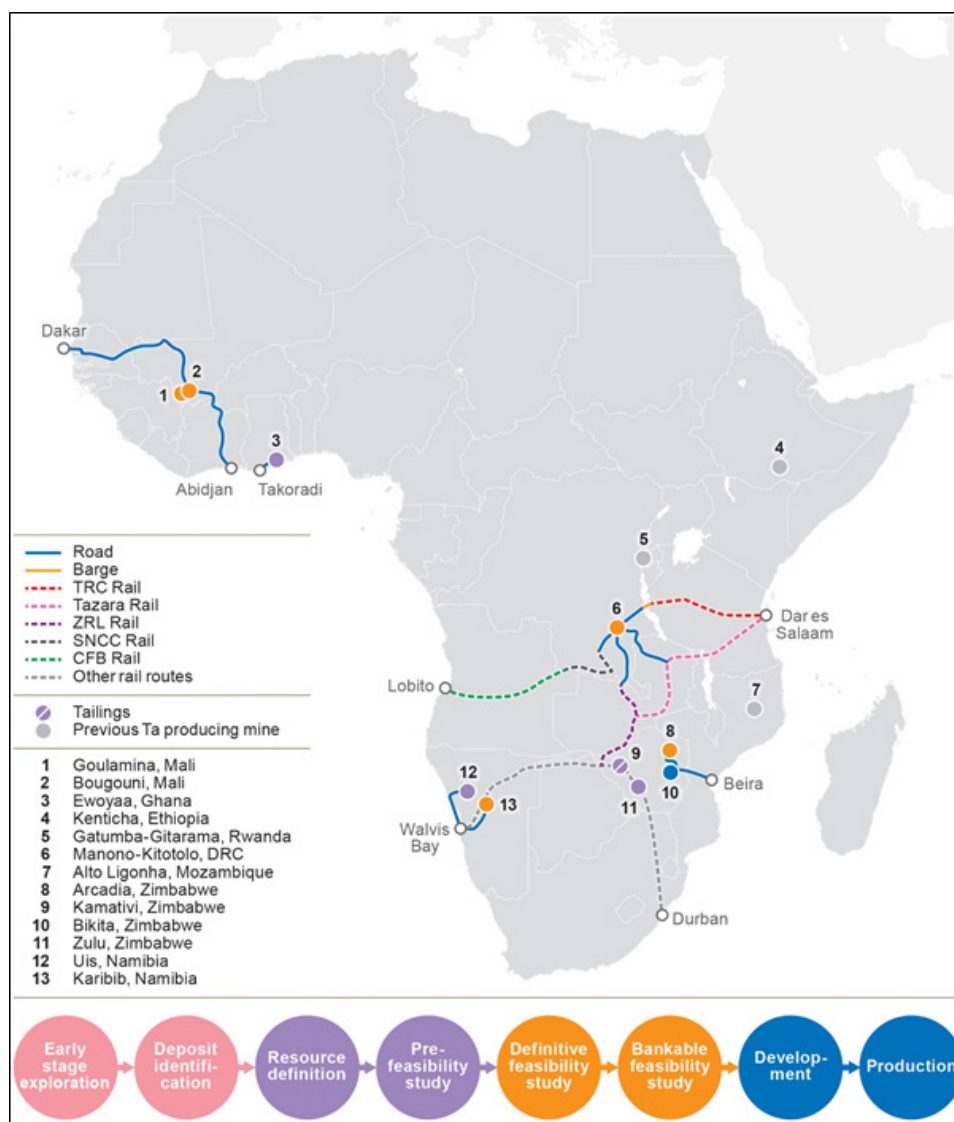


Fig. 1. Map of Africa showing the main lithium pegmatite resources, and relevant road, rail, and port infrastructure. Circles indicating the localities are coloured by the lithium exploration phase that has been reached as per the timeline. Map outline © ESRI; map from Goodenough et al. (2021).

and show evidence of the magmatic-hydrothermal transition, with primary minerals replaced by later assemblages.

Only one mine in Africa has consistently produced lithium in recent years: Bikita in Zimbabwe. However, Zimbabwe has very extensive lithium pegmatites in addition to Bikita, including Arcadia and Zulu within the Archaean craton, and Kamativi in the Proterozoic mobile belt of NW Zimbabwe. A few other lithium pegmatite occurrences have been recorded in African Archaean cratons, most notably at Vredefort in South Africa (Rajesh et al., 2020), but few have been studied in detail. In West Africa, the major lithium pegmatites are Paleoproterozoic, and associated with the Birimian orogen; the best-explored examples are in Mali and Ghana. Mesoproterozoic lithium pegmatites are well-known in Central Africa, particularly the major Manono-Kitotolo pegmatites in the DRC (Dewaele et al., 2016), and examples of a similar age also occur at Kamativi in Zimbabwe and in Namaqualand on the South Africa-Namibia border (Ballouard et al., 2020). The last major episode of lithium pegmatite formation occurred in association with the Pan-African orogenic events and is exemplified by the pegmatites in the Damara Belt of Namibia.

We have recently established a four-stage paragenesis for the Kamativi pegmatite of Zimbabwe (Shaw et al., in press). Stage 1, magmatic crystallisation, includes the formation of lithium minerals such as spodumene; stage 2, albitisation, involves partial replacement of stage 1 assemblages by quartz-albite intergrowths with the introduction of cassiterite and columbite group minerals (CGMs); stage 3, greisenisation, is demonstrated by quartz and muscovite replacing earlier minerals, with continued cassiterite and CGM growth; and stage 4 is a lower-temperature alteration leading to the formation of cookeite, sericite, analcime and apatite. Our ongoing work, combined with review of published literature, shows that a similar paragenesis applies for many African lithium pegmatites, but with different stages being variably dominant, and with differing lithium minerals. For example, petalite is a major lithium mineral in the Archaean pegmatites of Zimbabwe, where it is formed in stage 1, and is also present in the pan-African pegmatites of Namibia. Stage 3 appears to be less significant in the Paleoproterozoic pegmatites of West Africa (Wilde et al., 2021) but very significant in some Central African examples (Hulsbosch and Muchez, 2020).

Understanding the mineralogy and paragenesis of lithium pegmatites is a critical step in the development of the lithium supply chain in Africa, as it underpins the mineral processing steps that are essential for any mine. Worldwide, spodumene is the main mineral currently processed for chemicals of the purity required for batteries. Although there has been substantial research into processing of other minerals, petalite is most typically used in the ceramics industries, and lepidolite is not yet processed at a commercial scale. Thus, although many of the lithium pegmatites described above have been explored to an advanced stage, none are currently producing lithium for the battery supply chain (Goodenough et al., 2021). In recent years petalite concentrate produced at Bikita and Arcadia in Zimbabwe, and lepidolite concentrate from the Karibib pegmatite project in Namibia, have been exported for further processing and refining. There is clear potential for Africa's lithium resources to make an important economic contribution, but this should be placed in the context of the wider supply

chain; in particular, the potential for regional cooperation on mineral processing, refining, and production of lithium chemicals deserves further consideration.

- Ballouard, C., Elburg, M. A., Tappe, S., Reinke, C., Ueckermann, H. and Daggart, S., 2020. Magmatic-hydrothermal evolution of rare metal pegmatites from the Mesoproterozoic Orange River pegmatite belt (Namaqualand, South Africa). *Ore Geology Reviews*, 116, 103252.
<https://doi.org/10.1016/j.oregeorev.2019.103252>
- Dewaele, S., Hulsbosch, N., Cryns, Y., Boyce, A., Burgess, R. and Muchez, P., 2016. Geological setting and timing of the world-class Sn, Nb-Ta and Li mineralization of Manono-Kitotolo (Katanga, Democratic Republic of Congo). *Ore Geology Reviews*, 72, 373-390.
<https://doi.org/10.1016/j.oregeorev.2015.07.004>
- Goodenough, K. M., Deady, E. A. and Shaw, R. A., 2021. Lithium resources, and their potential to support battery supply chains, in Africa. *British Geological Survey, Keyworth, Nottingham*.
<http://nora.nerc.ac.uk/id/eprint/530698/>
- Hulsbosch, N. and Muchez, P., 2020. Tracing fluid saturation evolution and multiphase cassiterite mineralisation of the Gatumba pegmatite dyke system (NW Rwanda). *Lithos*, 354-355, 105285.
<https://doi.org/10.1016/j.lithos.2019.105285>
- Melcher, F., Graupner, T., Gäbler, H.-E., Sitnikova, M., Oberthür, T., Gerdes, A., Badanina, E. and Chudy, T., 2017. Mineralogical and chemical evolution of tantalum-(niobium-tin) mineralisation in pegmatites and granites. Part 2: Worldwide examples (excluding Africa) and an overview of global metallogenetic patterns. *Ore Geology Reviews*, 89, 946-987.
<https://doi.org/10.1016/j.oregeorev.2016.03.014>
- Rajesh, H. M., Knoper, M. W., Belyanin, G. A., Safonov, O. G. and Schmidt, C., 2020. Petalite postdating spodumene in pegmatite as a consequence of the ~2.02 Ga meteorite impact in the Vredefort structure, southern Africa. *Lithos*, 376-377, 105760.
<https://doi.org/10.1016/j.lithos.2020.105760>
- Shaw, R. A., Goodenough, K. M., Deady, E. A., Nex, P., Ruzvidzo, B., Rushton, J. and Mounteney, I., in press. The magmatic-hydrothermal transition in lithium pegmatites: petrographic and geochemical characteristics of pegmatites from the Kamativi area, Zimbabwe. *Canadian Mineralogist*.
- Wilde, A., Otto, A. and McCracken, S., 2021. Geology of the Goulamina spodumene pegmatite field, Mali. *Ore Geology Reviews*, 134, 104162.
<https://doi.org/10.1016/j.oregeorev.2021.104162>

Session 4: Selected critical mineral deposits I

Wednesday November 17, 16:30 PST (0:30 GMT)

List of speakers

Chair: Evan Orovan, British Columbia Geological Survey and Centre of Ore Deposit and Earth Sciences, University of Tasmania

Marcus Haynes, Geoscience Australia
The potential for critical minerals: Australia's contribution to the global supply chain

Helen Degeling, Geological Survey of Queensland
Strategic resources and the new economy: Queensland's critical mineral potential

Vladimir Lisitsin, Geological Survey of Queensland
Critical minerals in traditional deposit types in the Mount Isa region, Queensland, Australia

Carl Spandler, Department of Earth Sciences, University of Adelaide
Unconformity-related REE deposits of the Browns Range, Australia

Evan Orovan, British Columbia Geological Survey and Centre of Ore Deposit and Earth Sciences, University of Tasmania
The Trial Harbour Ni skarn, Zeehan mineral field, western Tasmania

Michael G. Gadd, Geological Survey of Canada
Critical minerals in Paleozoic hyper-enriched black shales

Question and answer period

The potential for critical minerals: Australia's contribution to the global supply chain

Marcus Haynes^{1a}, Zhehan Weng¹, David Huston¹, Stuart Walsh²

¹ Geoscience Australia, Canberra, ACT 2609, Australia

² Monash University, Melbourne, VIC 3800, Australia

^a corresponding author: marcus.haynes@ga.gov.au

To date, Australian interest in mineral criticality has largely focused on the critical minerals of other nations and on the opportunities for Australia to act as a supplier of these commodities (Skirrow et al., 2013; Mudd et al., 2018). The Exploring for the Future program is positioning Australia as a reliable and responsible supplier of critical minerals by identifying new opportunities for mineral supply. To realize these opportunities, Australia needs to do more than identify what minerals are critical, but also to understand the drivers of criticality and how to optimally facilitate supply. These are complex issues, involving international supply chains and market forces (e.g., Emsbo et al., 2021), but – within the sphere of influence of a Government geological survey – they touch on endowment, geological prospectivity, and economic and regulatory policy settings. Here, we analyze the above factors to outline the primary controls on realizing the potential critical mineral ventures, and of how these vary regionally. We focus principally on two aspects of the problem: critical mineral endowment analysis and prediction, and economic potential appraisal.

One of the main challenges in analyzing critical mineral potential is the absence of data on their endowment. Geoscience Australia's Mineral Potential Mapper tool (accessible on Geoscience Australia's portal; <https://portal.ga.gov.au>) has been successful in driving exploration for major commodities and, implicitly, their associated critical minerals. However, more work is needed to map specific critical mineral prospectivity. Data sets of ore geochemistry have enabled predicting critical mineral endowment in ores and tailings, where data might otherwise be difficult to collect (Huston and Brauhart, 2017). This is a coarse approximation but does facilitate new research questions and enables prioritizing strategic targets for follow-up study. The work of the Critical Minerals Mapping Initiative (CMMI) facilitates extensions to the framework for these approaches. Combining the international Critical Minerals in Ores dataset (Champion et al., 2021) with data from industry reports we can reappraise the critical mineral production opportunities around known deposits. For example, examination of the cobalt to nickel ratio in different types of nickel deposits in Australia reveals cobalt-potential of lateritic-

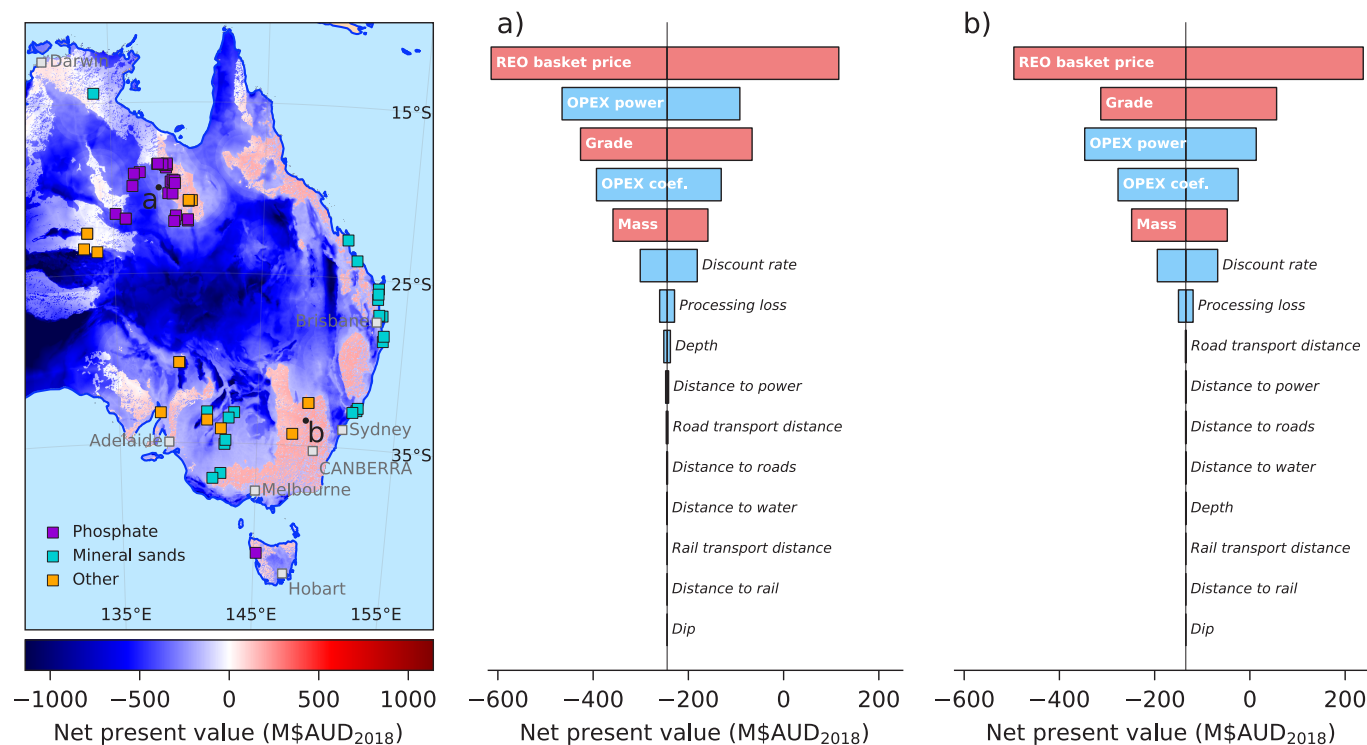


Fig 1. Economic modelling of a hypothetical rare-earth element deposit across eastern Australia. Left, net present value as a function of spatial location (i.e., subject to the distribution of infrastructure and sedimentary cover), overlain by the locations of mines and deposits for potential rare-earth element mineral systems including sedimentary phosphate, heavy mineral sands, and others (e.g., alkaline intrusives apatite/fluorite veins, skarn). Centre and right, sensitivity of net present value at locations **a)** and **b)** to changes in the model input parameters. Parameters are ranked by the magnitude of their impact on the model. Red bars reflect positive correlation; blue bars reflect negative correlation.

nickel deposits (ratio of 0.102) that are about double that of komatiite-hosted nickel sulphide deposits (ratio of 0.053). These results warrant rethinking the economic potential from Australia's laterite endowments.

To illustrate the analysis of economic potential for critical mineral developments in Australia, we calculate an ensemble of models for rare-earth oxide deposits across eastern Australia. Despite present limited production, Australia has identified geological potential for rare-earth element deposits covering multiple different mineral systems (Hoatson et al., 2011). Our economic modelling is undertaken using the open-source Bluecap software (Walsh et al., 2020), accessible via GitHub (<https://github.com/GeoscienceAustralia/bluecap>) and through the Economic Fairways Mapper tool on Geoscience Australia's portal. The Economic Fairways Mapper combines large-scale infrastructure and geological datasets to evaluate the mining, processing, administrative, and infrastructure expenses of mining operations across Australia (e.g., Haynes et al., 2020). Crucially, in examining these systems, we have recognised a paucity of data on which to calibrate capital and operational expenditure cost functions, particularly for critical minerals. Nevertheless, sensitivity and uncertainty analysis can provide insights into the opportunities and challenges facing the development of these deposits (Fig. 1). The above tools and analysis methods provide a unique perspective to understand how geological potential, research and policy settings can influence critical mineral supply.

Geoscience Australia acknowledges all landholders, communities, and traditional custodians who have supported our work in rural, regional, and remote Australia to deliver this work. This work is undertaken under the Exploring for the Future program funded by the Australian government. This abstract is published with the permission of the CEO of Geoscience Australia.

Champion, D., Raymond, O., Huston, D., Van Der Wielen, S., Sexton, M., Bastrakov, E., Schroder, I., Butcher, G., Hawkins, S., Lane, J., McAlpine, S., Czarnota, K., Britt, A., Granitto, M., Hofstra, A., Kreiner, D., Emsbo, P., Kelley, K., Wang, B., Case, G., Graham, G., Lauzière, K., Lawley, C., Gadd, M., Pilote, J-L., Létourneau, F., Lisitsin, V., and Haji Egeh, A., 2021. Critical Minerals in Ores - geochemistry database. Geoscience Australia, Canberra.

<http://pid.geoscience.gov.au/dataset/ga/145496>

Emsbo, P., Lawley, C., and Czarnota, K., 2021. Geological surveys unite to improve critical mineral security. *Eos*, 102.

<https://doi.org/10.1029/2021EO154252>

Haynes, M.W., Walsh, S.D.C., Czarnota, K., Northey, S.A., and Yellishetty, M., 2020. Economic fairways assessments across Northern Australia. Geoscience Australia, Canberra.

<http://dx.doi.org/10.11636/133681>

Hoatson, D.M., Jaireth, S., and Mieztis, Y., 2011. The major rare-earth-element deposits of Australia: geological setting, exploration, and resources. Geoscience Australia, Canberra.

Huston, D.L. and Brauhart, C.W., 2017. Critical commodities in Australia - An assessment of extraction potential from ores. Record 2017/014. Geoscience Australia, Canberra.

<http://dx.doi.org/10.11636/Record.2017.014>

Mudd, G.M., Werner, T.T., Weng, Z.-H., Yellishetty, M., Yuan, Y., McAlpine, S.R.B., Skirrow, R.G., and Czarnota, K., 2019. Critical minerals in Australia: A review of opportunities and research needs. Record 2018/051. Geoscience Australia, Canberra.

<http://dx.doi.org/10.11636/Record.2018.051>

Skirrow, R.G., Huston, D.L., Mernagh, T.P., Thorne, J.P., Dulfer, H., and Senior, A., 2013. Critical commodities for a high-tech world: Australia's potential to supply global demand. Geoscience Australia, Canberra.

<http://pid.geoscience.gov.au/dataset/ga/76526>

Walsh, S.D.C., Northey, S.A., Huston, D., Yellishetty, M., and Czarnota, K., 2020. Bluecap: A geospatial model to assess regional economic-viability for mineral resource development. *Resources Policy*, 66, 101598.

<https://doi.org/10.1016/j.resourpol.2020.101598>

Strategic resources and the new economy: Queensland’s critical mineral potential

Helen Degeling^{1a}

¹ Geological Survey of Queensland, Brisbane, QLD 4000, Australia

^a helen.degeling@resources.qld.gov.au

The new economy is the ecosystem of changes required for the energy transition away from carbon-emitting fuels towards electrified technology and battery energy storage. The term ‘new economy’ acknowledges the economic, policy, and community sentiment transitions that accompany these changes. It also embraces concepts of the circular economy, in which waste has inherent value and is constantly recycled. Building strength, volume, circularity, and sustainability into the new aspects of an industry traditionally driven purely by market demand and focused on conventional base and precious metals requires government support and leadership.

The Queensland Government’s New Economy Minerals Initiative aims to support the growth and development of the

critical minerals industry in our state. In Queensland, critical mineral endowment is dominated by copper, cobalt, silver, tin, tungsten, indium and rare earth elements (Fig. 1). Whilst there are abundant known resources as well as significant exploration upside for these minerals, one of the greatest opportunities lies in the re-assessment of historical mine waste, including tailings. This form of ‘secondary prospectivity’ represents a strategic opportunity to obtain value from an otherwise worthless liability, remediate existing environmental problems (e.g., acid-forming waste) and satisfy circular economy principles that are becoming increasingly embedded in forward-thinking policy.

Some of Queensland’s largest cobalt resources, for example, lie in the tailings dams and mine waste of world-class copper

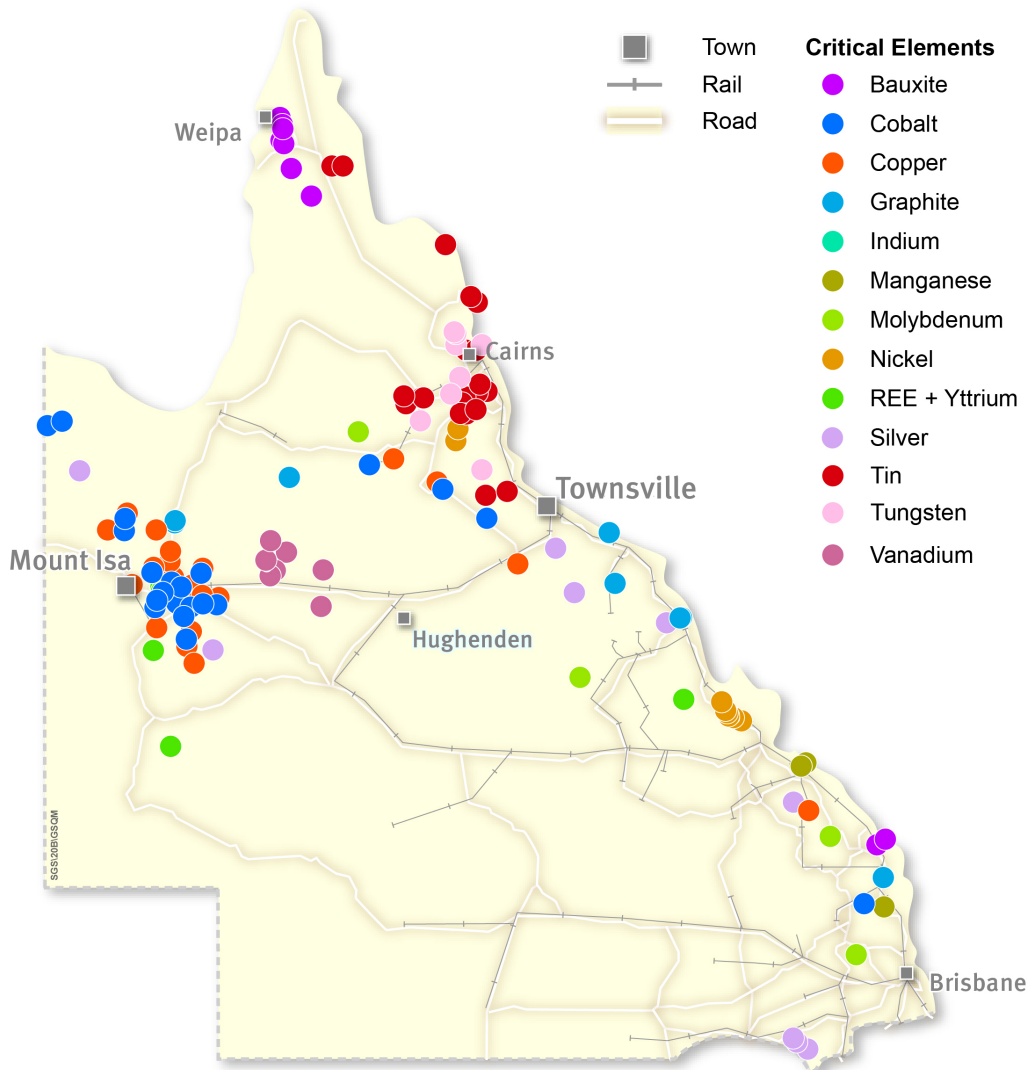


Fig. 1. Location of critical mineral deposits and mineral occurrences throughout Queensland.

mines such as the Mt. Isa mine. Innovative research and partnership, including with the University of Queensland and the Japan Oil, Gas and Metals National Corporation (JOGMEC), is examining this opportunity to introduce circular economy principles, and develop new understanding for the efficient extraction of cobalt from pyrite. Key sites of interest include the Capricorn Copper mine and the Rocklands copper mine. Some companies in Queensland are already exploiting mine waste as a resource, including New Century at the Century zinc mine, and EQ Resources at the Mt. Carbine tungsten mine. However, these examples pursue only the primary commodity of the original operation. Our research addresses critical, or new economy minerals that may have been ignored by the original operators, such as cobalt associated with copper, rare earth elements in phosphorite, and indium with tin.

The Queensland Department of Resources, in collaboration with the Sustainable Minerals Institute at the University of Queensland and Geoscience Australia, aims to produce an inventory of critical mineral potential in significant sites of mine waste across Queensland. The inventory will include mineralogical and deportment analysis to inform a preliminary understanding of metallurgical challenges and solutions in each case.

To date, 17 sites have been sampled and characterized for critical mineral potential since early 2020. These sites demonstrate secondary prospectivity for copper, cobalt, indium, tin, tungsten, and rare earths. They demonstrate clearly that our first step when it comes to critical minerals, is to understand what we already have but might have missed or overlooked.

Further to the critical mineral challenge is transitioning government agencies, such as geological surveys, to take a whole ‘ecosystem’ view, rather than just the pure geology and research feeding into the traditional exploration style. This approach compartmentalizes each component of the ecosystem, or step of the supply chain, such that no one agency has a view of the whole within their jurisdiction.

Processing and extraction challenges (including geopolitical monopolies) affect the attractiveness of a product on the international market, and therefore impact appetite for exploration. The ESG credentials of a company (or chain of companies), from greenfields exploration all the way through to production, manufacturing and export, is being examined and made visible in ways never before experienced by the resources sector. Sustainable processing research, traceability trials, domestic battery manufacture; these are all factors that must be considered in parallel with traditional geological mapping and prospectivity analysis.

Each of these activities stimulates interest from industry, investors, community, and downstream manufacturers. Without a path to market, there is no point exploring, and so an entire ‘ecosystem’ view, is a key component for government, and geological surveys, to consider when supporting the burgeoning critical minerals industry. Anything less is setting up the new economy to fail.

Critical minerals in traditional deposit types in the Mount Isa region, Queensland, Australia

Vladimir Lisitsin^{1a} and Courtney Dhnaram¹

¹Geological Survey of Queensland, Brisbane QLD 4000, Australia

^a corresponding author: vladimir.lisitsin@dnrm.qld.gov.au

The Mount Isa Province in northwest Queensland (Fig. 1) is well known for its world-class base metal, silver, and phosphate deposits of several distinct types including: Proterozoic Iron Oxide Copper-Gold (IOCG); orogenic copper (sediment-hosted copper); siliciclastic-carbonate (SEDEX) Zn-Pb-Ag; siliciclastic-mafic (Broken Hill-type) Pb-Ag-Zn; and Cambrian phosphorites (terminology of Hofstra et al., 2021). In addition to ‘traditional’ main commodities and

common by-products, deposits of these types are also known to contain significantly elevated concentrations of several critical minerals that could potentially be economic by-products (Huston and Brauhart, 2017). However, there are limited publicly available geochemical data to adequately characterize the economic significance of traditional deposit types in the region as potential sources of critical commodities. Geological Survey of Queensland (Australia) has undertaken a program

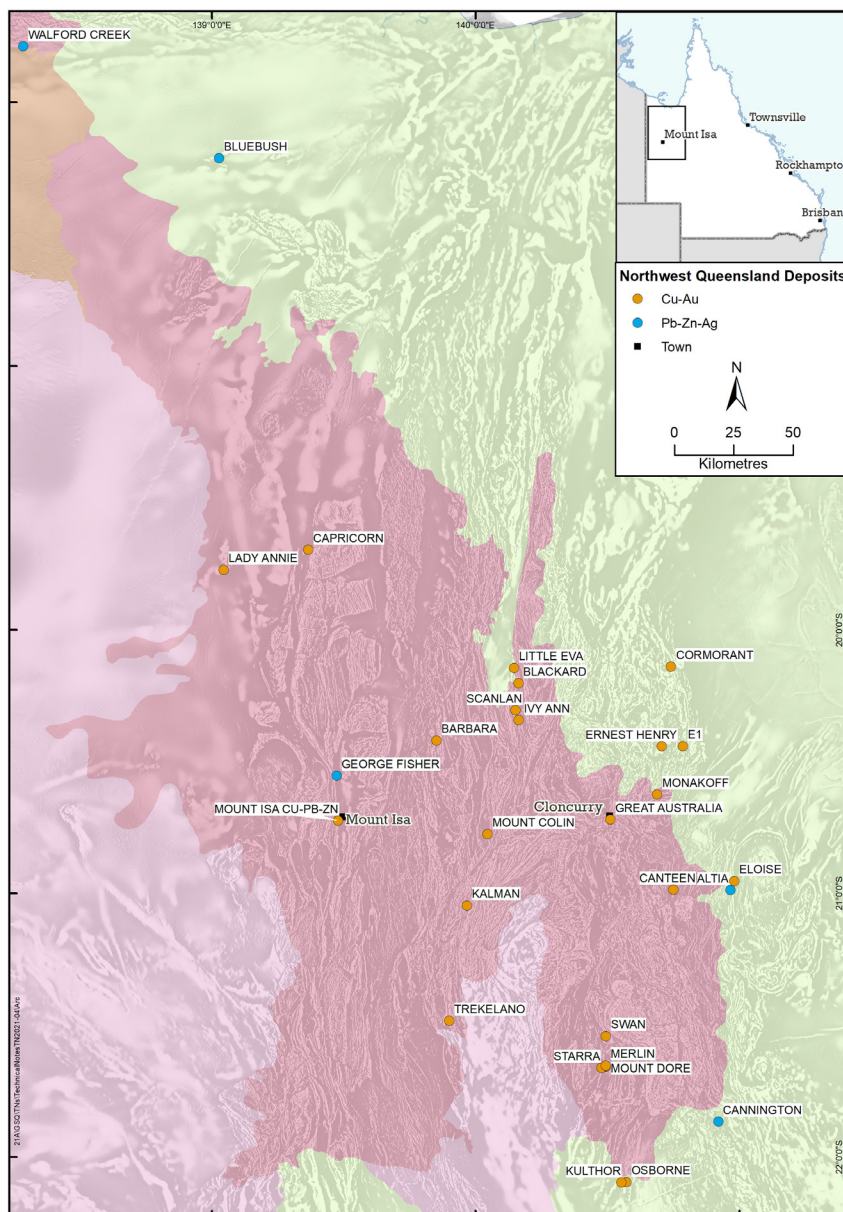


Fig. 1. Copper-gold and lead-zinc-silver deposits within the Mount Isa Province investigated as part of this study.

of systematic geochemical and mineralogical characterization of key deposit types in the Mount Isa Province to assess their endowment of critical minerals.

The program encompassed: targeted systematic acquisition of representative drill core and ore samples from multiple deposits of different geological types; continuous hyperspectral and XRF scanning of drill core; and comprehensive multi-element geochemistry on multiple samples (20-200) from each deposit. Major- and trace-element geochemistry (up to 67 elements) used a combination of industry-standard digestion methods and analytical techniques: four-acid digestion and ICP-MS/OES (48 elements); lithium metaborate fusion and ICP-MS/OES (31 elements); fire assay and ICP-MS (Au, Pt, Pd); Leco furnace (C, S); KOH fusion - ion chromatography (F); Aqua regia-ICP-MS (Hg, Se, Te); and specialized HNO₃-HF digestion with orthophosphoric acid leach and ICP-MS finish (Ge). QA/QC procedures (in addition to those undertaken by a major reputable accredited commercial laboratory) included routine use of: matrix-matched Certified Reference Materials (at least 1 per 20 samples) and field duplicates; and barren quartz 'washing' of crushing and pulverising equipment after each sample (to minimize cross-sample contamination).

Copper-gold mineralization in most IOCG deposits, characterised by complexity and variability of geochemical signatures between individual deposits, is significantly enriched in one or more critical minerals. Average concentrations of cobalt are commonly in the 300–800 ppm range, locally with higher grades (0.1–0.2% Co) in individual samples and mineralized zones. Rhenium is strongly enriched only in some Mo-rich IOCG and affiliated deposits (such as Merlin and Kalman, where average grades exceed 3 ppm Re and locally >30 ppm). REEs (mostly light, i.e., La, Ce) are significantly enriched in parts of only several IOCG deposits in the region and rarely exceed bulk concentrations of >1,000 ppm total REE.

Cobalt is also significantly enriched in parts of sediment-hosted ('orogenic') copper deposits in the western Mount Isa Province (Mount Isa Copper, Capricorn Copper, Mount Oxide, Lady Annie, Walford Creek), where concentrations in copper mineralization are commonly in the 100–1,000 ppm Co range, with individual samples and cobalt-rich zones of some deposits reaching 0.15–0.2% Co.

Major siliciclastic-carbonate (SEDEX) Zn-Pb-Ag deposits in the western Mount Isa Province (Mount Isa Zn-Pb, Hilton) have a common geochemical signature of enriched Pb-Ag-Cd-Zn-Tl-Sb-As and contain elevated Ge. Germanium concentrations in Zn mineralization are commonly 10–20 ppm Ge, locally exceeding 40 ppm Ge in individual samples.

Major Cambrian phosphorite deposits of the Georgina Basin typically contain 300-800 ppm TREE (up to 2,000 ppm in some deposits) in fresh phosphorite, with notable relative enrichment of mid- to heavy- REE (HREE/LREE = 1). Crandalite-rich products of surface weathering of phosphorites are characterised by significant further REE enrichment, with >1% total REE identified in individual highly weathered samples.

Hofstra, A., Lisitsin, V., Corriveau, L., Paradis, S., Peter, J., Lauzière, K., Lawley, C., Gadd, M., Pilote, J., Honsberger, I., Bastrakov, E., Champion, D., Czarnota, K., Doublier, M., Huston, D., Raymond, O., VanDerWielen, S., Emsbo, P., Granitto, M., and Kreiner, D., 2021. Deposit classification scheme for the Critical Minerals Mapping Initiative Global Geochemical Database: U.S. Geological Survey Open-File Report 2021–1049, 60p.

<https://doi.org/10.3133/ofr20211049>

Huston, D. L., and Brauhart, C. 2017. Critical commodities in Australia: an assessment of extraction potential from ores. Record 2017/14, 34p. Geoscience Australia, Canberra.

<http://dx.doi.org/10.11636/Record.2017.014>

Unconformity-related REE deposits of the Browns Range, Australia

Carl Spandler^{1a}, Teimoor Nazari-Dehkordi², Nicholas H.S. Oliver³, and Jessica Walsh¹

^{1a} Australian Critical Minerals Research Centre, The University of Adelaide, South Australia

² Department of Geology, University of Johannesburg, Johannesburg, South Africa

³ HCOVGlobal Consultants, QLD 4812, Australia

^a corresponding author: carl.spandler@adelaide.edu.au

The imperative for diversity of supply of rare earth elements (REE) is driving exploration for new styles of mineralization across the globe. This is particularly relevant to heavy REEs for which there are few alternative sources outside of China. We document a new heavy REE ore style found in Western Australia, but which may have global distribution. The heavy REE mineralization is hosted in metasedimentary rocks as numerous orebodies of variable size and grade distributed across a large district of northwestern Australia (Fig. 1a). The focus of mining and exploration activity has been in the Browns Range Dome (Fig. 1b, c) where a total mineral resource of 9.26 Mt at

0.67 % total rare earth oxides has been defined. The orebodies are mainly close to a regional unconformity between Archean Browns Range Metamorphics (arkosic metasedimentary rocks) and overlying Proterozoic sandstones of the Birrindudu Group. The orebodies consist predominantly of xenotime [(Y,HREE)PO₄] plus quartz with minor florencite [LREEAl₃(PO₄)₂(OH)₆], and occur along steeply dipping structures in a stockwork of hydrothermal veins and breccias.

In-situ U-Pb dating of xenotime from several deposits/prospects yielded an age range for mineralization of 1.65 to 1.60 Ga. This timeframe has no local coeval magmatism or

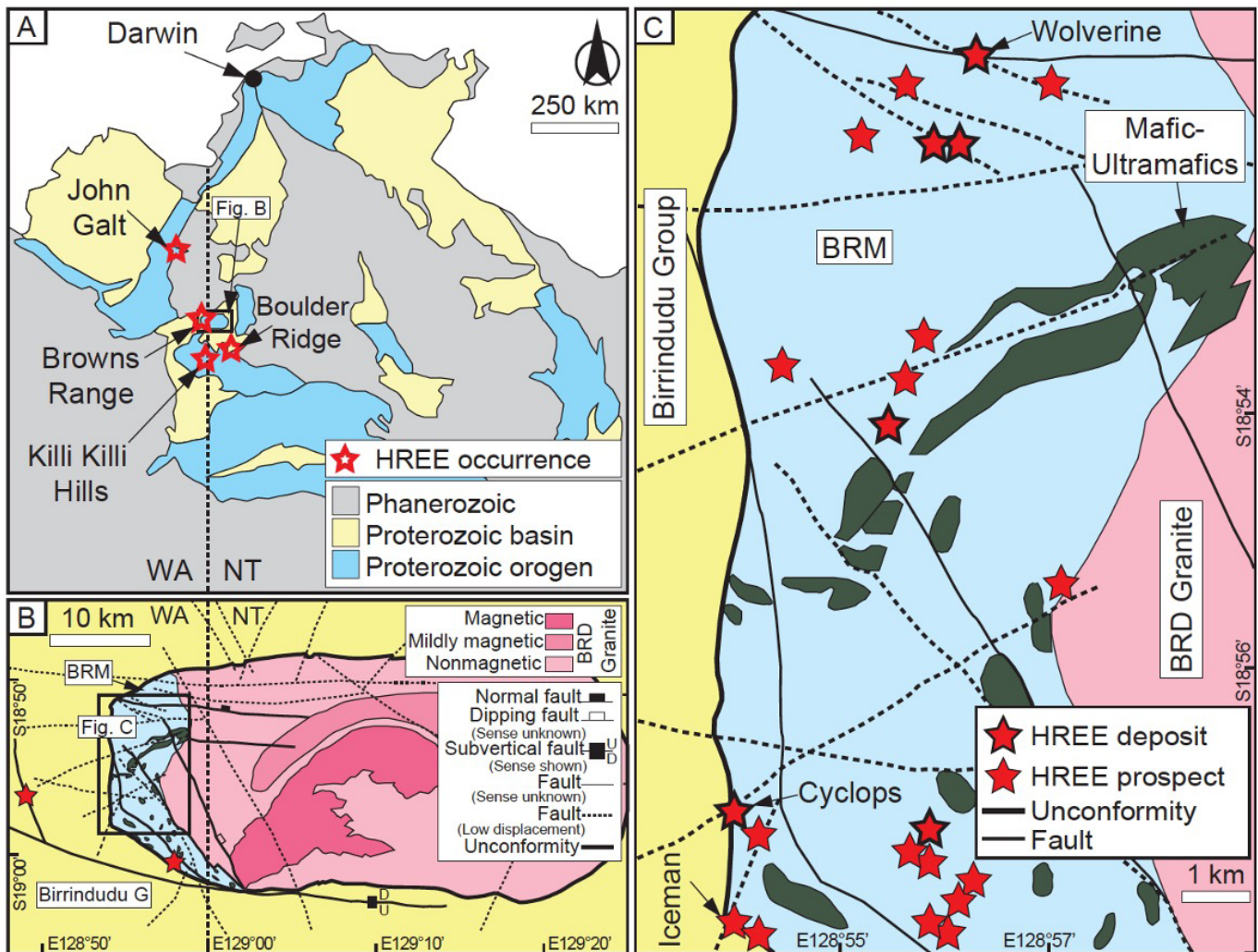


Fig. 1. a) Location of the HREE deposits and prospects in NW Australia. b) Geology of the Browns Range Dome. c) HREE deposits and prospects in the western part of the Browns Range Dome. BRM = Browns Range Metamorphics. Note, the boundary between the BRM and Birrindudu Group sedimentary rocks is a regional unconformity.

orogeny and is significantly younger than the ca. 1.8 to 1.72 Ga local metamorphism. The mineralization does, however, coincide with distal continental collision events with the North Australian Craton, including the initiation of the Isan Orogeny and Liebig Orogeny along the eastern and southern margins of the craton. Far-field stresses from these events are invoked as drivers of large-scale fluid flow and fault (re)activation in the region.

Samples of the Browns Range Metamorphics are variably depleted in heavy REE compared to typical sedimentary protoliths and also have non-radiogenic Nd isotope compositions that are comparable to the orebodies, but quite distinct from the igneous rocks or other sedimentary rocks (Birrindudu Group) across the North Australian Craton. These observations demonstrate that the ore metals were derived directly from the Browns Range Metamorphics. Based on mineralogical, geochemical, and fluid inclusion data, we propose that H₂O-CaCl₂-NaCl (up to 25 wt.% salinity) fluids leached REE from the Browns Range Metamorphics, and subsequently mixed with P-bearing acidic fluids in fault zones, especially near the unconformity between the Browns Range Metamorphics and overlying Birrindudu Group sandstones. Mixing of these fluids led to REE mineral precipitation and ore formation.

This style of REE mineralization is unlike any other known REE ore style and herein we refer such deposits as 'unconformity-related REE'. The closest analogue to this ore style globally is the Maw zone, which formed in a very similar geological setting in the Athabasca Basin, Canada. There is great potential for further unconformity-related REE deposits to be found in intracontinental basins close to regional unconformities between Archean basement rocks and overlying Proterozoic sedimentary sequences. Our ongoing research is examining the geological conditions required to form this ore style, and particularly, the role of Archean detrital zircons in basement metasedimentary rocks as sources of REE (and P?) for mineralization.

The Trial Harbour Ni skarn, Zeehan mineral field, western Tasmania

Evan A. Orovan^{1,2a}, Emmet O'Keefe¹, Lejun Zhang¹, and David R. Cooke¹

¹ ARC Research Hub for Transforming the Mining Value Chain (TMVC), Centre of Ore Deposit and Earth Sciences, University of Tasmania, Tasmania, Australia

² British Columbia Geological Survey, Ministry of Energy, Mines and Low Carbon Innovation, Victoria, BC V8W 9N3, Canada

^a corresponding author: evan.orovan@gov.bc.ca

The physicochemical properties of nickel make it ideal as an alloy for stainless steel and an important component in rechargeable batteries and other green technologies. These applications have convinced many jurisdictions to classify nickel as a critical material and to recognize its major economic and industrial importance. Thus, gaining an understanding of how nickel forms in the environment is required to support exploration and mining and to ensure a continuous supply as we move to a green future.

Magmatic differentiation and segregation of immiscible sulphide liquids are key processes in the formation of many Ni sulphide deposits. However, the unconventional Ni sulphide mineralization at Trial Harbour (Zeehan mineral field, western Tasmania; Fig.1) is related to serpentinization of ultramafic rocks from an ophiolite sequence and hydrothermal and metasomatic processes spatially and temporally associated

with nearby granites. The host rocks form part of the Dundas Trough, which is a curved belt of Palaeozoic rocks that also host Cambrian volcanic massive sulphide base metal and gold deposits (e.g., Hellyer), porphyry-related Cu-Au deposits (e.g., Mt Lyell), Devonian Sn skarn deposits (e.g., Renison Bell), and other epigenetic deposits associated with granite emplacement.

The Ni sulphide mineralization at Trial Harbour is hosted by steeply dipping, serpentinized Cambrian intrusive rocks of the McIvor Hill ultramafic complex and juxtaposed volcanoclastic sedimentary rocks of the Crimson Creek Formation (Cambrian). Mineralization mostly occurs within the hydrothermal or metamorphic aureole of the Heemskirk granite (Late Devonian), where different tenors of skarn alteration are expressed. In calcareous horizons of the Crimson Creek Formation, the skarn alteration defines a prograde assemblage of andraditic garnet, diopside pyroxene, anorthite, and titanite that has

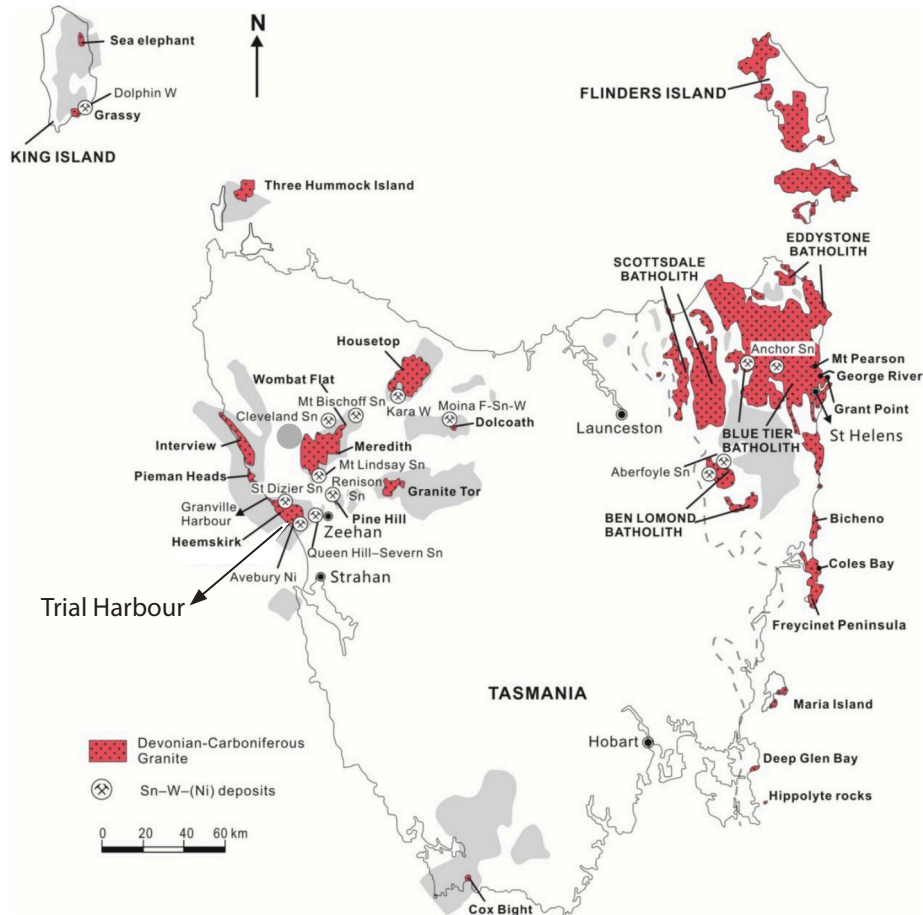


Fig. 1. Distribution of Devonian-Carboniferous granites in Tasmania. The Trial Harbour Ni skarn is immediately south of the Heemskirk granite in western Tasmania. After Hong (2016).

been overprinted by prehnite, muscovite, epidote, and apatite. Within the ultramafic rocks the prograde assemblage lacks garnet, contains abundant magnetite, and is overprinted by a hydrous assemblage of serpentine, phlogopite and Fe-chlorite. Locally, cumulate textures are partly preserved with serpentine pseudomorphs after olivine. In both domains, mineralization typically occurs as blebby to semi-massive pentlandite with pyrite and sphalerite, and as patches and veins of Mn-oxides, shandite ($\text{Ni}_3\text{Pb}_2\text{S}_2$), hazelwoodite (Ni_3S_2) and pentlandite with inclusions of sphalerite and galena. Locally, metal concentrations reach 4500 ppm Ni, 2600 ppm Zn, and 1000 ppm Pb (from pXRF results), with the highest concentrations near the Nickel Reward mine showing. Locally, these Ca and Fe-Mg skarns are crosscut by Sn-bearing tourmaline and quartz veins near the contact with the Heemskirk granite, and by later carbonate and chalcedony veins and cemented breccias.

The coincidence between the concentrations of Ni with Zn, Pb, and Sn is an uncommon relationship in ultramafic rocks. Previous work on the nearby Avebury Ni deposit (Kamenetsky et al., 2016) showed that serpentinization of a sufficient volume of olivine-bearing ultramafic rocks can release enough Ni to account for the concentration observed locally, and that remobilization of Ni from a previously formed magmatic deposit is not required. This model is consistent with observations at Trial Harbour, where it is envisaged that serpentinization-related liberation of Ni from olivine was incorporated into late-stage hydrous fluids that emanated from the Heemskirk granite and precipitated as oxides and sulphides under hydrothermal skarn conditions.

New LA-ICP-MS U-Pb analyses from the early prograde skarn assemblage provide ages of 357.3 ± 3.1 Ma (MSWD = 0.70) using hydrothermal titanite and 354.6 ± 7.1 Ma (MSWD = 1.6) using andraditic garnet. An $^{40}\text{Ar}/^{39}\text{Ar}$ age on distal retrograde phlogopite returned a plateau age of 362.30 ± 0.38 Ma (MSWD = 1.38). These ages overlap with the emplacement age of the nearby Heemskirk granite (362.8–358.0 Ma), tying the age of mineralization to magmatism. These results are consistent with the geochemical and textural observations that Trial Harbour mineralization is hydrothermal and that it formed during emplacement of the Heemskirk granite (cf. Keays and Jowitt, 2013). Recognition of the geological relationships between granite emplacement, ultramafic bodies, and permissive serpentinization may be an important update to Ni exploration models.

- Hong, W., 2016. Magmatic-hydrothermal volatile exsolution and mineralisation in Tasmania Sn granites. PhD thesis, University of Tasmania, Hobart, Australia, 282 p.
- Kamenetsky, V.S., Lygin, A.V., Foster, J.G., Meffre, M., Maas, R., Kamenetsky, M.B., Goemann, K., and Beresford, S.W., 2016. A story of olivine from the McIvor Hill complex (Tasmania, Australia): Clues to the origin of the Avebury metasomatic Ni sulfide deposit. *American Mineralogist*, 101, 1321-1331.
- Keays, R.R., Jowitt, S.M., and Callaghan, T., 2013. The Avebury Ni deposit, Tasmania: A case study of an unconventional nickel deposit. *Ore Geology Reviews*, 52, 4-17.

Critical minerals in Paleozoic hyper-enriched black shales

Michael G. Gadd^{1a}, Jan M. Peter¹, and Daniel Layton-Matthews²

¹Geological Survey of Canada, Ottawa, ON K1A 0E8, Canada

²Queen's Faculty for Isotope Research, Department of Geological Sciences and Geological Engineering, Queen's University, Kingston, ON K7L 3N6, Canada

^acorresponding author: michael.gadd@canada.ca

Hyper-enriched black shale (HEBS), also referred to as highly metalliferous black shale (Johnson et al., 2017), is an important global repository for Zn, Ni, Cu, Mo, Se, U, V, Cr, Co, Ag, Au, Re, platinum-group elements (PGE), and rare-earth elements (REE; Jowitt and Keays, 2011). Many of the chemical elements contained within HEBS are deemed critical minerals (or critical raw materials) within Canada (Natural Resources Canada, 2021) and also globally (e.g., Australia and United States of America). Yukon and British Columbia HEBS contain up to 7.4 wt.% Ni, 2.7 wt.% Zn, 0.38 wt.% Mo, 400 ppb Pt, 250 ppb Pd, 160 ppb Au, and 58.5 ppm Re. The polymetallic (including many critical minerals) nature of this deposit type is intriguing and provides the impetus to understand their genetic controls and develop an exploration model.

The best-known example of HEBS in Canada is the Nick Ni-Zn-Mo-PGE-Re-Au prospect, Yukon (Hulbert et al., 1992), which was discovered in 1981 by Cominco while following up on a Geological Survey of Canada stream-sediment survey. The nickel sulphide layer at the Nick prospect is thin (3–10 cm) and discontinuously crops out over a strike length of 100 km. This style of mineralization has been recognized in many locations across northern Yukon, including at Peel River, Moss, Monster River and the Rein showing (Fig. 1). Polymetallic HEBS have also been documented in the Kechika trough (Peter et al., 2018), which is the southern extension of the Selwyn basin in northeastern British Columbia (Fig. 1). The HEBS mineralization that underlies the Cardiac Creek clastic-dominated Ag-Pb-Zn-Ba deposit in British Columbia is mineralogically and geochemically similar to that in Yukon (Peter et al., 2018).

The sources of metals and drivers of mineralization for HEBS remain controversial. This is because few clues are preserved as to the depositional controls of mineralization, many of the metals that constitute HEBS do not commonly occur together in most ore systems, and mineralization is geographically widespread. There are two prevailing genetic models to explain the salient features of HEBS mineralization: 1) precipitation from hydrothermal fluids vented at the seafloor and 2) direct precipitation of metals from ambient seawater. The first model proposes that metals are sourced through the flow of hydrothermal (and possibly hydrocarbon-bearing) hydrothermal basin fluids along synsedimentary growth faults (Steiner et al., 2001). The second model proposes that combined organic matter remineralization, low siliciclastic sedimentation rates, and effective chemical trapping promoted the accumulation and preservation of sulphide minerals on the seafloor (Lehmann et al., 2007). Metal deposition may have been further enhanced by high primary productivity (Lehmann et al., 2016) and/or Fe-Mn-oxyhydroxide particulate shuttling (Gadd et al., in press). In either model, sulfur was probably derived from seawater sulfate, which was reduced by the interaction of

microbes and organic matter via the process of bacterial sulfate reduction. Resultant sulphide mineralogy is predominantly pyrite, Ni sulphides (e.g., millerite or vaesite), and sphalerite, and sulphide mineral textures strongly indicate mineralization from earliest diagenesis through later diagenesis. Rare, late sulphide veins indicate that sulphide precipitation likely ceased during latest diagenesis; this is supported by tightly constrained radiometric ages at the Nick (390.7 ± 5.1 Ma), Peel River (387.3 ± 4.4 Ma), and Moss (389.4 ± 5.7 Ma) localities. Although radiometric ages for HEBS at Akie are more complex, the age of organic-rich mudstone 3 m above HEBS is well constrained (380.2 ± 3.6 Ma; Fig. 2). Close agreement between conodont biostratigraphic and radiometric ages (Fig. 2), provides strong support that HEBS mineralization was a synsedimentary and basin-scale phenomenon.

Given the occurrence of HEBS at the stratigraphic contact between the Road River Group and the Canol Formation, together with the recessive weathering of the host rocks,

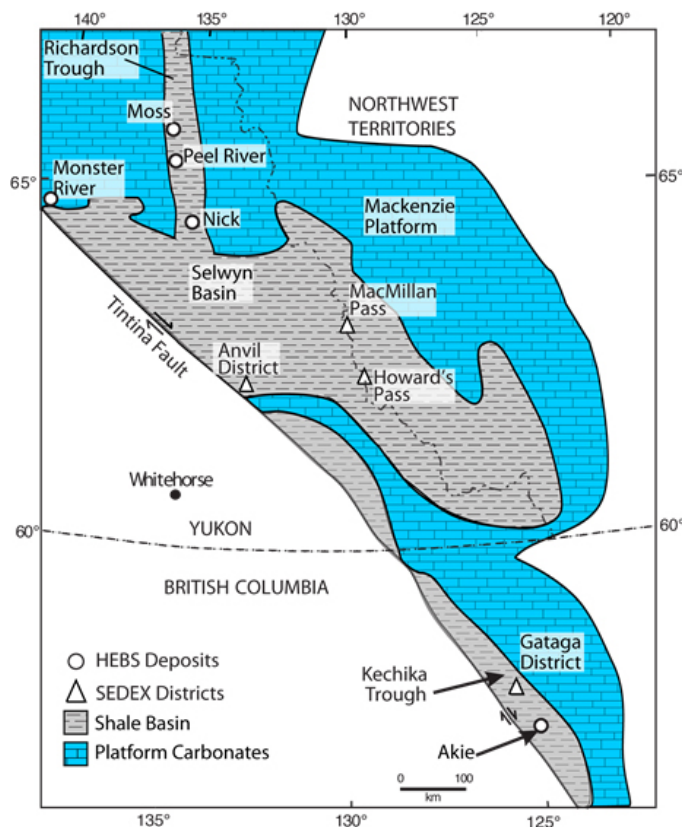


Fig. 1. Map of the Ancestral North American passive continental margin displaying locations of key hyper-enriched black shale (HEBS) localities and sedimentary exhalative (SEDEX) Zn-Pb districts in British Columbia and Yukon (modified from Goodfellow, 2007).

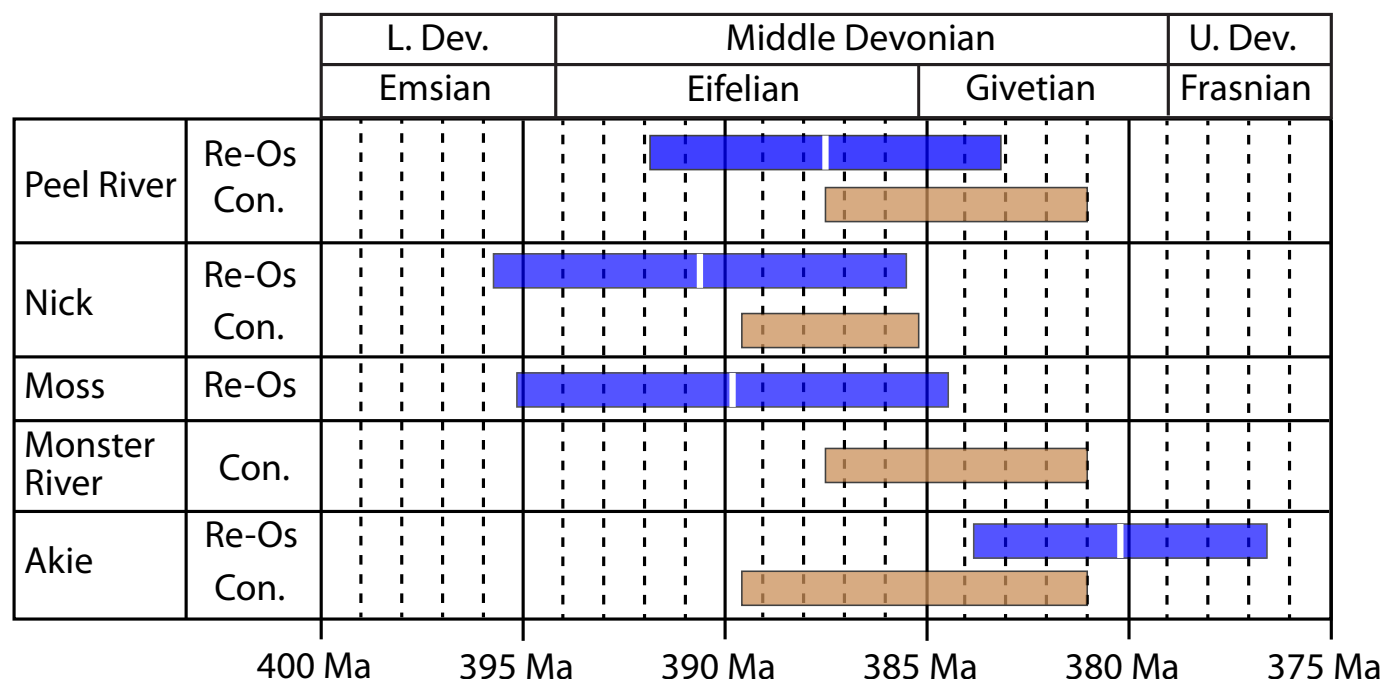


Fig. 2. Comparison of Re-Os isochron ages (Re-Os; vertical white bars are age and horizontal blue bars are 2σ uncertainty) of HEBS showings compared with conodont (Con.) biostratigraphic ages (horizontal tan bars). Ages of conodont biozones are from Becker et al. (2020).

exploration for HEBS mineralization should be focused on bedrock exposures in high-relief areas such as stream and river cuts, and cliff faces. That HEBS are coeval at localities separated by 100s to 1000s of km indicates a strong potential for further discoveries elsewhere along the stratigraphic contact between the Road River Group and the Canol Formation.

Becker, R. T., Marshall, J. E., Da Silva, A.-C., Agterberg, F., Gradstein, F. M., and Ogg, J. G., 2020. The Devonian Period. In: Gradstein, F. M., Ogg, J., Schmitz, M., and Ogg, G., (Eds.), *Geologic Time Scale 2020*, Elsevier, pp. 733-810.

Gadd, M. G., Peter, J. M., Hnatyshin, D., Creaser, R., Gouwy, S. A., and Fraser, T. A., 2020. A Middle Devonian basin-scale precious metal enrichment event across northern Yukon (Canada). *Geology*, 48, 242-246.

Gadd, M. G., Peter, J. M., and Layton-Matthews, D., in press. Genesis of hyper-enriched black shale Ni-Mo-Zn-Pt-Pd-Re mineralization in the northern Canadian Cordillera. In: Peter, J. M., and Gadd, M. G., (Eds.), *Geological Survey of Canada Bulletin* 617.

Goodfellow, W. D., 2007. Base metal metallogeny of the Selwyn Basin, Canada: Mineral Deposits of Canada: A Synthesis of Major Deposit-Types, District Metallogeny, the Evolution of Geological Provinces, and Exploration Methods. In: Goodfellow, W.D., (Ed.), *Mineral Deposits of Canada*, Geological Association of Canada, Special Publication, 5, pp. 553-579.

Hulbert, L.J., Gregoire, D., Paktunc, D., and Carne, R., 1992. Sedimentary nickel, zinc, and platinum-group-element mineralization in Devonian black shales at the Nick property, Yukon, Canada: a new deposit type. *Exploration and Mining Geology*, 1, 39-62.

Lehmann, B., Nägler, T. F., Holland, H. D., Wille, M., Mao, J., Pan, J., Ma, D., and Dulski, P., 2007. Highly metalliferous carbonaceous shale and Early Cambrian seawater. *Geology*, 35, 403-406.

Lehmann, B., Frei, R., Xu, L., and Mao, J., 2016. Early Cambrian black shale-hosted Mo-Ni and V mineralization on the rifted margin of the Yangtze Platform, China: reconnaissance chromium isotope data and a refined metallogenic model. *Economic Geology*, 111, 89-103.

Johnson, S.C., Large, R.R., Coveney, R.M., Kelley, K.D., Slack, J.F., Steadman, J.A., Gregory, D.D., Sack, P.J., and Meffre, S., 2017. Secular distribution of highly metalliferous black shales corresponds with peaks in past atmosphere oxygenation. *Mineralium Deposita*, 52, 791-798.

Jowitt, S.M. and Keays, R.R., 2011. Shale-hosted Ni-(Cu-PGE) mineralisation: a global overview. *Applied Earth Science; Transactions of the Institution of Mining and Metallurgy: Section B*, 120, 187-197.

Lehmann, B., Nägler, T.F., Holland, H.D., Wille, M., Mao, J., Pan, J., Ma, D., and Dulski, P., 2007. Highly metalliferous carbonaceous shale and Early Cambrian seawater. *Geology*, 35, 403-406.

Natural Resources Canada, 2021, Critical Minerals <https://www.nrcan.gc.ca/our-natural-resources/minerals-mining/critical-minerals/23414> [accessed July 26, 2021]

Peter, J. M., Bocking, N., Gadd, M. G., Layton-Matthews, D., and Johnson, N., 2018. Textural and mineralogical characterization of a Ni-Zn-rich black shale occurrence at the Akie property, Kechika Trough, northern British Columbia, and comparison with examples from Yukon. In: Rogers, N., (Ed.), *Targeted Geoscience Initiative: 2017 report of activities, volume 1*, Geological Survey of Canada, Open File 8358, pp. 207-216.

Steiner, M., Wallis, E., Erdtmann, B.-D., Zhao, Y., and Yang, R., 2001. Submarine-hydrothermal exhalative ore layers in black shales from South China and associated fossils — insights into a Lower Cambrian facies and bio-evolution. *Palaeogeography, Palaeoclimatology, Palaeoecology*, 169, 165-191.

Session 5: Selected critical mineral deposits II

Thursday November 18, 13:30 PST (21:30 GMT)

List of speakers

Chair: Allen Andersen, United States Geological Survey

Mark W. Bultman, United States Geological Survey
Potential for concealed critical mineral deposits in the northern Trans-Pecos region of West Texas and southern New Mexico from a new aeromagnetic survey

Kathryn E. Watts, United States Geological Survey
Temporal and petrogenetic links between Mesoproterozoic alkaline and carbonatite magmas at Mountain Pass, California

Frank Santaguida, First Cobalt Corp.
New cobalt-copper resources: New perspectives from the Iron Creek project, Idaho cobalt belt

Craig Bow, Group Ten Metals Inc.
Precious and base metal mineralization within the Peridotite zone of the Stillwater Complex, Montana, USA

Thomas R. Benson, Lithium Americas Corp.
Geology of the Thacker Pass deposit in the McDermitt Caldera, Nevada: The largest and highest grade known sedimentary lithium resource in the United States

Fiorella Sist, Controlled Thermal Resources (US) Inc.
Development of a mineralized brine resource: The Hell's Kitchen lithium and power project, Salton Sea, USA

Question and answer period

Potential for concealed critical mineral deposits in the northern Trans-Pecos region of West Texas and southern New Mexico from a new aeromagnetic survey

Mark W. Bultman^{1a}

¹U.S. Geological Survey, Tucson, AZ 85719, USA

^ambultman@usgs.gov

The northern Trans-Pecos magmatic province of west Texas and southern New Mexico (Fig. 1) hosted alkaline magmatism from 48 to 16 Ma. The area was under a compressional stress regime from 48 to 26 Ma and nearly all the felsic rocks in the area were emplaced during this time, mainly during the 37–26 Ma period. Transition from compressional to extensional tectonics occurred from 32 to 20 Ma and subsequent magmatism was almost exclusively mafic. Rhyolite and rhyolite porphyry laccoliths, emplaced during the compressional regime, were intruded into Cretaceous sedimentary rocks and are enriched in rare earth elements (REEs) and other critical minerals. Included in these intrusions are the 34–36 Ma intrusive rhyolites of the Sierra Blanca Mountains, Texas (Fig. 1), which host the Round Top heavy REE deposit. In addition, alkaline igneous rocks in the Cornudas and Hueco Mountains, both located in Texas and New Mexico (Fig. 1), also show high concentration of REEs. Potential mineral occurrences of interest in the region include: REE in highly fractionated rhyolites, REE-thorium-uranium veins, REE-fluorine veins, copper-REE-fluorine veins, REE-fluorine breccia pipes, iron skarns, porphyry molybdenum, and carbonatites.

An aeromagnetic and aeroradiometric survey was flown over the region in January and February of 2021 with the following objectives: 1) Detect regional trends, fractures, or patterns that may be responsible for the locations of the Tertiary alkaline intrusions; 2) Identify magma sources and plumbing systems for the Tertiary alkaline intrusions; and 3) Identify potential concealed Tertiary alkaline intrusions that may represent concealed critical mineral deposits. The survey covered approximately 5,800 square kilometers; flight lines were spaced at 200 m and draped at 125 m altitude. The survey region was split into four blocks due to terrain. Three blocks with rugged terrain required the survey to be flown by a helicopter in those areas. These blocks include: 1) Hueco Mountains block in the northwest part of the survey; 2) Cornudas Mountains block in the northern part of the survey; and 3) Sierra Blanca Mountains block in the southern part of the survey (Fig. 1). Lying in between and connecting these three blocks is the Middle block which was flown with a fixed-wing aircraft (Fig. 1).

Based on the aeromagnetic data, outcropping Tertiary intrusive rocks were observed to have much larger magnetic anomalies than the Cretaceous sediments in which they are located likely due to higher magnetic susceptibilities. This was especially true in the Cornudas Mountains and to a lesser extent in the Sierra Blanca and Hueco Mountains. In order to observe these high susceptibility rocks at depth, matched bandpass filtering (Phillips, 2001) of the aeromagnetic data was used to separate shallow short-wavelength anomalies from deeper longer wavelength anomalies.

Matched bandpass filtering is based on the fact that the Fourier amplitude spectrum of a potential field can be modelled by a linear combination of potential fields each produced by a horizontal layer of sources at a given depth. Each horizontal layer is called an equivalent source and the depth of each equivalent source is found by fitting a linear segment (in log space) of the form $B * k^n * e^{-(k/z)}$ where k is the radial wavenumber, n is 0 for a magnetic dipole and -1 for a magnetic half-space, B is a constant, and z is depth (Phillips, 2001). The number of linear segments used to describe the entire Fourier amplitude spectrum determines the number of equivalent sources. While the spatial distribution of magnetic sources is rarely confined to a given depth, matched bandpass filtering has proven to be a useful way to perform approximate depth separation of anomalies (Phillips, 2001).

Since the amplitudes of anomalies from each equivalent source can vary dramatically and decreases with increasing depth, the data are statistically standardized by subtracting the mean of all data from a given equivalent source and dividing by its standard deviation. Relative amplitude of the standardized anomalous magnetic field can then be used to separate rocks with larger anomalies from smaller anomalies allowing for the visualization of only rock with a high magnetic susceptibility, presumably the Tertiary intrusive rocks.

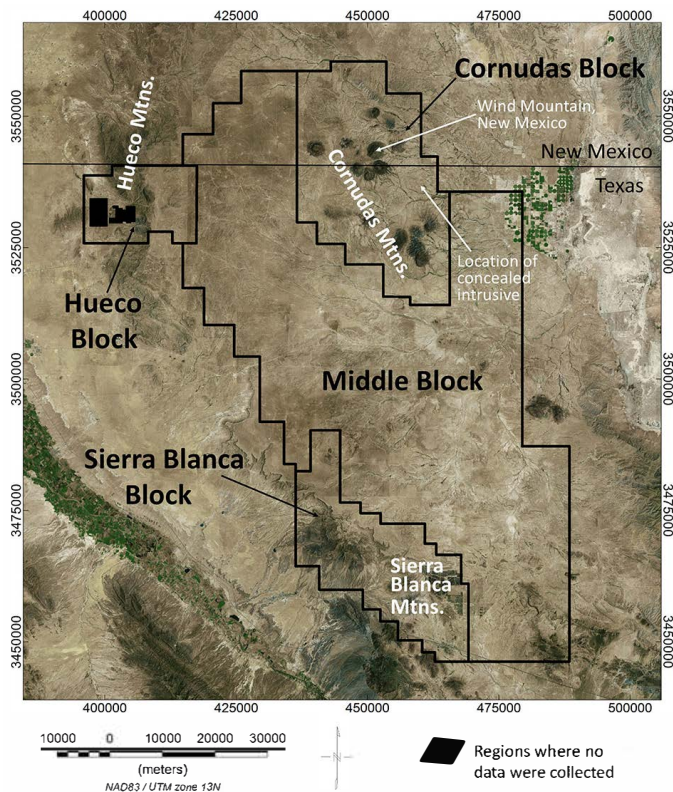


Fig. 1. The northern Trans-Pecos Magmatic Province including the outline of Trans-Pecos aeromagnetic/aeroradiometric survey blocks, Texas and New Mexico.

Figure 2 displays a 3-dimensional model of the standardized anomalous magnetic field of five equivalent sources from matched bandpass filtering in the Cornudas block of the Trans-Pecos aeromagnetic survey (Fig. 1). An additional model layer was needed between the two deepest equivalent sources to generate a continuous 3-dimensional model and this layer was generated by linear interpolation. Data from the model are clipped below a standardized anomalous magnetic field value of zero meaning that approximately half of the data in the model are removed. The resulting model displays rock with the highest 50 percent of standardized anomalous magnetic field values and is thought to represent the rock with high magnetic susceptibilities, inferred to be the Tertiary intrusive rocks. This is verified by the fact that the high susceptibility rock in the model that reaches the surface is spatially coincident with

outcrop of Tertiary intrusive rock in all cases (Fig. 2). One example of this is shown, Wind Mountain, New Mexico, which is an exposed nepheline syenite laccolith and located on both Figs. 1 and 2. Figure 2 displays multiple horizontal and vertical feeder systems for the observed intrusions. It also locates several potential concealed intrusions that approach but do not breach the surface. One such concealed intrusion is labeled in Fig. 2 and it and others may represent potential for concealed critical mineral resource occurrences.

Phillips, J.D., 2001, Designing matched bandpass and azimuthal filters for the separation of potential-field anomalies by source region and source type, Australian Society of Exploration Geophysicists Extended Abstracts, 2001:1, 1-4
<https://doi.org/10.1071/ASEG2001ab110>

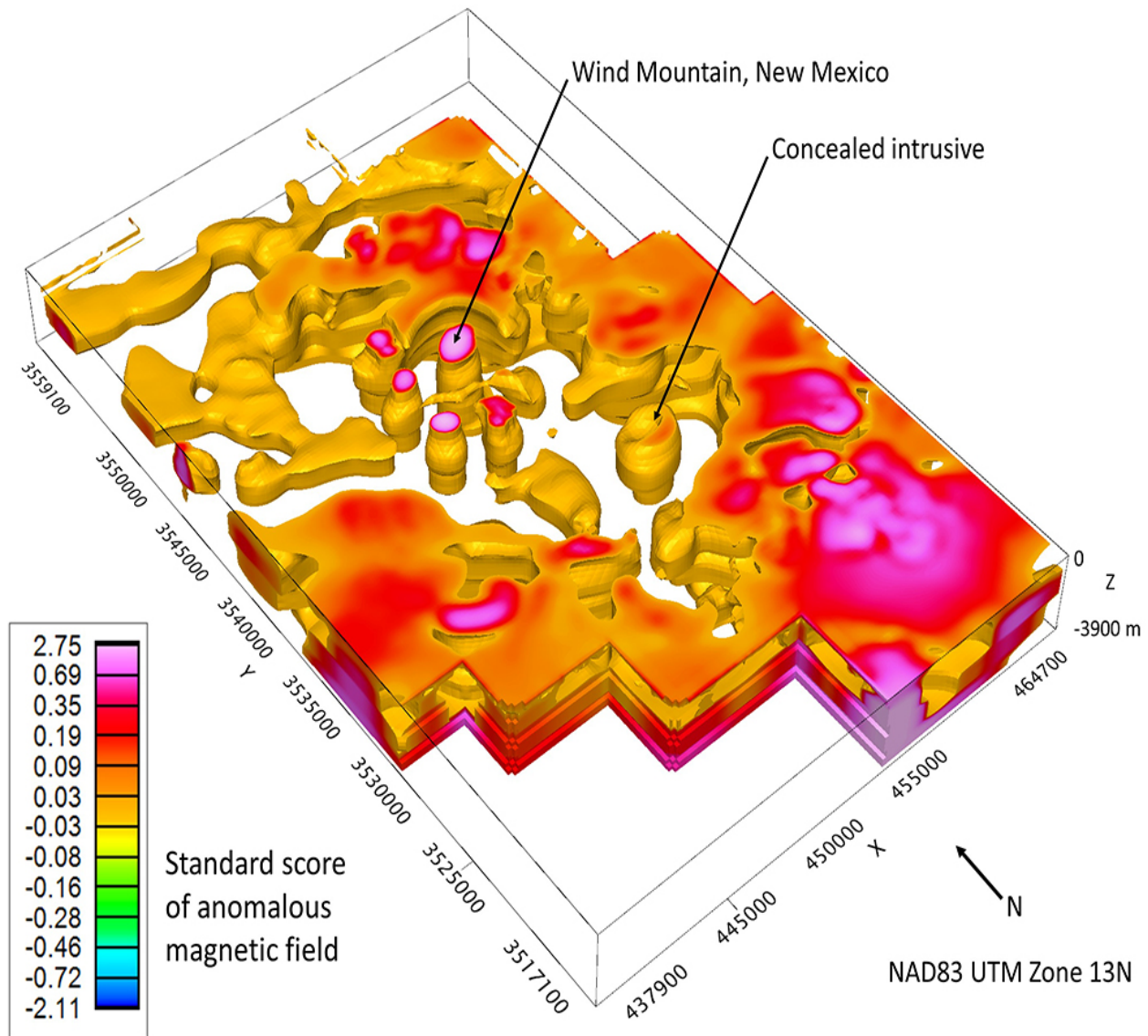


Fig. 2. Three-dimensional representation of high susceptibility rock in the Cornudas Block (Fig. 1), Trans-Pecos aeromagnetic survey. Only rocks with an anomalous magnetic field standard score greater than 0.0 are shown which includes approximately one-half of the rock in the Cornudas block. Wind Mountain, New Mexico is labeled for locational purposes as is a likely Tertiary intrusive that does not breach the surface.

Temporal and petrogenetic links between Mesoproterozoic alkaline and carbonatite magmas at Mountain Pass, California*

Kathryn E. Watts^{1a}, Gordon B. Haxel², and David M. Miller³

¹ U.S. Geological Survey, Spokane, Washington 99201, USA

² U.S. Geological Survey, Flagstaff, Arizona 86001, USA

³ U.S. Geological Survey, Moffett Field, California 94025, USA

^a corresponding author: kwatts@usgs.gov

*The following abstract and figures are excerpted from Watts et al. (2021).

Mountain Pass is the site of the most economically important rare earth element (REE) deposit in the United States. Mesoproterozoic alkaline intrusions are spatiotemporally associated with a composite carbonatite stock that hosts REE ore. Understanding the genesis of the alkaline and carbonatite magmas is an essential scientific goal for a society in which critical minerals are in high demand and will continue to be so for the foreseeable future. We present an ion microprobe study of zircon crystals in shonkinite and syenite intrusions to establish geochronological and geochemical constraints on the igneous underpinnings of the Mountain Pass REE deposit. Silicate whole-rock compositions occupy a broad spectrum (50–72 wt % SiO₂), are ultrapotassic (6–9 wt % K₂O; K₂O/Na₂O = 2–9), and have highly elevated concentrations of REEs (La 500–1,100× chondritic). Zircon concordia ²⁰⁶Pb/²³⁸U–²⁰⁷Pb/²³⁵U ages (Fig. 1) determined for shonkinite and syenite units are 1409 ± 8, 1409 ± 12, 1410 ± 8, and 1415 ± 6 Ma (2σ). Most shonkinite dikes are dominated by inherited Paleoproterozoic xenocrysts, but there

are sparse primary zircons with ²⁰⁷Pb/²⁰⁶Pb ages of 1390–1380 ± 15 Ma for the youngest grains. Our new zircon U-Pb ages for shonkinite and syenite units overlap published monazite Th-Pb ages for the carbonatite orebody and a smaller carbonatite dike. Inherited zircons in shonkinite and syenite units are ubiquitous and have a multimodal distribution of ²⁰⁷Pb/²⁰⁶Pb ages that cluster in the range of 1785–1600 ± 10–30 Ma. Primary zircons have generally lower Hf (<11,000 ppm) and higher Eu/Eu* (>0.6), Th (>300 ppm), Th/U (>1; Fig. 2), and Ti-in-zircon temperatures (>800°C) than inherited zircons. Oxygen isotope data reveals a large range in δ¹⁸O values for primary zircons, from mantle (5–5.5‰) to crustal and supracrustal (7–9‰). A couple of low-δ¹⁸O outliers (2‰) point to a component of shallow crust altered by meteoric water. The δ¹⁸O range of inherited zircons (5–10‰) overlaps that of the primary zircons. Our study supports a model in which alkaline and carbonatite magmatism occurred over tens of millions of years, repeatedly tapping a metasomatized mantle source, which endowed

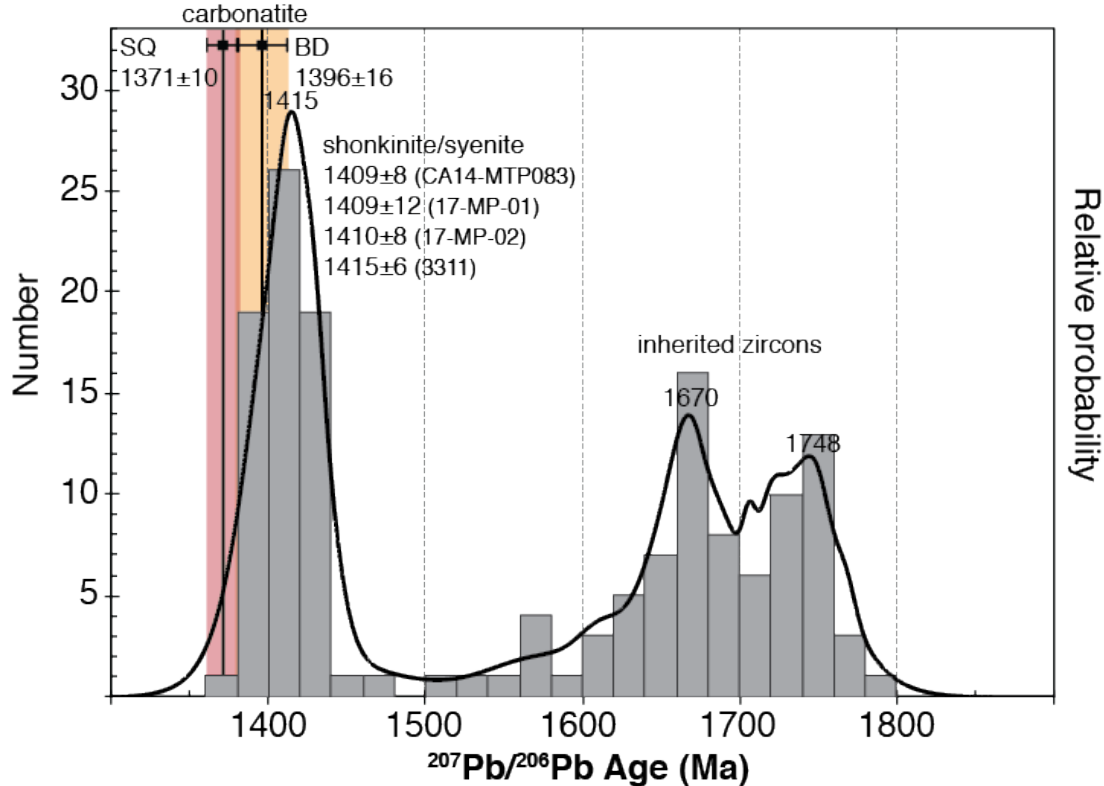


Fig. 1. Zircon geochronology summary for shonkinite-syenite samples, showing histogram and probability function for concordant ²⁰⁷Pb/²⁰⁶Pb age data. Zircon concordia ages (±2σ) of the shonkinite-syenite samples are listed, and monazite Th-Pb ages for carbonatite samples from the Sulphide Queen (SQ) and Birthday (BD) localities (Poletti et al., 2016) are included for reference.

magmas with elevated REEs and other diagnostic components (e.g., F, Ba). Though this metasomatized mantle region existed for the duration of Mountain Pass magmatism, it probably did not predate magmatism by substantial geologic time (>100 m.y.), based on the similarity of 1500 Ma zircons with the dominantly 1800–1600 Ma inherited zircons, as opposed to the 1450–1350 Ma primary zircons. Mountain Pass magmas had diverse crustal inputs from assimilation of Paleoproterozoic and Mesoproterozoic igneous, metaigneous, and metasedimentary rocks. Crustal assimilation is only apparent from high spatial resolution zircon analyses and underscores the need for mineral-scale approaches in understanding the genesis of the Mountain Pass system.

Poletti, J.E., Cottle, J.M., Hagen-Peter, G.A., and Lackey, J.S., 2016. Petrochronological constraints on the origin of the Mountain Pass ultrapotassic and carbonatite intrusive suite, California. *Journal of Petrology*, 57, 1555-1598.
 Watts, K.E., Haxel, G.B., and Miller, D.M., 2021 (in press). Temporal and petrogenetic links between Mesoproterozoic alkaline and carbonatite magmas at Mountain Pass, California. *Economic Geology*
<https://doi.org/10.5382/econgeo.4848>

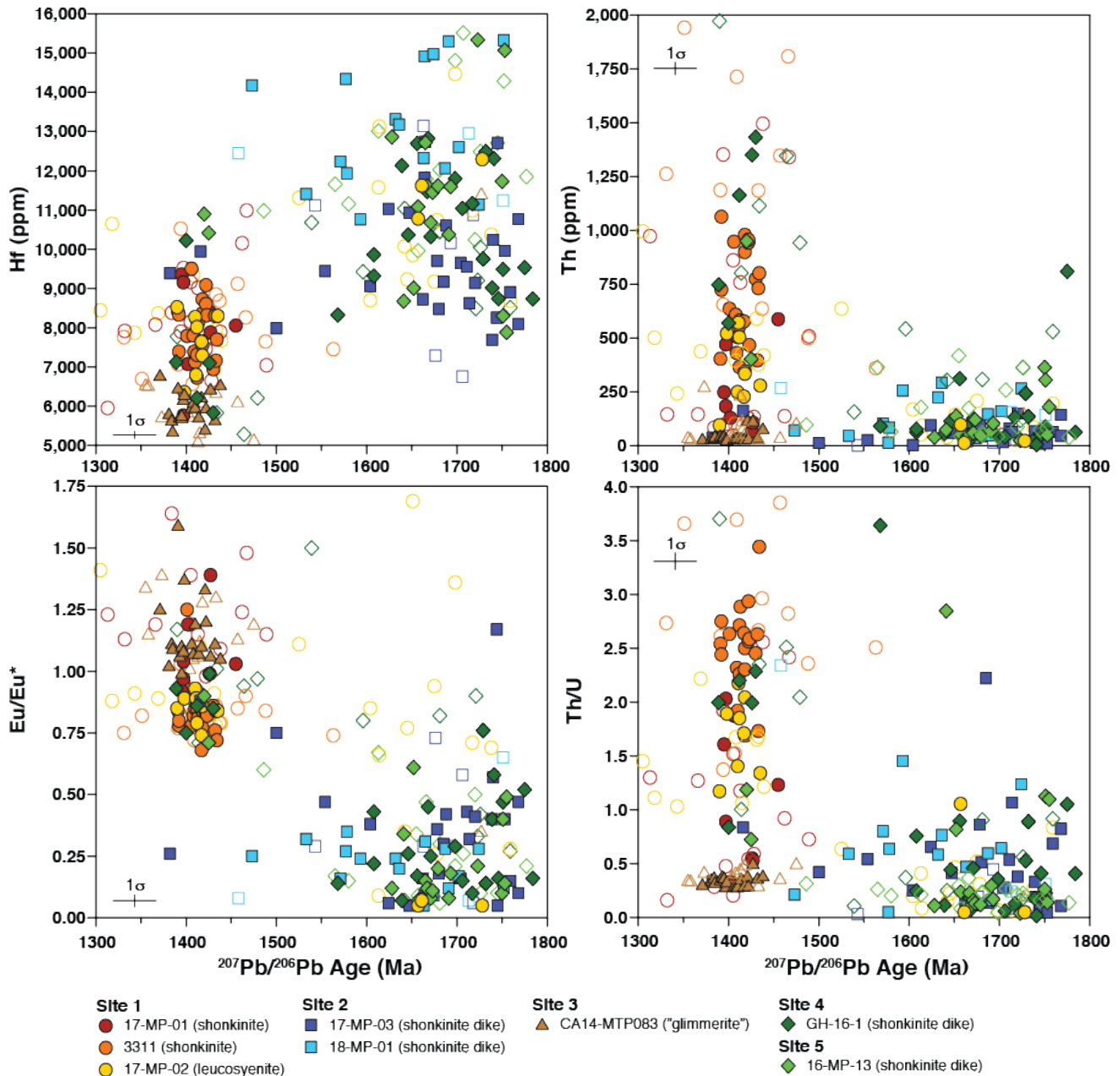


Fig. 2. Zircon Hf, Eu/Eu*, Th, and Th/U versus $^{207}\text{Pb}/^{206}\text{Pb}$ age for Mountain Pass shonkinite-syenite series rocks. Concordant zircon grain spots for each sample group are shown in the colored symbols; open-colored symbols of the same type show discordant zircon grain spots. Average 1σ error bars are included in the corner of each panel.

New cobalt-copper resources: New perspectives from the Iron Creek project, Idaho cobalt belt

Frank Santaguida^{1a}

¹ First Cobalt Corp., Toronto, ON M5C 2L7, Canada
^a fsantaguida@firstcobalt.com

The Iron Creek cobalt-copper project in central Idaho is in the Mesoproterozoic Idaho cobalt belt (ICB), a fertile mining district containing several historical operations and undeveloped cobalt-copper±gold resources. Initially explored from 1967 to 1971, the Iron Creek property saw little activity in the past 40 years. With the growing global demand for cobalt, recent exploration has expanded the previously known cobalt and copper resources (Ristorcelli and Schlitt, 2019). Several mineralized zones are exposed at the property, but to date, only the Iron Creek deposit has been extensively explored (Fig. 1).

Mineralization is largely stratabound, contained within siltite-rich metasedimentary rocks. Metamorphism is lower greenschist grade and sedimentary structures in the host rocks are locally well-preserved, typically outside of mineralized zones. Thin, cm-scale, quartzite layers are prominent in the main mineralized zones at Iron Creek relative to rocks in the immediate hanging-wall. Stratigraphic markers have not been recognized in the host rock sequence, although one unit

containing siderite porphyroblasts has been traced continuously in the footwall of the mineralized zone.

Mineralogy of the ore metals is relatively simple; cobalt occurs primarily in pyrite and copper in chalcopyrite (Fig. 2a). Cobalt is concentrated in pyrite along crystallographic boundaries, as well as within the cores of coarse pyrite grains (Fig. 2b). Pyrite lenses are interlayered with the host siltite, but locally transect bedding. In places, pyrite is semi-massive and up to 15m in true thickness. Chalcopyrite is disseminated, but also occurs as stringers cross-cutting the pyrite lenses and as well-developed stringers in the siltite hanging-wall in the western portion of the resource. Locally, brecciated rocks and shear zones are developed sub-parallel to bedding containing thicker mineralized intervals. Regionally, the metasedimentary rocks that host cobalt-copper mineralization and define the ICB are within the Apple Creek Formation a succession estimated to be more than 15,000m thick that has been mapped continuously along a strike length of 100 km (Burmester et al., 2016).

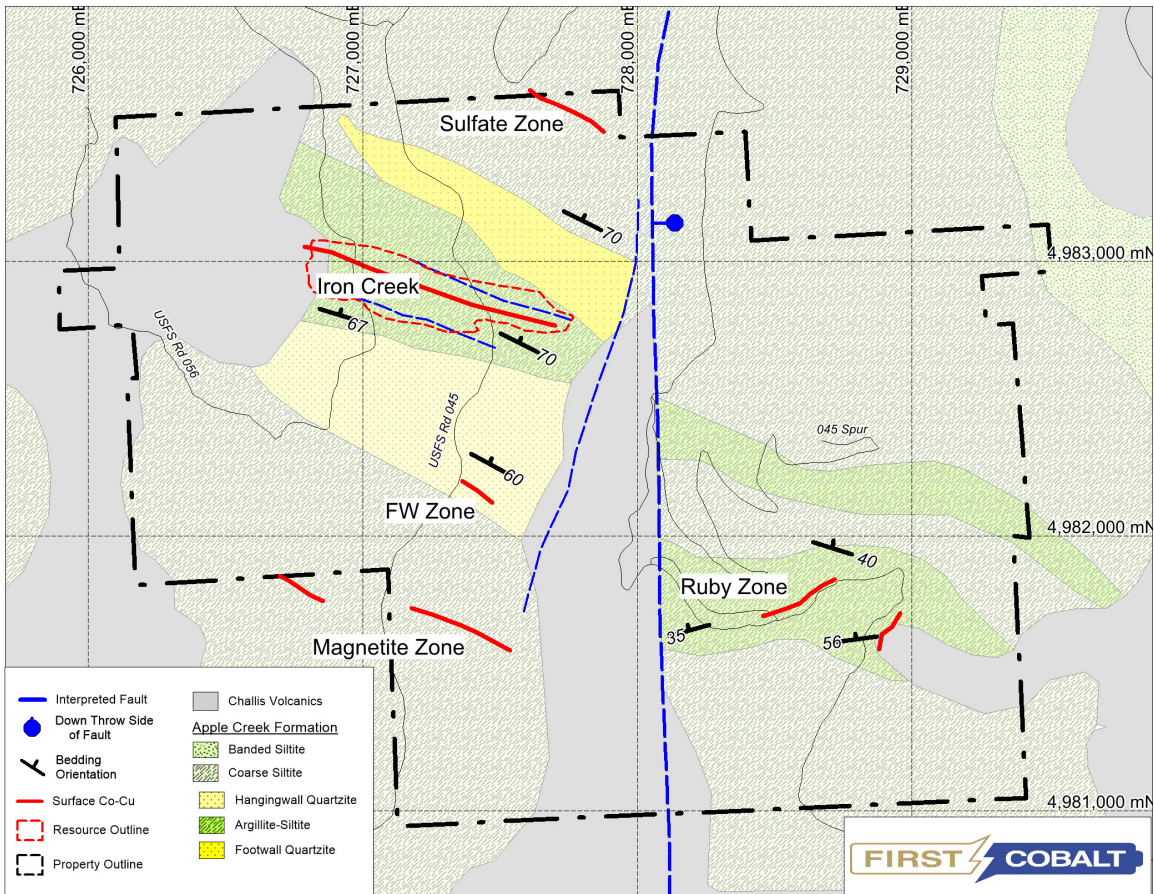


Fig. 1. Bedrock geology of the Iron Creek property.

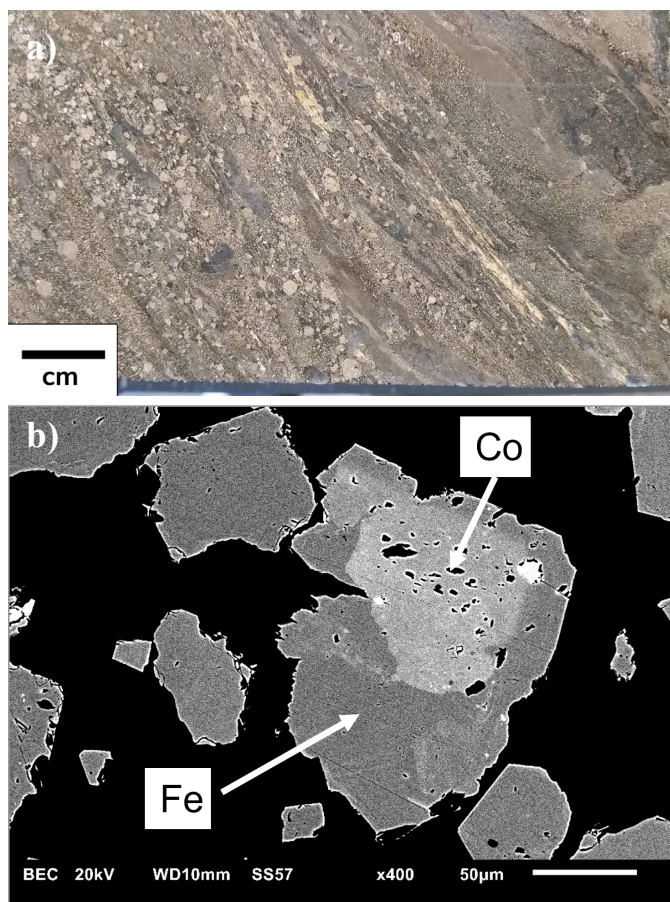


Fig. 2. a) Typical high-grade cobalt ore texture with semi-massive pyrite and chalcopyrite in drill core from the Iron Creek deposit. b) Backscattered electron image of a typical cobalt-rich pyrite grain; brighter area within grain is enriched in cobalt.

In 2020, a NI43-101 compliant resource was released for an underground-only mining scenario including an Indicated Resource of 2.374 million tonnes grading 0.26% Co and 0.61% Cu, and an Inferred Resource of 2.950 million tonnes grading 0.22% Co and 0.68% Cu, using a cutoff grade of 0.18% Co Equivalent, which is calculated as Co (%) + Cu/10 (%). Mineralization remains open along strike and down dip.

Most known cobalt-copper deposits in the ICB occur approximately 60 km northwest of Iron Creek; collectively called the Blackbird Mining District (Slack, 2012; Bookstrom et al., 2016). Blackbird-type deposits are predominantly stratabound lenses of cobaltite, chalcopyrite, and iron sulphides within metamorphosed siltite higher in the Apple Creek Formation. Individual deposits such as Blackbird, Chicago, and Ram consist of several lenses that commonly occur along multiple stratigraphic horizons. Host rocks are conspicuously biotite-rich and extend beyond mineralization. Gold is also concentrated with Co and Cu. The biotite-rich host rocks that are traced across the ICB transect the general bedding trends of the Apple Creek Formation at shallow angles. Some cobalt mineralization in the ICB is also associated with tourmaline-rich breccias and veins that locally cross-cut stratigraphy at high angles for several 100 m.

Slack et al. (2017) proposed that the Blackbird cobalt-copper deposits originated from a range of mineralizing processes,

from diagenetic to epigenetic; the latter occurring both before and during metamorphism. At the Blackbird deposits, geochronological, and geochemical evidence suggests links to the post-sedimentary composite granite-gabbroic plutons, dating the main stage of cobalt mineralization at younger than 1,370 Ma, approximately 30 Ma later than the host rocks (Slack, 2012; Aleinikoff et al., 2012). The Iron Creek deposits are also considered to have formed by processes similar to that of an iron-rich endmember of a magmatic-hydrothermal system, akin to iron-oxide-copper-gold models (Hitzman et al., 2017).

- Aleinikoff, J.N., Slack, J.F., Lund, K., Evans, K.V., Fanning, C.M., Mazdab, F.K., Wodden, J.L., and Pillers, R.M., 2012. Constraints on the timing of Co-Cu±Au mineralization in the Blackbird district, Idaho, using SHRIMP U-Pb ages of monazite and xenotime plus zircon ages of related Mesoproterozoic orthogneisses and metasedimentary rocks. *Economic Geology* 107, 1143-1175.
- Bookstrom, A.A., Box, S.E., Cossette, P.M., Frost, T.P., Gillerman, V.S., King, G.R., and Zirakparvar, N.A., 2016. Geologic history of the Blackbird Co-Cu district in the Lemhi sub-basin of the Belt-Purcell Basin. In: MacLean, J.S., and Sears, J.W. (Eds.), *Belt Basin: Window to Mesoproterozoic Earth*. Geological Society of America Special Paper, 522, pp. 185–219.
- Burmester, R.F., Lonn, J.D., Lewis, R.S., and McFadden, M.D., 2016. Stratigraphy of the Lemhi sub-basin of the Belt Supergroup. In: MacLean, J.S., and Sears, J.W. (Eds.), *Belt Basin: Window to Mesoproterozoic Earth*. Geological Society of America Special Paper 522, pp. 121-137.
- Hitzman, M.W., Bookstrom, A.A., and Slack, J.F., 2017. Cobalt-styles of deposits and the search for primary deposits, U.S. Geological Survey Open-File Report 2017-1155, 47p.
- Ristorcelli, S.J. and Schlitt, J. Technical Report with Updated Estimate of Mineral Resources for the Iron Creek Cobalt-Copper Project, Lemhi County, Idaho, USA. National Instrument 43-101 Report.
- Slack, J.F., 2012. Strata-bound Fe-Co-Cu-Au-Bi-Y-REE deposits of the Idaho Cobalt Belt: Multistage hydrothermal mineralization in a magmatic-related iron oxide copper-gold system. *Economic Geology* 107, 1089-1113.
- Slack, J.F., Kimball, B.E., and Shedd, K.B., 2017. Critical mineral resources of the United States—economic and environmental geology and prospects for future supply. U.S. Geological Survey Professional Paper 1802-F, 40p.

Precious and base metal mineralization within the Peridotite zone of the Stillwater Complex, Montana, USA

Craig Bow^{1a}, Michael Rowley¹, Michael Ostenson¹, Justin Modroo¹, Allen Andersen²

¹ Group Ten Metals, Vancouver, BC V6C 1T2, Canada

² U.S. Geological Survey, Spokane, WA 99201, USA

^a corresponding author: craigb@csbplats.com

The Stillwater Complex is a 2.7 Ga layered mafic-ultramafic intrusion, host to the world-class J-M Reef Pd-Pt deposit. Group Ten Metals is exploring for base and precious metals along 25 strike kilometres of prospective mafic and ultramafic rocks that include multiple target types and individual prospects (Fig. 1).

The Stillwater Complex stratigraphy is divided into three major units based on proportions of cumulus minerals. Group Ten’s exploration efforts focus primarily within the lower third of the intrusion, from the Basal series, which occurs at the footwall contact, upwards into the Ultramafic series

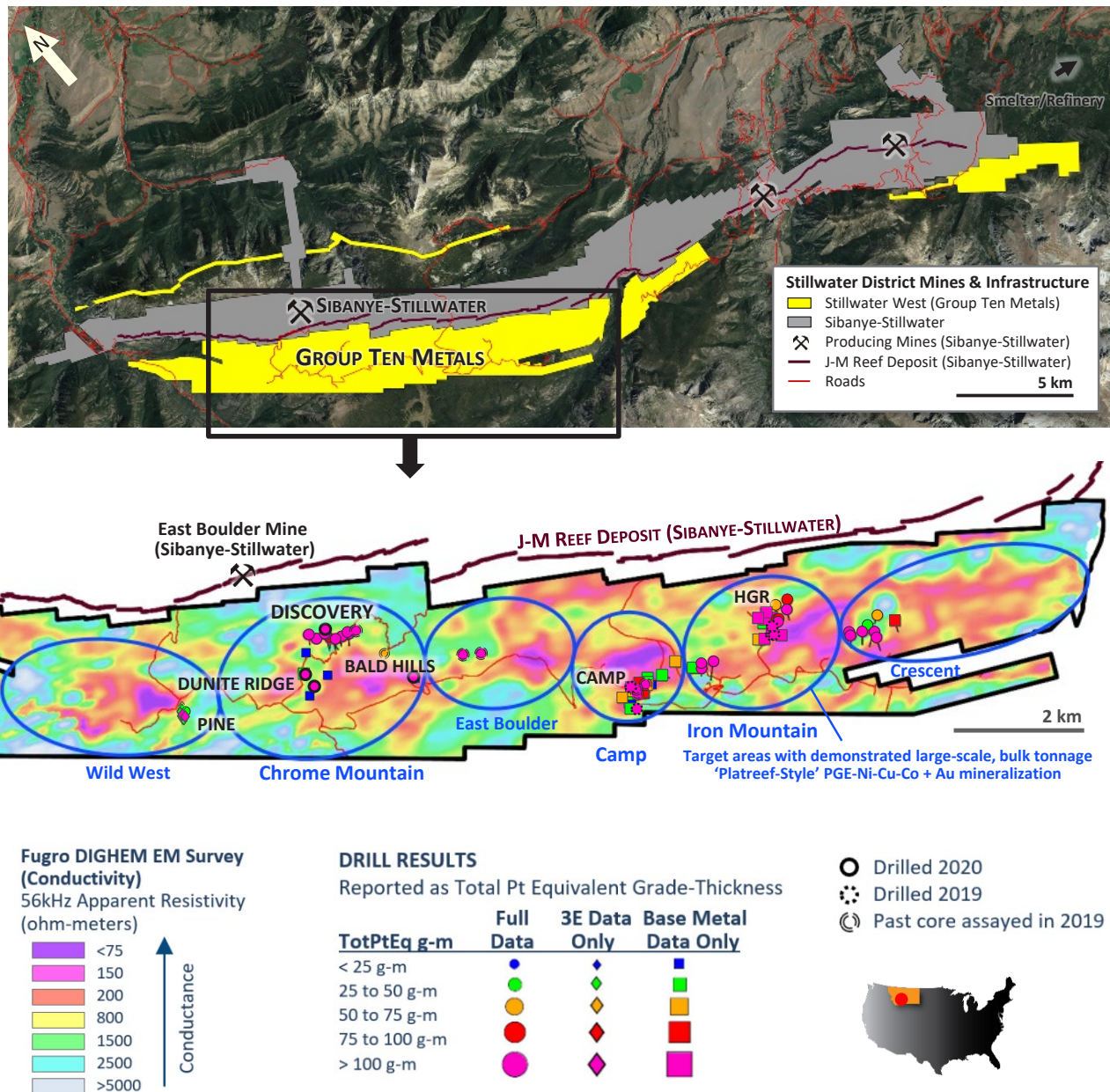


Fig. 1. Selected drill results over geophysics for the Stillwater West PGE-Ni-Cu-Co + Au project, Stillwater Complex, Montana, USA.

(1400 m) divided into a lower Peridotite zone and an upper Bronzite (orthopyroxenite) zone. Conventionally, rocks of the Peridotite zone have been interpreted to be repetitive, laterally continuous, and layered sequences of olivine, chromite,

olivine-chromite, olivine-orthopyroxene, and orthopyroxene cumulates. However, this interpretation was developed from observations in the eastern portion of the complex, far from our focus areas. Our detailed mapping and that of previous

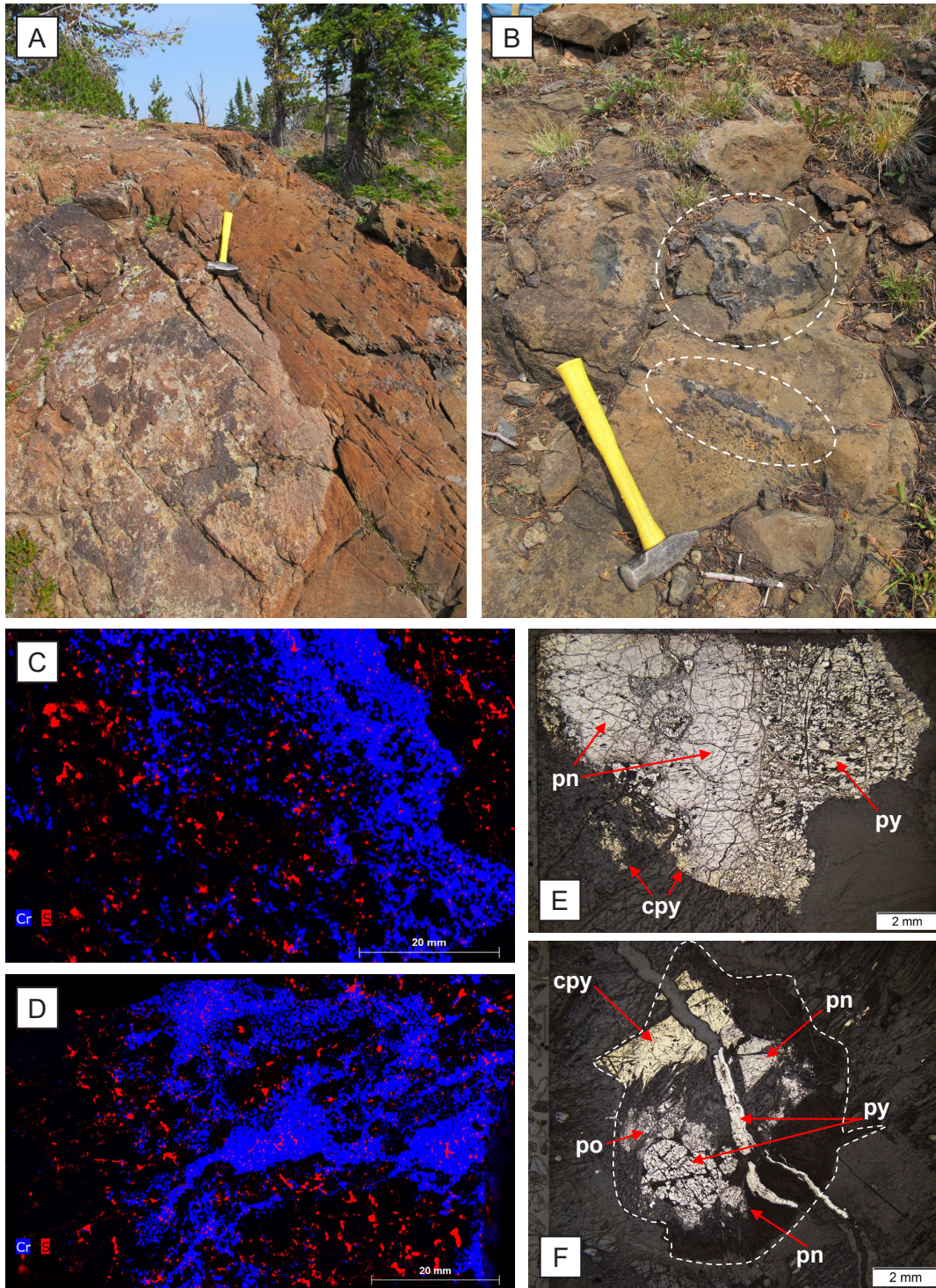


Fig 2. **a)** Discordant dunite mass (right) cross-cutting bronzite cumulate (left) at the western base of Chrome Mountain. **b)** Chromite schlieren in discordant dunite near Chrome Mountain. **c, d)** X-ray element maps showing Cr (chromite, blue) and S (sulphides, red) distribution in drill core samples from the Chrome Mountain area. Images captured using a Bruker M4 Tornado housed at the Colorado School of Mines. **e, f)** Reflected light images of rounded sulphide globules that occur peripheral to chromite schlieren. Major sulphide minerals are pyrite (py), pentlandite/violarite (pn), chalcopyrite (cpy), and minor pyrrhotite (po). Dashed line surrounds an alteration halo and possible original boundary of the sulphide globule.

companies, consistently paints a very different picture. We have found a thinner Peridotite zone than what is described in the eastern part of the complex, lacking in both lateral continuity and easily discernable cyclicality.

Based on an analysis of more than 50 years of historical exploration, one that considered differing commodity focus, land positions, analytical menus, and deployed petrogenetic models, our initial focus is in the Iron Mountain and Chrome Mountain sectors (Fig. 1). Group Ten Metals completed diamond drilling in these areas during 2019-2020 and currently has two drills turning.

At Iron Mountain, the primary targets are contact-type Ni-Cu-PGE magmatic sulphides in the Basal series and lower Peridotite zone, near the footwall contact of the complex. Drill holes from 2019 penetrated basement rock rafts to intersect underlying mineralized ultramafic rocks. Important objectives include establishing the PGE tenor of sulphide mineralization drilled by AMAX in the 1970s. Re-analysis of core from AMAX drill hole 355-71 at Iron Mountain revealed a narrow zone of disseminated sulphides with high gold concentrations (up to 14.3 g/t) and moderate PGE concentrations (3.7 to 4.8 g/t Pt+Pd). Recent SEM-EDS thin section mapping shows that the high gold is accompanied by abundant nickeline and a Ni-Bi sulphide mineral.

At Chrome Mountain, mapping has established that magmatic layering was disturbed or destroyed across large areas. Correlations of marker units (for example, chromitite seams) become problematic along a W-NW axis within which normal igneous stratigraphy has been disrupted by or converted to discordant dunite masses (Fig. 2a), pyroxenite pegmatitic rocks, and what appear to be magmatic breccias. This unusual assemblage of rock types is accompanied by significant and previously underappreciated PGE mineralization related to chromite schlieren (Fig. 2b) and minor but persistent base metal sulphides. Core samples from 2020 are currently being prepared for detailed instrumental study.

Interstitial sulphides and larger sulphide globules (up to 1 cm) are proximal to the cm- to dm-scale chromite schlieren and rafted blocks (Fig. 2c-f). Platinum-group minerals (PGM) occur as discrete grains concentrated along the outer margins of these sulphide globules (within ca. 1 mm) in association with silicate alteration minerals. Using a TESCAN TIMA-X automated mineralogy system in bright phase mode, more than 20 different PGM were identified including, bismuth tellurides (e.g., michenerite, merenskyite), arsenides (e.g., sperrylite), antimonides (e.g., mertieite, isomertieite), and arsenic-sulphides (e.g., hollingworthite, irarsite). The spatial distribution of PGM within alteration halos is probably due to replacement along sulphide globule margins through reaction with hydrothermal fluids, causing an inward-migrating sulphide boundary. Sulfur loss through sulphide mineral replacement could explain the higher ore tenors within this area of disrupted stratigraphy.

Disclaimer: Any use of trade, firm, or product names is for descriptive purposes only and does not imply endorsement by the U.S. Government.

Geology of the Thacker Pass deposit in the McDermitt Caldera, Nevada: The largest and highest grade known sedimentary lithium resource in the United States

Thomas R. Benson^{1,2,a}

¹ Lithium Americas Corporation, Vancouver, BC V6C 1E5, Canada

² Lamont-Doherty Earth Observatory, Palisades, NY 10964, USA

^a tom.benson@lithiumamericas.com

The ongoing global electrification of the automobile industry is resulting in a rapidly increasing demand for lithium (Li) for use in Li-ion batteries. Most industry analysts now project demand to surpass expected supply by mid-decade, leading to a “lithium rush” for new Li resources. This is especially true for sedimentary-type lithium deposits in the United States, with several junior mining companies recently announcing new projects and staking new claims on Tertiary lacustrine sediments for this critical element.

Current data from JORC and SEDAR reports indicate that sedimentary resources in the United States contain Measured and Indicated (M and I) whole-rock Li grades less than 2,000 ppm Li: Rhyolite Ridge – 1,600 ppm Li; Tonopah – 1,253 ppm Li; Clayton Valley (Cypress) – 1,052 ppm Li; Clayton Valley (Noram) – 1,136 ppm Li; Big Sandy – 1,950 ppm Li. A notable exception is the Thacker Pass deposit in the McDermitt caldera

(mid-Miocene) in northern Nevada. This resource, hosted in the clay-rich caldera lake deposits, has a higher cutoff than the resource grades of the other published resources (2,000 ppm Li) and an average M&I resource grade of ~3,000 ppm Li (Ehsani et al., 2018). Whole-rock concentrations from drill core assays reach values up to ~9,000 ppm Li (Ehsani et al., 2018) and 10- μ m in situ SHRIMP-RG analyses of the clays are consistently ~1.5 wt. % (Benson, 2018). These Li-rich sediments are present throughout much of the ~40 x 30 km caldera, leading Castor and Henry (2020) to estimate a total Li mass of up to 120 Mt Li (640 Mt LCE) contained within the McDermitt caldera lacustrine sediments.

To better understand the geology and metallogeny of this uniquely high-grade and large deposit, Lithium Americas Corp. launched a new multi-institutional collaborative research project with over 20 researchers from universities and federal

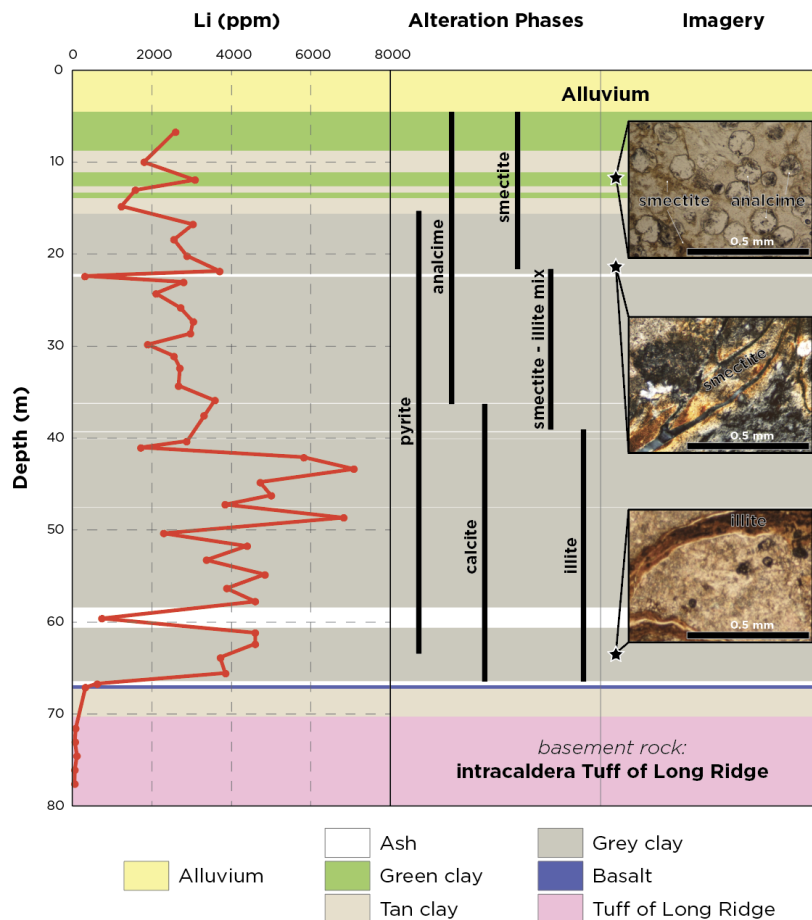


Fig.1. Representative whole-rock drill core assay data from the Thacker Pass project demonstrating consistently high Li concentrations > 2,000 ppm Li. Also shown are phases determined via X-ray diffraction and thin section images of different portions of the caldera lake sequence.

labs across North America in summer 2021. New data from this collaboration indicate that the bulk of the Li-bearing clays likely precipitated as neoformed Mg-rich, Al-poor (Stillings and Godfrey, 2018) trioctahedral smectites (hectorite) within a high-pH, high-alkalinity closed caldera lake system. At the base of the sedimentary section, the hectorite likely underwent thermal diagenesis to a Li-rich illite due to the interaction of hydrothermal fluids with meteoric water driven by devitrification and degassing of the underlying intracaldera Tuff of Long Ridge and residual magma (Ingraffia et al., 2020). This provided sustained high temperatures and added F-rich fluids and additional Li to the system, altering the smectites to illites and trapping most of the Li in the octahedral site of the illite. The illitic zone contains the extremely Li-rich clays, with whole-rock concentrations consistently over 4,000 ppm Li and up to 9,000 ppm Li (Fig. 1). Illite clay separates from this zone average 1.2 wt. % Li (Stillings and Godfrey, 2018).

We hypothesize that the McDermitt caldera lake sediments have a distinctively higher grade than other sedimentary resources because: 1) the magma chamber was initially enriched in Li (Benson et al., 2017); 2) the sediments formed in a closed lake system thermodynamically favorable for the precipitation of Mg-smectites; and 3) prolonged degassing of residual magma and devitrification of intracaldera tuff added excess fluids rich in Li to the base of the system (Fig. 2). The ongoing research with external collaborators aims to expand and improve upon this model using advanced mineral structure characterization techniques, Li and stable isotopic analyses, K-Ar, $^{40}\text{Ar}/^{39}\text{Ar}$, and U-Pb geochronology, melt inclusion analyses, trace element geochemistry, hydrogeochemistry, and 3D geological mapping.

- Benson, T.R., 2018. The volatility of lithium and implications for the formation of world-class hard rock, sedimentary, and brine deposits. American Geophysical Union Fall Meeting, Washington, District of Columbia. <https://agu.confex.com/agu/fm18/meetingapp.cgi/Paper/349035>
- Benson, T. R., Coble, M. A., Rytuba, J. J., and Mahood, G. A., 2017. Lithium enrichment in intracaldera rhyolite magmas leads to Li deposits in caldera basins. *Nature Communications*, 8. <https://doi.org/10.1038/s41467-017-00234-y>
- Castor, S. B., and Henry, C. D., 2020. Lithium-rich claystone in the McDermitt Caldera, Nevada, USA: Geologic, mineralogical, and geochemical characteristics and possible origin. *Minerals*, 10, 1-39. <https://doi.org/10.3390/min10010068>
- Ehsani, R., Fourie, L., Hutson, A., Peldiak, D., Spiering, R., Young, J., and Armstrong, K., 2018. Technical report on the pre-feasibility study for the Thacker Pass Project, Humboldt County, Nevada, USA for Lithium Americas, 238p. <https://www.lithiumamericas.com/resources/pdf/investors/technical-reports/thacker-pass/Technical-Report-Thacker-Pass.pdf>
- Ingraffia, J., Ressel, M.R., and Benson, T.R., 2020. Thacker Pass lithium clay deposit, McDermitt Caldera, north-central Nevada: Devitrification of McDermitt Tuff as the main lithium source. In: Koutz, F.R. and Pennell, W.M., (Eds.), *Vision for Discovery: Geology and Ore Deposits of the Great Basin*, Geological Society of Nevada 2020 Symposium Proceedings, Reno, Nevada, pp. 395-410.
- Stillings, L.L., and Godfrey, L.V., 2018. Isotopic Composition of Lithium in Lithium-bearing clays from the Southwestern US. American Geophysical Union Fall Meeting, Washington, District of Columbia. <https://agu.confex.com/agu/fm18/meetingapp.cgi/Paper/453650>

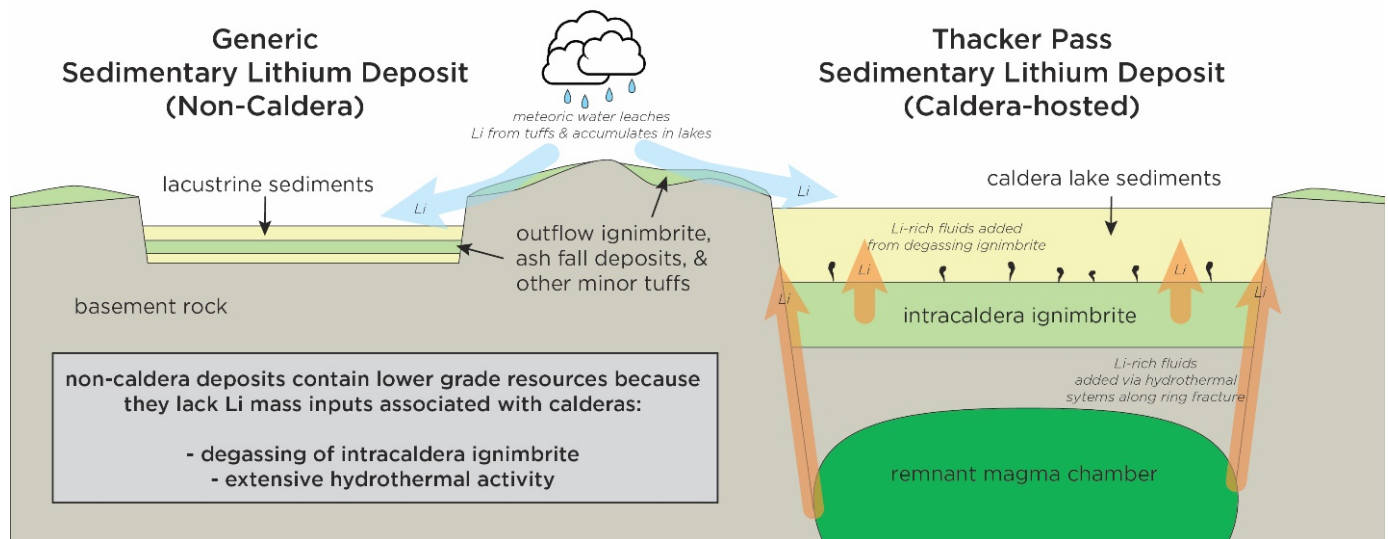


Fig. 2. Cartoon model illustrating the additional Li mass inputs to caldera lakes (orange arrows) not observed in lower grade non-caldera sedimentary Li deposits. In both scenarios, Li-bearing volcanic glass in ash layers and tuffs (blue arrows) contribute Li mass.

Development of a mineralized brine resource: The Hell’s Kitchen lithium and power project, Salton Sea, USA

Fiorella Sist^{1a}

¹ Controlled Thermal Resources (US) Inc, Imperial, CA 92251, USA
^afiorella.sist@cthermal.com

By combining geothermal power with direct lithium extraction (DLE), Controlled Thermal Resources (CTR) is setting new benchmarks to provide renewable energy to the western U.S. and to deliver the most sustainable, battery-grade lithium products in the world today. CTR’s Hell’s Kitchen Geothermal (HKG) power and lithium project is situated within the heart of the largest known geothermal resource in the world, called the Salton Sea Known Geothermal Resource Area (SSKGRA). For several decades the area has been home to several geothermal plants where their deep wells have tapped into the hot geothermal brine resource to extract the super-heated steam to drive turbines that produce electricity. In addition to the valuable heat contained in the hot brine is the rich concentration of dissolved minerals. The HKG technology will extract both the valuable heat and dissolved lithium, to produce both power and battery-grade lithium products at near-zero carbon footprint. This will be done by designing a fully integrated process that uses the well-established power

plant technology with novel DLE engineering techniques. This involves the use of renewable electricity and steam from the geothermal power plant to produce battery-grade lithium hydroxide in the adjacent DLE process. The fit-for-purpose plant design will use the available steam from geothermal brine to crystallize chemicals into final lithium products.

All the electricity, heat, and steam that drives these processes is produced onsite and has a near-zero carbon footprint, which is unique to geothermal-lithium operations and offers an environmental advantage relative to evaporation brine and hard rock resources that require burning fossil fuels to produce lithium. Furthermore, designing geothermal-lithium facilities from a greenfield site has advantages in comparison to ‘bolting on’ DLE processes to established geothermal facilities or other types of industrial units. For example, some geothermal power plants currently employ triple-flash technology to produce power (Fig. 1). In this process, the hot brine undergoes three consecutive separation stages: high pressure (HP); standard

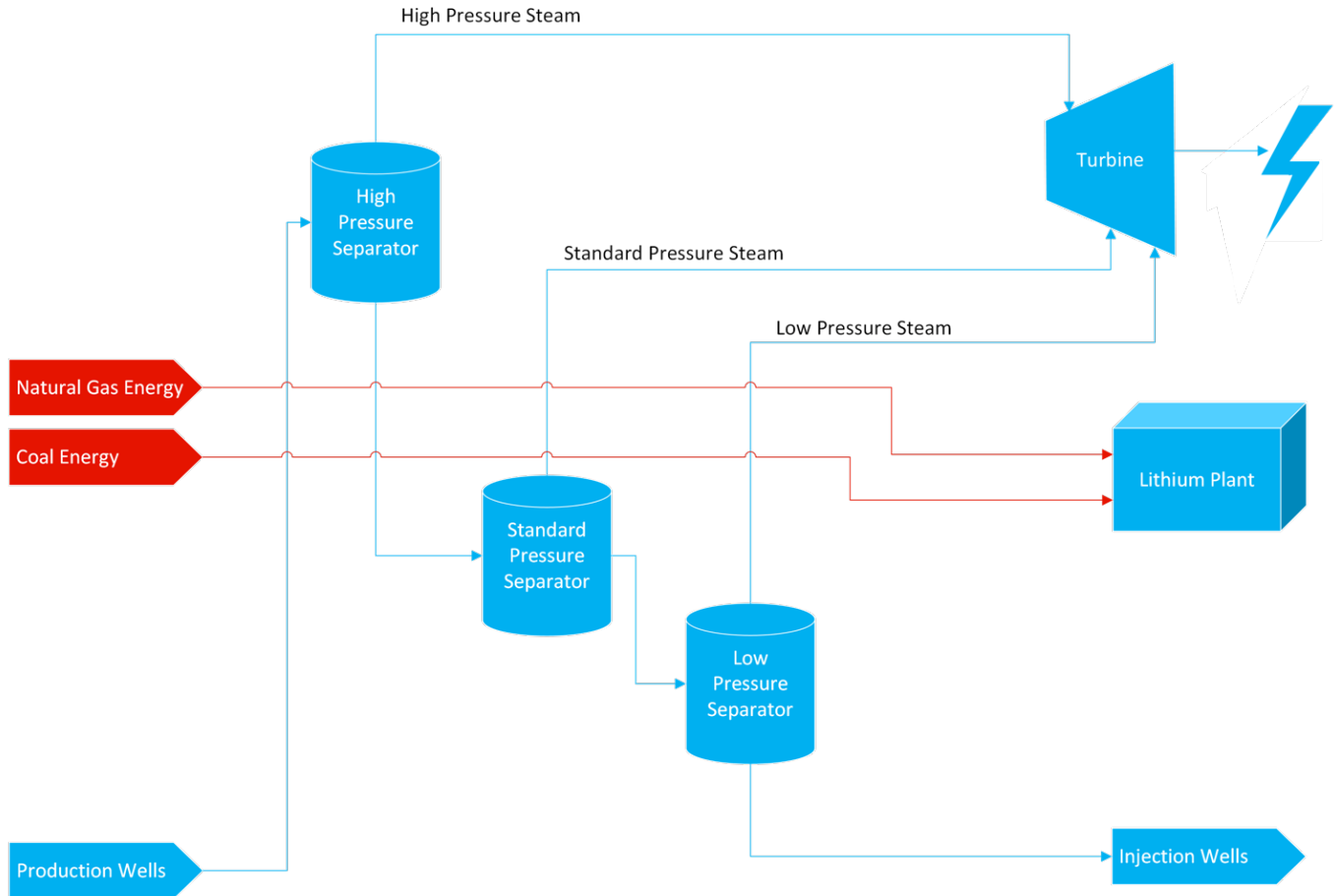


Fig.1. Triple flash plant design.

pressure (SP); and low pressure (LP). The steam flows generated at each stage are then directed to the turbine to produce electricity. The HKG process will instead use single-flash technology, where a fully integrated power generation and lithium production plant uses various steam flows (Fig. 2). In this process, the HP steam is directed to the turbine, while the SP and LP steam flows are used in the adjacent lithium production. Lithium production requires a significant amount of heat. In contrast to brownfield geothermal processes, which may need to generate heat by burning fossil fuels, the HKG design uses SP and LP steam in the lithium plant, thus eliminating the need for external power and heat. The HKG design involves a fully integrated power and lithium process that is built fit-for-purpose to distribute the steam efficiently, avoiding the need to import energy and thus yielding cost reductions and smaller carbon footprints.

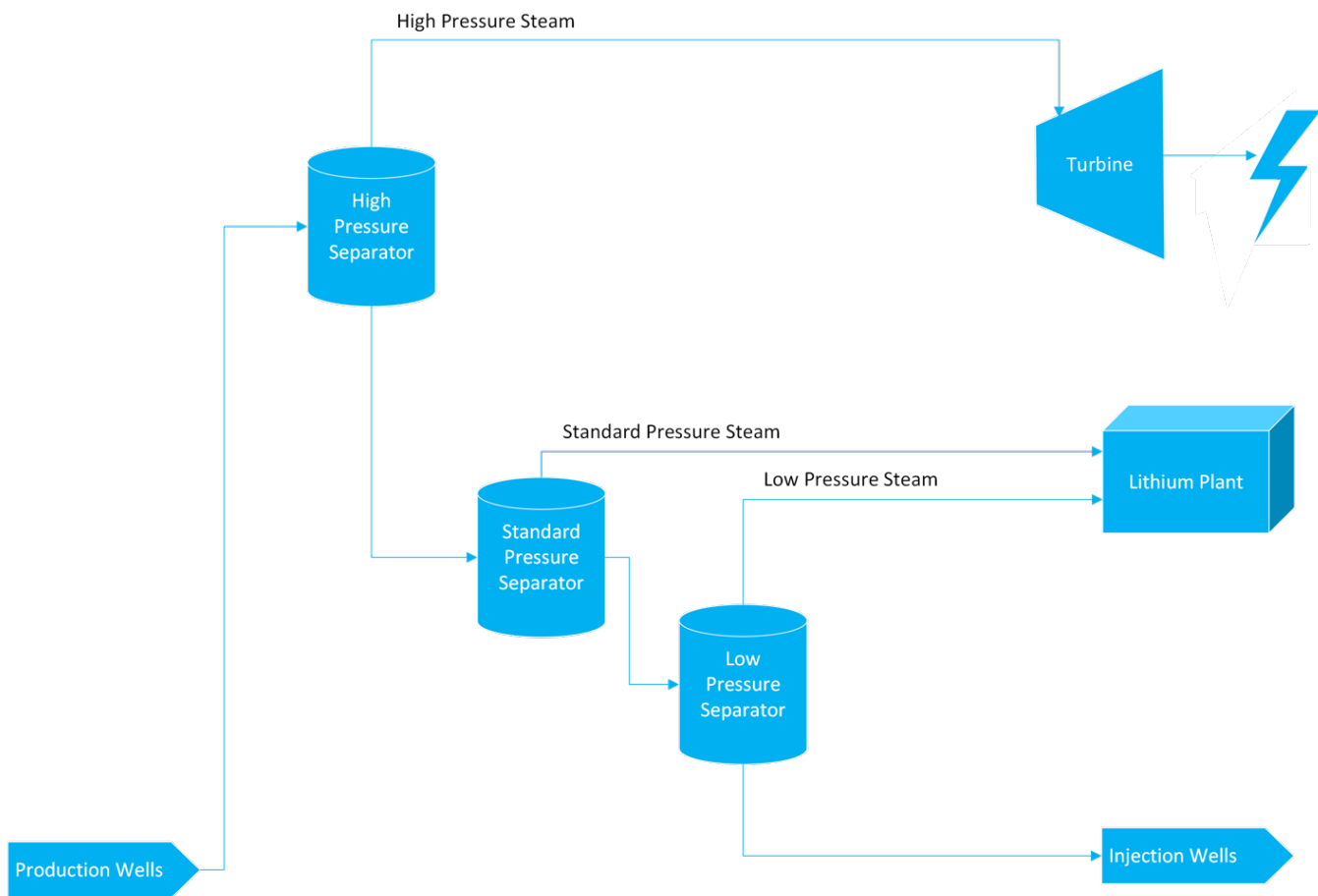


Fig.2. Single flash plant design.

Session 6: Exploration methods and technical considerations

Thursday November 18, 16:30 PST (0:30 GMT)

List of speakers

Chair: George Simandl, British Columbia Geological Survey

M. Beth McClenaghan, Geological Survey of Canada
Application of indicator mineral methods to critical material exploration

René Booyesen, Helmholtz Institute Freiberg for Resource Technology
Multi-scale and multi-source remote sensing of REEs in southern Africa

Mike D. Thomas, Geological Survey of Canada
Use of geophysical methods in exploration for critical materials

Sandra Lorenz, Helmholtz Institute Freiberg for Resource Technology
Outcrop sensing for the exploration of REEs and lithium

Tassos Grammatikopoulos, SGS Canada Inc.
Integration of process mineralogy in critical element deposits

John R. Goode, J.R. Goode and Associates
Rare earth elements: Challenges facing present and potential producers

Moritz Kirsch, Helmholtz Institute Freiberg for Resource Technology
Multi-source hyperspectral imaging of drill cores for the exploration of critical minerals

Question and answer period

Application of indicator mineral methods to critical material exploration

M. Beth McClenaghan^{1a}

¹ Geological Survey of Canada, Ottawa ON K1A 0E8, Canada

^a beth.McClenaghan@nrcan-rncan.gc.ca

Indicator minerals (IM) are mineral species that, when recovered as transported grains in clastic sediments, indicate the presence of a specific type of bedrock mineralization, hydrothermal alteration, or lithology. Their physical and chemical characteristics, which include a moderate to high density, facilitate their preservation and identification and allow them to be readily recovered from soil, glacial, stream, or eolian sediments and used to outline exploration targets that can be larger than their bedrock source. IM are separated from a sample, examined and, in some cases, analyzed chemically to provide information about the bedrock source that traditional sediment geochemical methods cannot, including nature of the ore or alteration and proximity to source. In the past 30 years, indicator mineral methods have expanded to become an important exploration method for a broad range of commodities including critical metals.

Numerous studies of known critical metal-bearing deposits have identified indicator mineral suites, their compositional ranges, and key chemical discrimination criteria (e.g., Cooke et al., 2017). Results of these bedrock studies can be applied to the minerals recovered from moderately heavy and heavy mineral fractions of sediment samples collected in regional exploration surveys. Individual mineral grains can be analyzed to determine their major and trace element and isotopic signatures and inclusion mineralogy to identify the specific style of mineralization that is the source of the grains. Historically, the focus has been on visual identification of indicator minerals in the sand-sized fraction, with subsequent mineral chemistry analysis by electron microprobe techniques. Modern mineral identification methods now also include automated mineralogy (e.g., MLA, QEMSCAN, TIMA, μ XRF) and laser ablation ICP-MS techniques applied to sand- and silt-sized mineral grains.

Porphyry copper deposits are significant sources of the critical metals Cu, Mo, and Re. IM methods useful for porphyry copper exploration include the ore minerals chalcocite, molybdenite (Fig. 1a,b), chalcocite, and gold as well as heavy (>3.2 g/cm³) oxide and silicate minerals such as andradite garnet, rutile, titanite, epidote, zircon and magnetite (e.g., Scott, 2005; Averill, 2011; Kelley et al., 2011; Plouffe and Ferbey, 2017; Chapman et al., 2018; Lee et al., 2021). The IM suite also includes mid-density (2.8 - 3.2 g/cm³) minerals such as tourmaline (Fig. 1c), apatite, and fluorite (Fig. 1d; e.g., Averill, 2011; Mao et al., 2016; Beckett-Brown et al., 2021) and the secondary mineral jarosite (Kelley et al., 2011; McClenaghan et al., 2020). Several case studies at known deposits have shown how IM chemistry can be used to link the minerals in sediment samples to their mineralized source rocks (e.g., Pisiak et al., 2017; Mao et al., 2017; Plouffe et al., 2021).

Rare earth element deposits hosted in carbonatites, peralkaline complexes, peraluminous granites, and granitic pegmatites also contain IM that can be readily recovered

from sediments samples. These minerals include pyrochlore (Fig. 1e), columbite-tantalite, spodumene, monazite (Fig. 1f), bastnaesite, allanite, fluorite (Fig. 1d), and spodumene (e.g., Makin et al., 2014; Mao et al., 2015, 2017; MacKay and Simandl, 2015; MacKay et al., 2016). Regional surveys and case studies around these deposits demonstrate how IM methods can be applied to REE exploration (e.g., Tripp et al., 2009; MacKay et al., 2015; Lehtonen et al., 2011; Simandl et al., 2017; McClenaghan et al., 2019).

Other critical metal deposits for which IM can be especially useful include Sn and W deposits because they can contain particularly rugged minerals such as cassiterite, scheelite, and topaz (Fig. 1g,h; e.g., McClenaghan et al., 2017a,b). Recent studies of scheelite chemistry demonstrate how mineral chemistry can provide insights into mineralization type upstream or up-ice of these IMs in sediment samples (Poulin et al. 2017, 2018).

- Averill, S.A. 2011. Viable indicators in surficial sediments for two major base metal deposit types: Ni-Cu-PGE and porphyry Cu. *Geochemistry: Exploration, Environment, Analysis*, 11, 279-291.
- Beckett-Brown, C.E., McDonald, A.M., McClenaghan, M.B., Plouffe, A., and Ferbey, T., 2021. Investigation of tourmaline characteristics in bedrock and surficial sediment samples from two Canadian porphyry copper systems. In: Schetselaar, E. and Plouffe, A. (Eds.), *Targeted Geoscience Initiative 5: Contributions to the understanding and exploration of porphyry deposits*, Geological Survey of Canada, Bulletin 616, pp. 109-135.
- Chapman, R.J., Allan, M.M., Mortensen, J.K., Wrighton, T.M., and Grimshaw, M.R., 2018. A new indicator mineral methodology based on generic Bi-Pb-Te-S mineral inclusion signature in detrital gold from porphyry and low/intermediate sulfidation epithermal environments in Yukon Territory, Canada. *Mineralium Deposita*, 53, 815-834.
- Cooke, D.R., Agnew, P., Hollings, P., Baker, M., Chang, Z., Wilkinson, J.J., White, N.C., Zhang, L., Thompson, J., Gemmill, J.B., Fox, N., Chen, H. and Wilkinson, C.C., 2017. Porphyry Indicator Minerals (PIMS) and porphyry vectoring and fertility tools (PVFTS) – Indicators of mineralization styles and recorders of hypogene geochemical dispersion halos. In: Tschirhart, V. and Thomas, M.D. (Eds.) *Proceedings of Exploration 17: Sixth Decennial International Conference on Mineral Exploration*, pp. 457-470.
- Kelley, K.D., Eppinger, R.G., Lang, J., Smith, S.M., and Fey, D.L., 2011. Porphyry Cu indicator minerals in glacial till samples as an exploration tool: example from the giant Pebble porphyry Cu-Au-Mo deposit, Alaska, USA. *Geochemistry: Exploration, Environment, Analysis*, 11, 321-334.
- Lee, R.G., Plouffe, A., Ferbey, T., Hart, C.J.R., Hollings, P., and Gleeson, S.A., 2021. Recognizing porphyry copper potential from till zircon composition: A case study from the Highland Valley porphyry district, south-central British Columbia; *Economic Geology*, 116, 1035-1045.
- Lehtonen, M., Laukkanen, J., and Sarala, P., 2011. Exploring RE and REE mineralization using indicator minerals. In: *Indicator Mineral Methods in Mineral Exploration, Workshop 3, 25th International*



Fig. 1. Colour photographs of sand-sized indicator minerals recovered from sediment samples down ice or downstream of critical metal deposits in Canada. **a)** chalcopyrite, **b)** molybdenite, **c)** tourmaline, **d)** fluorite, **e)** pyrochlore, **f)** monazite, **g)** cassiterite, and **h)** scheelite. Photographs by Michael J. Bainbridge Photography.

Applied Geochemistry Symposium, Rovaniemi, Finland, Association of Applied Geochemists, pp. 13-18.
 Mao, M., Simandl, G.J., Spence, J., and Marshall, D., 2015. Fluorite trace-element chemistry and its potential as an indicator mineral: Evaluation of LA-ICP-MS method. In: Simandl, G.J. and Neetz, M., (Eds.) Symposium on Strategic and Critical Materials Proceedings, November 13-14, 2015, Victoria, British Columbia. British Columbia Ministry of Energy and Mines, British Columbia Geological Survey Paper 2015-3, pp. 251-264.
 Mao, M., Rukhlov, A., Rowins, S., Spence, J., and Coogan, L.A., 2016. Apatite trace element compositions: A robust new tool for mineral exploration. *Economic Geology*, 111, 1187-1222.

Mao, M., Rukhlov, A.S., Rowins, S.M., Hickin, A.S., Ferbey, T., Bustard, A., Spence, J., and Coogan, L.A., 2017. A novel approach using detrital apatite and till geochemistry to identify covered mineralization in the TREK area of the Nechako Plateau, British Columbia. In: Ferbey, T., Plouffe, A., and Hickin, A.S., (Eds.), *Indicator Minerals in Till and Stream Sediments of the Canadian Cordillera*. Geological Association of Canada Special Paper Volume 50, Topics in Mineral Sciences 47, pp. 191-243.
 Mackay, D.A.R. and Simandl, G.J., 2015. Pyrochlore and columbite-tantalite as indicator minerals for specialty metal deposits *Geochemistry: Exploration, Environment, Analysis*. 15, 167-178.
 Mackay, D.A.R., Simandl, G.J., Grcic, B., Li, C., Luck, P., Redfearn,

- M. and Gravel, J., 2015. Evaluation of Mozley C800 laboratory mineral separator for heavy mineral concentration of stream sediments in exploration for carbonatite-related specialty metal deposits: case study at the Aley carbonatite, British Columbia (NTS 094B), Canada. In: Geoscience BC Summary of Activities 2014. Geoscience BC, Report 2015-1, pp. 111–122.
- Mackay, D.A.R., Simandl, G.J., Ma, W., Redfean, M. and Gravel, J., 2016. Indicator mineral-based exploration for carbonatites and related specialty metal deposits—A QEMSCAN® orientation survey, British Columbia, Canada. *Journal of Geochemical Exploration*, 165, 159-173.
- Makin, S.A., Simandl, G.J. and Marshall, D., 2014. Fluorite and its potential as an indicator mineral for carbonatite-related rare earth element deposits. In: *Geological Fieldwork 2013*. British Columbia Ministry of Energy and Mines, British Columbia Geological Survey, Paper 2014-1, pp. 207–212.
- McClenaghan, M.B., Parkhill, M.A., Pronk, A.G., and Sinclair, W.D., 2017a. Indicator mineral and till geochemical signatures of the Mount Pleasant W-Mo-Bi and Sn-Zn-In deposits, New Brunswick, Canada. *Journal of Geochemical Exploration*, 172, 151-166.
- McClenaghan, M.B., Parkhill, M.A., Pronk, A.G., Seaman, A.A., McCurdy, M., and Leybourne, M.I., 2017b. Indicator mineral and till geochemical signatures associated with the Sisson W-Mo deposit, New Brunswick, Canada. *Geochemistry: Exploration, Environment, Analysis*, 17, 297-313.
- McClenaghan, M.B., Paulen, R.C. and Kjarsgaard, I.M., 2019. Rare Metal indicator minerals in bedrock and till at the Strange Lake peralkaline complex, Quebec and Labrador, Canada. *Canadian Journal of Earth Sciences*, 56, 857-869.
- McClenaghan, M.B., McCurdy, M.W., Garrett, R.G., Beckett-Brown, C.E., and Casselman, S.G., 2020. Indicator mineral signatures of the Casino porphyry Cu-Au-Mo deposit, Yukon. *Geological Survey of Canada*, Open File 8711.
- Pisiak, L.K., Canil, D., Plouffe, A., Ferbey, T., and Lacourse, T., 2017. Magnetite as an indicator mineral in the exploration of porphyry deposits; a case study in till near the Mount Polley Cu-Au deposit, British Columbia, Canada. *Economic Geology*, 112, 919–940.
- Plouffe, A., and Ferbey, T., 2017. Porphyry Cu indicator minerals in till: a method to discover buried mineralization. In: Ferbey, T., Plouffe, A., and A. Hickin, A. (Eds.) *Indicator minerals in till and stream sediments of the Canadian Cordillera*. Geological Association of Canada, Special Volume 50, Topics in Mineral Sciences 47, pp. 129–159.
- Plouffe, A., Acosta Gongora, P., Kjarsgaard, I.M., Petts, D., Ferbey, T., and Venance, K.E., 2021. Detrital epidote chemistry: detecting the alteration footprint of porphyry Cu mineralisation in the Canadian Cordillera. In: Schetselaar, E. and Plouffe, A. (Eds.) *Targeted Geoscience Initiative 5: Contributions to the understanding and exploration of porphyry deposits: Geological Survey of Canada, Bulletin 616*, pp. 137-157.
- Poulin, R.S., McDonald, A., Kontak, D.J., and McClenaghan, M.B., 2017. On the spatial relationship between cathodoluminescence responses and the chemical composition of scheelite from geologically diverse ore-deposit environments. *The Canadian Mineralogist*, 54, 1147-1173.
- Poulin, R.S., McDonald, A., Kontak, D.J., and McClenaghan, M.B., 2018. Assessing scheelite as an ore-deposit discriminator using its trace-element and REE chemistry. *The Canadian Mineralogist*, 56, 265-302.
- Simandl, G.J., Mackay, D.A.R., Ma, X., Luck, P., Gravel, J., and Akam, C., 2017. The direct indicator mineral concept and QEMSCAN® applied to exploration for carbonatite and carbonatite-related ore deposits. In: Ferbey, T., Plouffe, A., and Hickin, A.S., (Eds.) *Indicator Minerals in Till and Stream Sediments of the Canadian Cordillera*. Geological Association of Canada Special Paper Volume 50, and Mineralogical Association of Canada Topics in Mineral Sciences Volume 47, pp. 175-190.
- Scott, K.M. 2005. Rutile geochemistry as a guide to porphyry Cu-Au mineralization, Northparkes, New South Wales, Australia. *Geochemistry: Exploration, Environment, Analysis*, 5, 247-253.
- Tripp, R.B., Bensen, W.M., Adams, D.T., Loweres, H.A., Lee, G.K., and Bailey, E.A. 2009. Europium-rich dark monazite - a potential new ore mineral for Alaska, USA. *EXPLORE* 145, 2-10.

Multi-scale and multi-source remote sensing of REEs in southern Africa

René Booyesen^{1a}, Robert Zimmermann¹, Robert Jackisch¹, Richard Gloaguen¹, Moritz Kirsch¹, and Sandra Lorenz¹

¹ Helmholtz-Institute Freiberg for Resource Technology, Freiberg, Germany

^a corresponding author: r.booyesen@hzdr.de

Technological advancements have led to an increased demand for rare earth elements (REEs), resulting in them becoming crucial to ensure the transformation towards green technologies (Dutta et al., 2016). At the same time, the world's REE supply is monopolized by a limited number of countries (Simandl, 2014). A renewed and sustainable exploration approach is required to ensure a more ethical and global supply of REEs. For this, we suggest the use of a multi-scale and multi-source remote sensing workflow. Conventional exploration methods typically involve extensive fieldwork and geochemical lab work supported by geophysical surveying. This approach however, can be constrained by several factors such as the area size and accessibility, climate, and finances as well as the lack of a social licence to operate. The suggested multi-scale, multi-source approach uses optical remote sensing data from multiple platforms with increasing spatial resolution. We use multispectral satellite data, plane-based hyperspectral data, unmanned aerial vehicle (UAV)-based hyperspectral data and validate the findings with in-situ measurements. Our suggested method can mitigate the disadvantages of traditional exploration techniques by allowing for fast, systematic, and dense surveying, particularly in inaccessible and remote areas with little infrastructure. Additionally, a generally less-invasive

technique garners a higher social acceptance for the mining and exploration community. We demonstrate our approach from work at the Marinkas Quellen carbonatite complex in Namibia.

The proposed multi-scale remote sensing workflow commences with the processing and geological analyses of satellite data. Optical satellite data, which we use for large-scale structural and geological mapping, are freely available and typically extend across a large area. However, freely available satellite data usually have a low spatial resolution (10-30 m) and most are multispectral. To solve these drawbacks, potential target areas identified with satellite data are then investigated with airplane-based hyperspectral imaging (HSI; e.g., HyMap data). HSI sensors usually acquire information in up to hundreds of contiguous spectral bands from the visible and near-infrared (VNIR) to the short-wave infrared (SWIR) part of the electromagnetic spectrum. They also offer a medium spatial resolution of a few m (average 5 m). This allows us to identify narrow absorption features and discern between characteristic spectral features better than with multispectral satellite data. Below we illustrate the use of HyMap data over the Marinkas Quellen carbonatite body where we applied supervised learning algorithms, in this case support vector machines (SVM), to identify and discriminate between carbonatite types (Fig. 1).

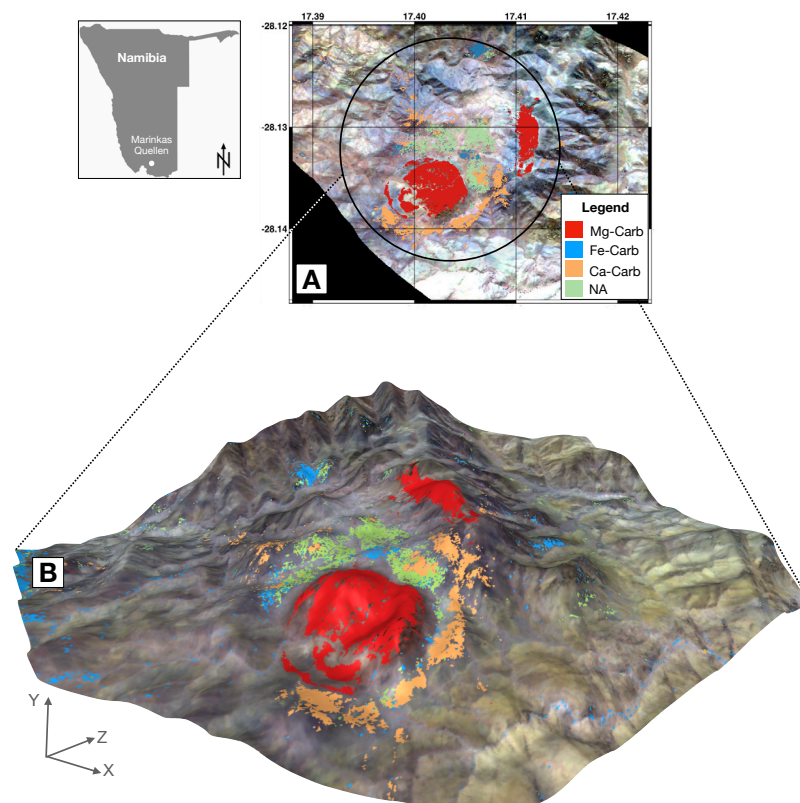


Fig. 1. Resulting HyMap data over the Marinkas Quellen carbonatite complex; inset shows its location in Namibia. **a)** SVM classification of the different carbonatite types at the complex overlain onto a HyMap false colour composite image. **b)** The classification result displayed onto a 3D model of the area.

We were able to improve the existing geological map, select target zones for further detailed investigation with UAVs, and be better informed before fieldwork.

Once in the field, we used a lightweight hyperspectral frame-based sensor (e.g., Senop Rikola) attached to a multi-rotor UAV to capture data in the VNIR with cm-scale spatial resolution. UAV-based hyperspectral data can bridge the spatial resolution gap between airplane-based data and ground measurements. Furthermore, areas inaccessible on foot can be safely surveyed with UAVs, with the added advantage of fast and flexible data acquisition. Before analyses, we apply robust pre-processing methods set out by Jakob et al. (2017) to the UAV-based hyperspectral data to ensure a geometrically and spectrally correct dataset. The workflow then allows for the creation of spatially continuous mineral maps over outcropping bodies to detect mineralized zones and improve sampling strategies. We highlight the benefits of UAV-based hyperspectral imaging from a selected target zone in Marinkas Quellen to map REEs in outcropping carbonatites (Fig. 2 a). Neodymium (Nd), a key pathfinder, has characteristic absorption features at 580 nm, 740 nm, and 800 nm of the electromagnetic spectrum (Turner et al., 2015). We were able to identify the 800 nm absorption feature in the hyperspectral data and used minimum wavelength mapping (MWM) to detect and map the presence of Nd (Fig. 2 b). To validate the results, we captured in-situ spectral measurements with a handheld spectrometer, which verified the presence of Nd through its characteristic absorption features. Additionally, samples were collected for mineralogical and geochemical analyses that included XRD, XRF and ICP-MS. The results indicated that high amounts of REEs are in the outcrop.

The proposed multi-scale remote sensing approach allows us to survey an area of interest rapidly, efficiently and safely. By

using the full potential of remote sensing data from satellite to UAV, we can take advantage of each platform's benefits and mitigate their drawbacks. Furthermore, accurate pre-processing of UAV-based hyperspectral data allowed us to directly detect REEs in an outcrop. Currently, our UAVs approach has been restricted to the acquisition of VNIR data, which limits the amount of rock types that can be identified. However, we are currently working on acquiring UAV-based hyperspectral SWIR data to extend mineral mapping abilities. We thank the Geological Survey of Namibia for their continuous support during field work and for supplying the HyMap data over the Marinkas Quellen carbonatite body.

- Booyesen, R., Jackisch, R., Lorenz, S., Zimmermann, R., Kirsch, M., Nex, P. A. M., and Gloaguen, R., 2020. Detection of REEs with lightweight UAV-based hyperspectral imaging. *Scientific Reports*, 10, 1-12.
- Dutta, T., Kim, K.H., Uchimiya, M., Kwon, E.E., Jeon, B.H., Deep, A., and Yun, S.T., 2016. Global demand for rare earth resources and strategies for green mining. *Environmental Research*, 150, 182-190.
- Jakob, S., Zimmermann, R., and Gloaguen, R., 2017. The need for accurate geometric and radiometric corrections of drone-borne hyperspectral data for mineral exploration: Mephysto—A toolbox for pre-processing drone-borne hyperspectral data. *Remote Sensing*, 9, 88.
- Simandl, G.J., 2014. Geology and market-dependent significance of rare earth element resources. *Mineralium Deposita*, 49, 889-904.
- Turner, D., Rivard, B., and Groat, L., 2015. Visible to shortwave infrared reflectance spectroscopy of rare earth element minerals. In: Simandl, G.J., and Neetz, M. (Eds.), *Symposium on critical and strategic materials proceedings*. British Columbia Geological Survey Paper 2015-03, pp. 219-229.

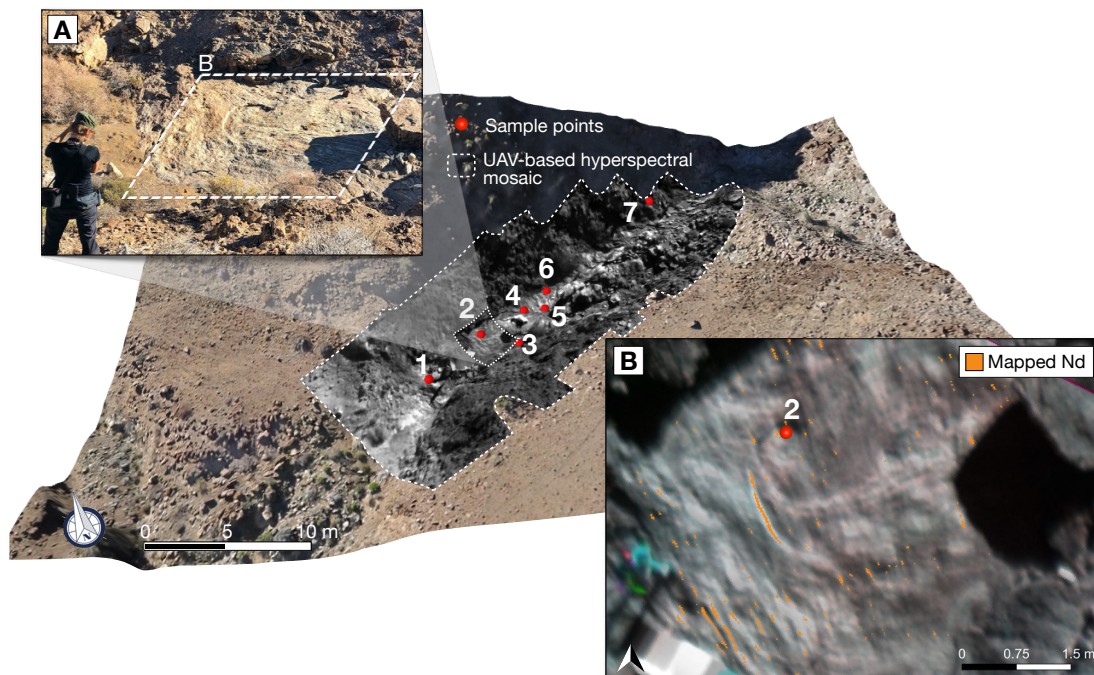


Fig. 2. UAV-based hyperspectral mosaics from a target at the Marinkas Quellen carbonatite complex overlain onto a 3D model indicating sampling locations for ground validation. **a)** Field photo of the area with sample site 2 used for REE mapping. **b)** Close up of the area with sample site 2; mapped Nd in orange overlain onto the UAV-based false colour composite image (modified after Booyesen et al., 2020).

Use of geophysical methods in exploration for critical materials

M.D. Thomas^{1a}

¹ Geological Survey of Canada, Ottawa ON K1A 0E8, Canada

^a mike.thomas@nrcan-rcan.gc.ca

The Canadian list of critical materials contains 31 materials (Government of Canada, 2021). Considering current concerns with climate change and the environment that promote major initiatives to phase out petroleum-powered vehicles and to shift to battery-powered electric vehicles, this study focuses on geophysical exploration for certain critical materials required for state-of-the-art batteries and environmentally friendly technology such as grid-storage. These critical materials include aluminum, cobalt, copper, graphite, lithium, nickel and tantalum.

Geophysical exploration for mineral resources, including those listed above, depends on a contrast in measured physical properties between the mineralization or host rock and adjacent crust. The principal physical properties are density, magnetization, conductivity/resistivity, chargeability, and radioactivity. Depending on size of the target, accessibility, level of detail required, and other factors, gravity, magnetic, electromagnetic (EM)/electrical, and radiometric surveys can be conducted in the air and/or on the ground.

Copper is extracted from a variety of geological settings that include porphyry copper, sedimentary rock-hosted stratabound copper, magmatic sulphide and volcanogenic massive sulphide (VMS) deposits. Exploration for copper mineralization is aided by the generally high densities, magnetic susceptibilities, and electrical conductivities of copper-bearing and associated minerals. For example, in gold-rich porphyry copper deposits gold is typically present in potassic alteration zones commonly associated with high contents of magnetite, making radiometric and magnetic surveys viable exploration tools.

VMS deposits contain mineral assemblages favouring direct detection by several geophysical methods. These assemblages may include pyrite, pyrrhotite, chalcopyrite, sphalerite, galena, magnetite, and hematite. The Bathurst mining camp, New Brunswick, is testament to the success of EM surveys leading to several major discoveries in the 1950s. A newly developed airborne EM system defined several anomalies, and resulted in the first airborne EM success, discovery of the Heath Steele lead-zinc deposit. The efficacy of combined EM and magnetic surveys in VMS exploration is exemplified by discovery of the very small Camel Back deposit ($\leq 200\,000$ tonnes) with its stratiform portion comprising two subparallel lenses, each just roughly 4 m thick.

The challenge in discovering sedimentary stratabound copper deposits is their small thickness combined with large lateral dimensions. Furthermore, if they and their hosting strata are gently dipping, they may produce a long wavelength geophysical response that may be difficult to discern. Nevertheless, induced polarization/resistivity surveys over sedimentary-hosted stratiform copper deposits employing modern inverse techniques provided insight into distribution of mineralization, such as at the Kapunda copper deposit in Australia where a close correlation between copper distribution

and apparent chargeability is observed. On Somerset Island in the arctic, airborne gravity gradiometry and EM signatures correlating with mineralized intersections defined by historic drilling helped delineate stratiform copper mineralization. These successes in geophysical imaging of stratabound copper deposits mitigate concerns for the use of geophysics in their exploration.

Magmatic sulphides host both copper and nickel deposits, and airborne and ground EM surveys have played a major role in their exploration. The deposit in the Thompson nickel belt (Thompson mine) was discovered in the mid-1950s using the airborne EM system presumably used to discover the Heath Steele VMS deposit. In later years EM coverage extended to a depth of at least 1 km for large deposits using techniques such as audiomagnetotellurics surveys and borehole EM. The complex folded geology of Thompson ore bodies has been investigated by cross-hole seismic tomography (Fig. 1), outlining low velocity zones that correspond to sulphide zones intersected by drill-holes. The seismic method is a powerful tool for investigations at great depth, pertinent to mineralization in the Thompson belt and Sudbury structure, where deposits may lie at depths greater than 1 km, such as in the Sudbury structure where one deposit is 2.5 km deep. A 3D seismic experiment in the Sudbury structure imaged prominent circular and semicircular scattering events in horizontal (time) slices of the seismic data, with the strongest events at approximately 1.8 km depth, centred above known mineralization. Gravity surveys also contribute to investigation of magmatic sulphide deposits. The Voisey's Bay Ovoid ore

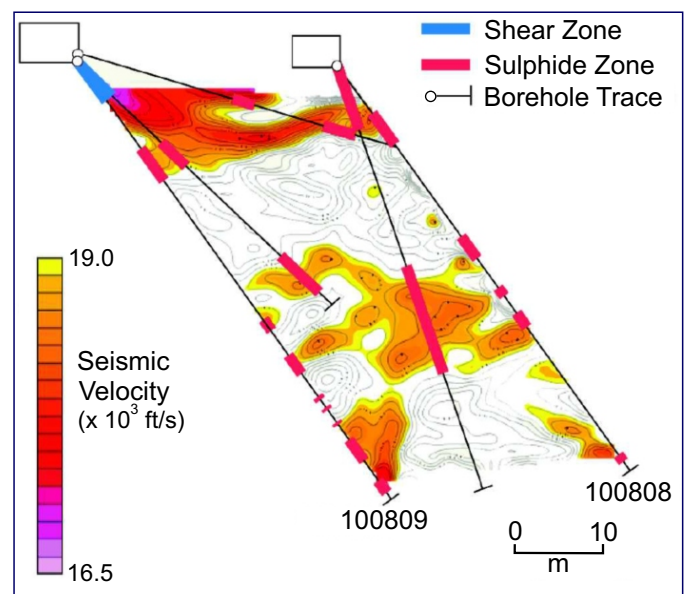


Fig. 1. Seismic tomographic image from the Thompson nickel belt, Manitoba (modified from King (2007)).

body, Labrador, discovered by outcropping NiS mineralization, was traced by EM and magnetic surveys into a wider, highly conductive zone, where drilling intersected the deposit. A subsequent ground gravity survey delineated a strong 4 mGal amplitude anomaly related entirely to massive sulphides, a 3D inversion of which (Fig. 2) delineated iso-surfaces at 0.8 g/cm^3 and 0.4 g/cm^3 that potentially bound the ore deposit.

airborne EM conductivity anomaly. Ground apparent conductivity traversing revealed many conductive structures, with peak conductivity representing individual graphite schist lenses.

Important sources of lithium and tantalum are pegmatites. The quest for exploration, therefore, is to find pegmatites rather than the mineral hosting the desired critical mineral. Geophysically,

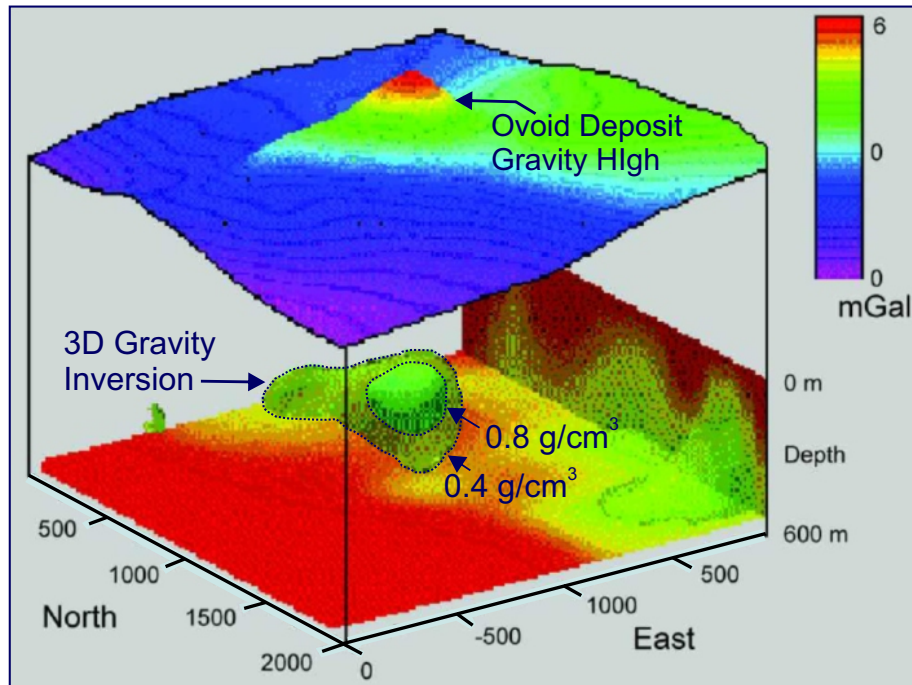


Fig. 2. 3D inversion of gravity data for Voisey's Bay Ovoid ore body showing iso-surfaces for recovered density contrasts of 0.8 g/cm^3 and 0.4 g/cm^3 (modified from King (2007)).

The main source of aluminum is bauxite ore. Several very large bauxite deposits are of the aluminous-laterite blanket type, occurring at or near the surface as flat-lying layers of variable thickness and extent. Generally, they are very thin, with a mean value for several deposits of approximately 5 m, and a maximum value of 80 m. No bauxite is mined in Canada, although there are several aluminum smelters and one refinery. Geophysical exploration for bauxite deposits is challenged by their small thicknesses, and their generally relatively flat-lying nature that result in gravity or magnetic signatures that would also be quite 'flat'. Electrical, EM, and seismic methods, apparently, are better suited to examine the characteristic layered geological setting. Seismic reflection surveys have been applied successfully over bauxite deposits (1 to 40 m thick) resting on a limestone palaeorelief in Bosnia and Herzegovina. Ground penetrating radar (GPR) is useful for defining near-surface bauxite deposits, augmenting speculative traditional approaches to estimate resources that rely on sparsely distributed boreholes.

Graphite production is mainly from flake graphite deposits hosted in metamorphic rocks. The high electrical conductivity of graphite makes EM methods the principal means of exploration. The roughly $2.0 \times 0.5 \text{ km}$ Vardfjellet graphite occurrence in Norway, which includes several subparallel and subvertical graphite-rich lenses, is coincident with a prominent

this is not easy given the broad similarities in mineralogy of felsic igneous rocks, though it has been proposed that lithium pegmatites have anomalously low magnetic susceptibility, and that associated magnetic lows could be detected by high-resolution, low-flying UAV magnetic surveys. In the Bird River belt, Superior Province, images of equivalent uranium (eU) defined by airborne radiometric surveys indicate that many stronger responses correlate with pegmatitic granites, or portions thereof, and pegmatites. In the same belt, the relatively high density of lithium-bearing spodumene within the Tanco deposit allowed delineation of the deposit by gravity surveys.

A significant proportion of global cobalt production is derived from laterites and as a by- or co-product of mining for other base metals, chiefly nickel and copper, exploration for which has been previously discussed.

Government of Canada. 2021. Canada announces critical minerals list. <https://www.canada.ca/en/natural-resources-canada/news/2021/03/canada-announces-critical-minerals-list.html> (Accessed: May 15, 2021).

King, A. 2007. Review of geophysical technology for Ni-Cu-PGE deposits. In: Milkereit, B. (Ed.), Proceedings of Exploration 07: Fifth Decennial International Conference on Mineral Exploration, 647-665.

Outcrop sensing for the exploration of REEs and lithium

Sandra Lorenz^{1a}, René Booyen¹, Sam Thiele¹, Robert Zimmermann¹, Moritz Kirsch¹, and Richard Gloaguen¹

¹ Helmholtz-Institute Freiberg for Resource Technology, Freiberg, Germany

^a corresponding author: s.lorenz@hzdr.de

Non-invasive technologies are key to ensure the sustainable exploration and mining of critical materials such as lithium and rare earth elements (REE), which are needed to fuel battery, magnet, and photovoltaic technologies for the transition towards low-carbon economies (Simandl, 2014; Heredia et al., 2020). Innovative sensing methods such as hyperspectral imaging allow the remote identification and high spatial resolution mapping of characteristic light-material interactions (“spectral fingerprints”) indicative of specific minerals and raw materials. These maps can be produced rapidly to support geological investigations during both exploration and mining. Accurate positioning of the spectral information in 3D space allows creating digital twins of outcrops and mines and integrating the spectral mapping results with other data such as from drill-cores or geochemical sampling. However, the low concentration and generally subtle spectral features associated with Li-bearing minerals and REEs present challenges for spectral mapping at the outcrop scale and, as a result, past approaches tended to use indirect methods based on, for example, mineral associations (Cardoso-Fernandes et al., 2020).

Direct mapping of REE and Li-minerals abundances is possible using high-resolution, high-quality spectral data and appropriate correction techniques. Sensor miniaturisation and development of new platforms now allow rapid data collection across large areas. These advances, combined with novel radiometric and geometric correction workflows (e.g., Thiele et al., 2021), recently allowed the direct detection of REE- and Li-bearing minerals at outcrop scale, using close-range ground-based (Boesche et al., 2015; Booyen et al., 2021) and drone-borne platforms (Booyen et al., 2020).

Two case studies of open pit mines, one from Siilinjärvi, Finland, (Fig. 1), the second from Uis, Namibia (Fig. 2) demonstrate direct 3D mapping of REE and Li mineralization. First, we captured ground-based photographs that were used for structure-from-motion, multi-view-stereo (SfM-MVS) photogrammetry to create digital 3D models/point clouds. We also acquired terrestrial hyperspectral data using a Specim AisaFENIX hyperspectral line scanner (push-broom scanner). The sensor covers the electromagnetic spectrum from 350 to 2500 nm over 384 spatial pixels and creates a datacube

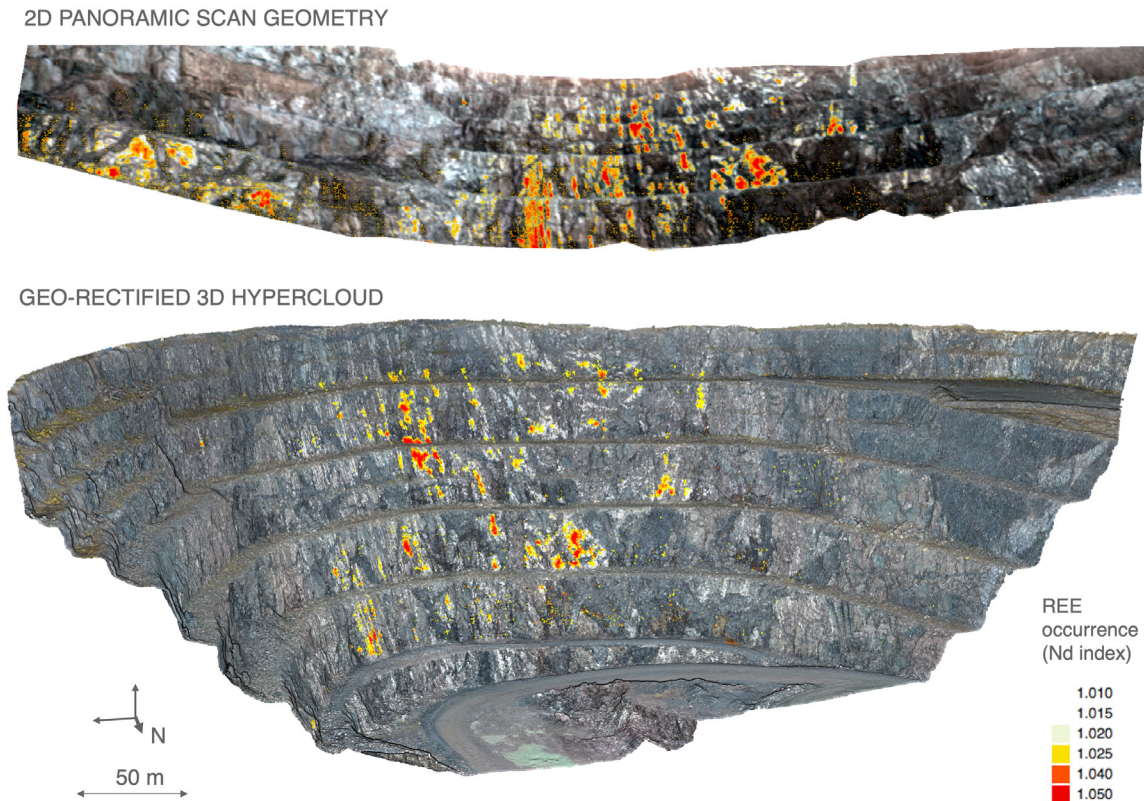


Fig. 1. Direct mapping of REE-bearing zones in the Siilinjärvi Main Pit (Finland) using the distinct absorptions of neodymium at 578 nm, 740 nm and 799 nm as pathfinder. The figure further illustrates the disadvantage of mapping in geometrically uncorrected 2D panoramic scan (top) compared to 3D located hypercloud (bottom), which preserves true spatial relations.

by steady rotation on a tripod. The resulting panoramic scan covers the important spectral features for both REE (578 nm, 740 nm and 799 nm for neodymium) and Li-bearing minerals (1593 nm and 1839 nm for cookeite, and 1538 nm, 1766 nm and 1850 nm for montebrasite). However, the results are subject to immense geometric distortion as well as radiometric influences that complicate spectral mapping, spatial localization, and scaling. We applied the processing workflow of Thiele et al. (2021) to perform accurate re-projection in original 3D space, as well as important radiometric and topographic corrections by combining the hyperspectral scans with the photogrammetric 3D point clouds. We subsequently mapped the occurrence of REEs and Li-bearing minerals based on their subtle characteristic spectral absorptions, and validated the occurrences by field sampling and mineralogical and elemental analysis.

Innovative remote sensing approaches allow us to rapidly create accurate digital twins of mine faces and natural geological outcrops. The 3D point clouds provide information on geological structure and can be populated with an arbitrary number of point-specific, high-dimensional spectral attributes to create so-called “hyperclouds”. Accurate processing and correction of the contained spectral information enables us to directly map the subtle spectral features indicative of Li- and REE-bearing minerals. Efficient remote mapping, even in complex terrains, is highly beneficial not only for initial targeting, but also for monitoring ore extraction, thus facilitating both exploration and optimized extraction.

We thank AfriTin and Yara Oy for support during field work, access to the mine site, and geological information and geochemical data.

- Boesche, N., Rogass, C., Lubitz, C., Brell, M., Herrmann, S., Mielke, C., Tonn, S., Appelt, O., Altenberger, U., and Kaufmann, H., 2015. Hyperspectral REE (Rare Earth Element) Mapping of Outcrops – Applications for Neodymium Detection. *Remote Sensing*, 7, 5160-5186.
- Booyesen, R., Jackisch, R., Lorenz, S., Zimmermann, R., Kirsch, M., Nex, P. A. M., and Gloaguen, R., 2020. Detection of REEs with lightweight UAV-based hyperspectral imaging. *Scientific Reports*, 10, 1-12.
- Booyesen, R., Lorenz, S., Thiele, S. T., Fuchsloch, W., Marais, T., Nex, P. A. M., and Gloaguen, R., (submitted). Accurate hyperspectral imaging of mineralized outcrops: An example from lithium-bearing pegmatites at Uis, Namibia. *Remote Sensing of Environment*.
- Cardoso-Fernandes, J., Teodoro, A. C., Lima, A., Perrotta, M., and Roda-Robles, E., 2020. Detecting Lithium (Li) mineralizations from space: current research and future perspectives. *Applied Sciences*, 10, 1785.
- Heredia, F., Martinez, A. L. and Surraco Urtubey, V., 2020. The importance of lithium for achieving a low-carbon future: overview of the lithium extraction in the ‘Lithium Triangle’. *Journal of Energy & Natural Resources Law*, 38(3), 213-236.
- Simandl, G., 2014. Geology and market-dependent significance of rare earth element resources. *Mineralium Deposita*, 49, 889-904.
- Thiele, S. T., Lorenz, S., Kirsch, M., Cecilia Contreras Acosta, I., Tusa, L., Herrmann, E., Möckel, R. and Gloaguen, R., 2021. Multi-scale, multi-sensor data integration for automated 3-D geological mapping. *Ore Geology Reviews*, 136, 104252.

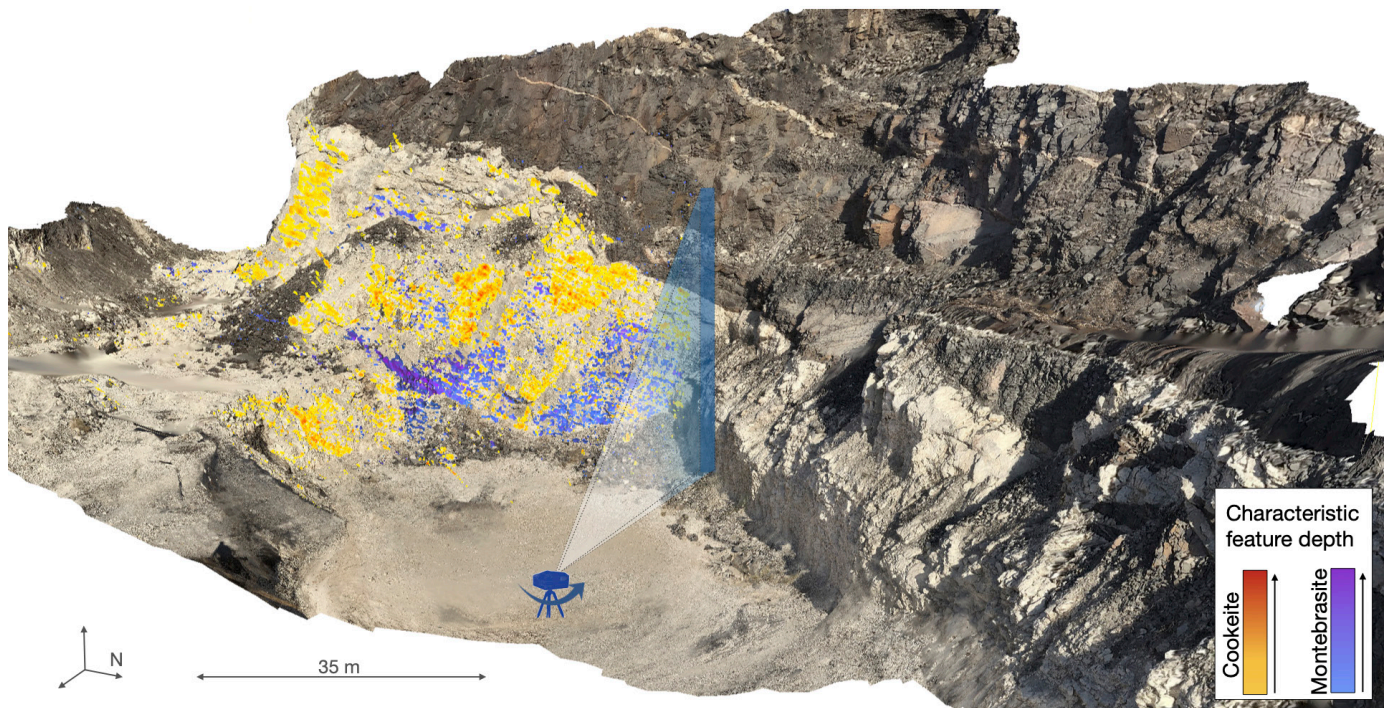


Fig. 2. 3D mineral map of the V1V2 pegmatite body at Uis (Namibia), indicating the occurrence of Li-bearing minerals cookeite and montebrasite based on their indicative spectral features at 1593 and 1538 nm, respectively (modified from Booyesen et al., submitted).

Integration of process mineralogy in critical element deposits

Tassos Grammatikopoulos ^{1,a}

¹ Natural Resources, SGS Canada Inc. Lakefield, ON K0L 2H0, Canada

^a tassos.grammatikopoulos@sgs.com

Quantitative automated mineralogy (QAM) using SEM-based instrumentation (QEMSCAN, MLA, TIMA-X) is widely applied to the study of ore deposits. Automated mineralogy, coupled with geological, geochemical, mineral chemistry and data analysis, are used to solve specific problems from exploration to mining. Most ore deposits bearing critical elements, including REE (rare earth elements), Li, and Nb, are complex. These deposits display a high degree of variability, owing to their inherent geological and mineralogical characteristics, which impact beneficiation. Mineral chemistry and other data can be integrated with QAM. Thus, the data can be applied to metallurgy and mineral processing to avoid extensive and time-consuming bench testing.

Proper mineral identification is critical because: 1) not all minerals are recoverable or rejected using the same process; 2) metals are hosted by a number of minerals; 3) certain minerals might be deleterious and others can carry harmful elements (e.g., U, Th). In most cases, REE deposits are complicated by the presence of multiple REE minerals (phosphates, silicates, fluorocarbonates, and oxides). The mineral speciation by QAM provides guidance to the zonation of the ore and recoverability of minerals and metals (Grammatikopoulos et al., 2013). Deposits can be mapped based on the ratios of heavy/light REE minerals, or REE silicates/phosphates/fluorocarbonates/oxides. REE phosphates and silicates float differently and rejection of either one can lead to low REE grades in concentrates. Geochemical analyses cannot alone be used to calculate the type of minerals and the metal distribution due to the multiple hosts of the minerals.

Grain size, exposure, liberation, and association can indicate the optimum liberation size target and possible grinding effects; recovery methods i.e., flotation using the exposure, or gravity upgrading using the specific gravity characteristics of the minerals. Figure 1 illustrates an example of monazite recoverability as a function of exposure and association by size fraction from a carbonatite composite with 80% passing 212 μm . The calculated liberation of monazite is low at ca. 41% and increases significantly below 106 μm and reaches ca. 60% in the -25 μm size fraction. Therefore, grinding below 106 μm would be required to improve liberation and further recover monazite. The grade and recovery relationships are difficult to understand without detailed mineralogical characterization because of the presence of multiple minerals that carry the REE.

Metal distribution is critical to understand the final recovery or potential contaminants or by-products. For example, spodumene, petalite, Li-bearing micas, and various Li phosphates in granitic pegmatite deposits can have significant internal variability that reflect the original zoning or alteration of the ore. Mineral chemistry analysis determined that Li, Cs, Rb, Ga, Fe can vary widely in spodumene, micas, and feldspars. QAM coupled with mineral chemistry is used to calculate the distribution of Li, Rb, and Cs. For example, spodumene

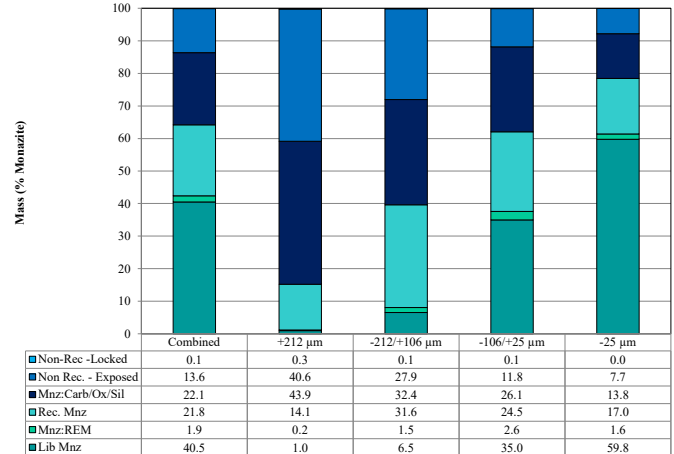


Fig. 1. Liberation of monazite by size fraction

accounts for 96% of the total Li. Micas and phosphates coupled with their low Li concentrations favour a spodumene concentrate, with minimum losses (Grammatikopoulos et al. 2021).

Figure 2 illustrates the theoretical grade-recoveries generated from the QEMSCAN (QS) analysis compared to the actual metallurgical (MET) values from a niobium project. Overall, the metallurgical recoveries fall between 60% and 80% of the total Nb in the samples. When the mineralogically predicted Nb_2O_5 grades and recoveries (QS-1) are higher than the metallurgical ones (MET-1), then this may be attributed to pyrochlore loss as: 1) fine grain size (<20 μm) due to entrainment; 2) coarse particles with poorly exposed surfaces; and 3) liberated coarse grains. Thus, retention flotation time must be increased to recover the fine particles, flash flotation used to recover the coarse and liberated pyrochlore particles, and regrinding the coarser middling particles implemented to increase liberation

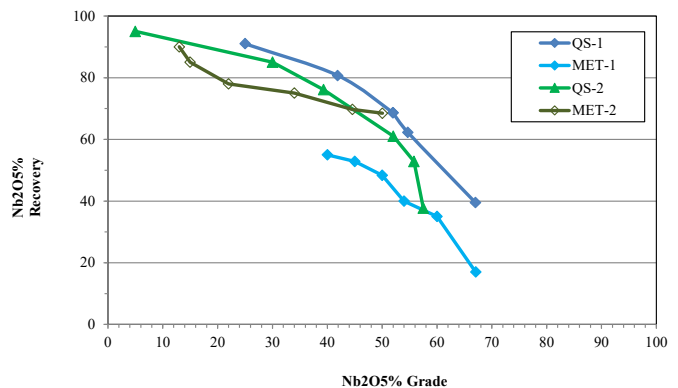


Fig. 2. Grade-recovery curves calculated from the QEMSCAN (QS) and metallurgical (MET) values (after Grammatikopoulos and Downing, 2020).

and surface exposure for flotation. Other samples yield similar mineralogical (QS-2) and metallurgical (MET-2) grades and recoveries (Fig. 2). In these samples, pyrochlore is about 10-20 µm coarser than that in the previous example, and middling particles contain pyrochlore with higher surface exposure and are better recovered. Therefore, the mineralogical information can explain the grade and recovery relations and assist the flotation process to improve the final niobium recovery.

QAM is important in REE, Li, Nb deposits because of the inherent mineralogical variability of the ores and the presence of metals in multiple minerals. It can define geological zones and domains for both exploration and mining. Furthermore, it sets realistic targets for final grades and recoveries, identifies the roots of the metal losses and is an absolute measure of metallurgical performance. Mineral attributes should be effectively integrated in mineral processing and flowsheet development, process optimization, and mine planning.

Grammatikopoulos, T., and Downing, S., 2020. The disruptive role of process mineralogy in geology and mineral processing industry. *Aspects in Mining & Mineral Science*, 5, 571-579.

Grammatikopoulos, T., Mercer, W., and Gunning, C., 2013. Mineralogical characterization using the QEMSCAN of the Nechalacho heavy rare earth metal deposit, Northwest Territories, Canada. *Canadian Metallurgical Quarterly*, 52, 265-277.

Grammatikopoulos, T., Aghamirian, M, Fedikow F., and Mayo T., 2021. Mineralogical characterization and preliminary beneficiation of the Zoro lithium project, Manitoba, Canada. *Mining, Metallurgy & Exploration*, 38, 329-346.

Rare earth elements: Challenges facing present and potential producers

John R. Goode^{1a}

¹ J.R. Goode and Associates, Toronto, ON M2N 6H9, Canada

^a jrgoode@sympatico.ca

Rare earth element (REE) projects include exploration, characterization and development of deposits, followed by mining or in-situ extraction, physical (commonly) and chemical upgrading to prepare an intermediate product, and separation of the REE for marketing (Goode 2019). Challenges that, if overcome, will allow a successful REE project stem from: 1) deposit type, mineralogy, and mining requirements; 2) REE grade; 3) location; and 4) project proponents.

Ionic clay deposits in China and Myanmar supply most of the world's heavy REE (HREE) and are processed by simple, low-cost, leach operations, commonly in-situ. Cerium is usually sequestered as thorium-bearing cerianite (Ce,Th)O₂. Deposits typically contain <0.1% REE and extend from surface to perhaps 20 m below surface meaning that a large area must be disturbed for a reasonable production rate therefore location is critical.

Mineral sand deposits are processed for zircon and/or ilmenite recovery and commonly contain monazite and xenotime, which can be economically co-recovered as high-grade concentrates. Historically, mineral sands were the primary REE source and are still exploited in India and restarted recently in the USA and Australia.

Hard rock deposits contain minerals such as bastnaesite, monazite, and eudialyte, and are usually low grade (typically <5% REE). The minerals are generally difficult to process, and beneficiation to greater than 40% rare earth oxide (REO – common assay convention) is usually essential to allow economical “cracking” of the minerals. Cracking processes need 1 to 3 tonnes of H₂SO₄ or NaOH per tonne of feed. Cracking ore at 4% REO will incur ten times the reagent cost per unit of REO as will a 40% REO concentrate. The minerals dictate the hydrometallurgical process. Caustic cracking works well with phosphate minerals and needs NaOH, CaO, and energy for the cracking process, HCl or HNO₃ to dissolve the REE, and other reagents for production of a mixed REE product. Acid baking is effective on many minerals and requires H₂SO₄ and energy for baking, and other reagents similar to those mentioned earlier. An oxidative roast and weak HCl leach are practised on bastnaesite concentrates at Mountain Pass in USA, and in Sichuan in China. Eudialyte is a REE silicate found in some deposits, (e.g., Kipawa in Canada, Tanbreez in Greenland, and Norra Karr in Sweden) and is readily dissolved in acid. but silica gel formation leads to difficulties and such ores are not now exploited.

Mining requirements for the ionic clay and mineral sands are minimal. Shallow hard rock deposits can be economically exploited by open pit. Mineralization at depth, such as the HREE-enriched Nechalacho Basal zone in Canada, which is 200 m below surface, can present major challenges to successful development. It is perhaps telling that there are presently no underground REE mines.

The grade of a REE deposit is a deceptive parameter. An ionic clay deposit at 0.1% REO will usually be far more attractive

than a eudialyte deposit at 10% REO. Most deposits only contain significant levels of the light REE (“LREE”), i.e., La to Gd. However, some deposits contain more than 5% of HREE, i.e., Tb to Lu plus Y, and have higher value. The basket value of the REE in some typical deposits, using Q1 2021 prices, are: LREE deposits, Mountain Pass - \$15/kg REO; Bayan Obo (China) - \$17/kg; Mt. Weld (Australia) - \$25/kg; HREE deposits: Strange Lake (Canada) - \$47/kg; Nechalacho - \$42/kg; Serra Verde (Brazil) - \$34/kg. Individual REO prices vary over time and one with high value today might have little value five years hence.

Assays for thorium and uranium are critical. Development of the Kvanefjeld deposit in Greenland, containing 1.43% REO and 0.036% U, is blocked because the project would necessarily make a uranium-bearing by-product. Lynas produces a flotation concentrate at its Mt. Weld mine containing 40% REO, 0.16% Th and 0.003% U which is shipped to its plant in Malaysia for processing. Concerns about radioactivity have forced Lynas to construct an expensive plant in Australia to produce a non-radioactive intermediate material to be sent to Malaysia. Monazite typically contains 58% REO, 8% ThO₂, and 0.3% U₃O₈. An operation handling 5,000 t/a of REO will have to deal with 690 t/a of ThO₂ and 26 t/a of U₃O₈ – contentious and highly regulated materials. The processing of US-sourced monazite at Energy Fuels' White Mesa uranium mill in USA is an imaginative solution to Th and U issues but is generally not available. Co-products (e.g., Fe, Nb, phosphate) can provide advantages. Bayan Obo is partially successful because the REEs are a by-product of iron ore operations. Several projects include co-products that might enhance economics including Tomtor in Russia (5.9% Nb₂O₅, 15% REO), Dubbo in Australia (1.85% ZrO₂, 0.87% REO), and Nolans in Australia (13% P₂O₅, 2.9% REO). However, co-product elements can be problematic through increased processing and marketing complexity.

Remote deposits frequently incur expensive power, supplies, and payroll. Examples include Tomtor, Strange Lake, and Nechalacho. Remote deposits might be successfully developed if the ore is high grade or can be upgraded to allow transport of material to a more favourable location. Local support and clear and stable local regulations are essential. Absence of these factors has hampered the development of several deposits including Kvanefjeld, Tanbreez, and in part, Lynas's Malaysian operation. Climatic conditions can render operations difficult and expensive. Examples include Tomtor, which can only mine during the winter, and Avalon's Nechalacho project which would operate the site all year but seasonally ship concentrate. Both situations increase capital costs and adversely affect cash flow.

REE technology is challenging. The market is complex and opaque. Experienced company management is critical. The proponent needs to determine how far down the supply chain the company should go. Options are to: 1) sell a mineral concentrate; 2) sell a chemical precipitate; 3) sell separated

Multi-source hyperspectral imaging of drill cores for the exploration of critical minerals

Moritz Kirsch^{1a}, Sandra Lorenz¹, René Booyen¹, Sam Thiele¹, Laura Tusa¹, Houda Saffi¹, Robert Zimmermann¹, Cecilia Isabel Acosta Contreras¹, Léa Géring¹, and Richard Gloaguen¹

¹ Helmholtz-Institute Freiberg for Resource Technology, Freiberg, Germany

^a corresponding author: m.kirsch@hzdr.de

Access to primary and secondary raw materials, particularly critical raw materials (CRM), is a prerequisite for a transition to a climate-neutral and circular economy and a successful delivery of the United Nations sustainable development goals (Ali et al., 2017). Resource- and energy-efficient exploration technologies such as hyperspectral imaging will aid discovery and evaluation of ore deposits, and thus contribute to sustaining a supply of CRM. Hyperspectral imaging provides fast, high-resolution, spatially continuous, and non-destructive mapping of minerals along drill cores. This spectroscopic technique uses the spectral reflectance and emission measured in hundreds of contiguous spectral bands to provide information about geological materials based on electronic and vibrational processes of bonded elements within minerals. Below we demonstrate the application of hyperspectral drill core scanning for the identification and mapping of CRMs using a case study of Li-bearing pegmatites in Uis, Namibia.

For data acquisition, we use a Specim Sisurock drill core scanner setup deployed in either lab or field environments (Fig. 1a,b) covering the visible to near-infrared and short-wave infrared (VNIR-SWIR), mid-wave infrared (MWIR), and long-wave infrared (LWIR) spectral regions (Fig. 1c). The raw data are processed in near-real time using a custom-built processing pipeline that automatically identifies new datasets, applies sensor corrections (dark current, lens correction, and conversion to reflectance) and then co-registers the hyperspectral data from each sensor based on automatically detected reference targets. Basic visualizations of each dataset (band ratios and minimum noise filter) are automatically generated using the Hylite open source toolbox (Thiele et al., 2021). These hyperspectral derivatives can then be virtually projected on the core using augmented reality (Fig. 1d) to facilitate data exploration and guide sampling. Innovative machine learning approaches are used for upscaling from quantitative (e.g., SEM-MLA)

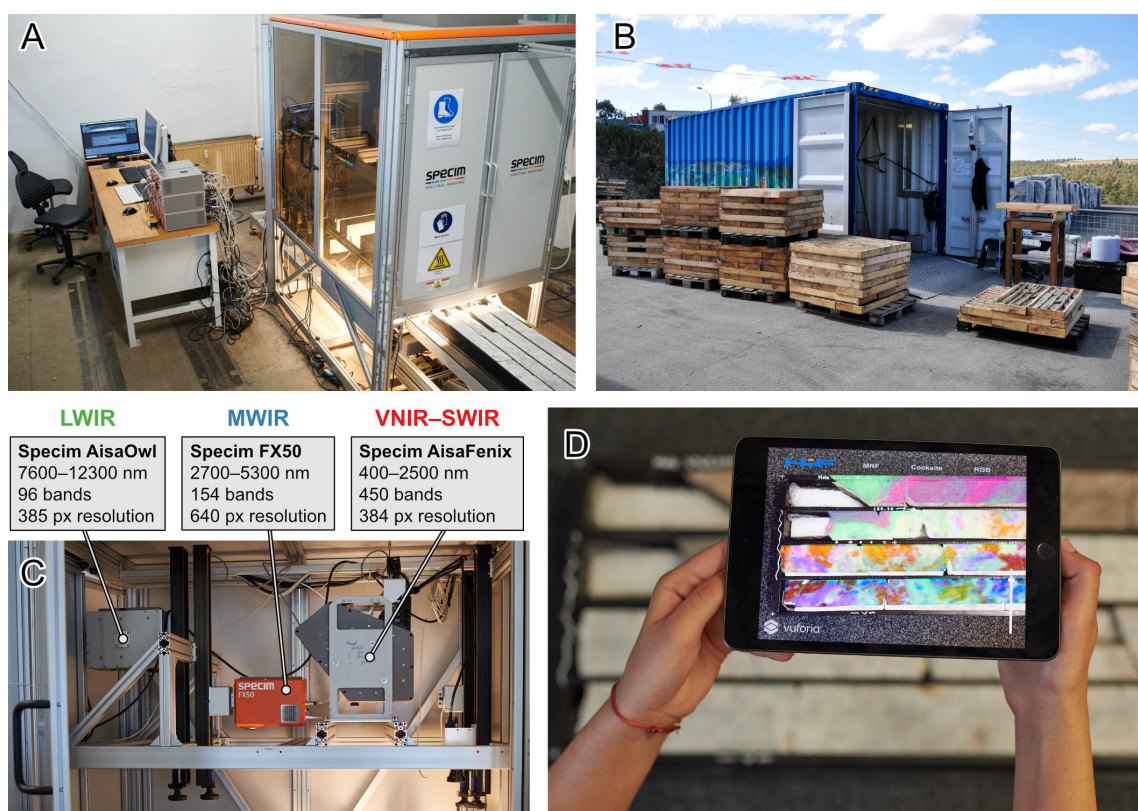


Fig. 1. Specim Sisurock hyperspectral drill core scanning facilities in lab **a**) and mobile **b**) setup with mounted sensors **c**) in the visible to near-infrared and short-wave infrared (VNIR-SWIR), mid-wave infrared (MWIR), and long-wave infrared (LWIR) range. **d**) Augmented reality used for direct visualization of hyperspectral results on the cores.

mineralogical data (Tusa et al., 2020) and for integrating geochemical and hyperspectral data in a superpixel-based framework (Contreras Acosta et al., 2020). The core imaging data can then rapidly be integrated in a 3D environment. Current developments include super-resolution, automatic segmentation and 3D simulations of categorical core data.

The Uis pegmatites are granitic lithium-caesium-tantalum (LCT) rare-element pegmatites, varying mostly in terms of accessory phase minerals (Fuchsloch et al., 2018). The drill cores chosen (Fig. 2) represent the main pegmatite body at the Uis mine. The mineral maps in the VNIR-SWIR range identify quartz and feldspar as the main host-rock minerals, whereas the VNIR-SWIR range is used to characterize a variety of minerals associated with hydrothermal alteration, including muscovite, Li-clay minerals, and Li-chlorite (cookeite), the latter of which is associated with quartz (Fig. 2).

Hyperspectral scanning allows for fast, non-invasive and efficient drill core mapping, providing a useful complement to core-logging performed by on-site geologists. We have also applied the method to rare earth element-hosting carbonatites from Delitzsch (Germany) and copper shales from Lusatia, (Germany) containing antimony, bismuth and cobalt, to show how hyperspectral imaging can be used to directly and indirectly map CRM in drill cores. Particularly for pegmatites and carbonates, extending the spectral range to the mid- and long-wave infrared adds valuable information on the mineralogical composition of CRM-hosting ores. Thus, integrating hyperspectral data across the VNIR-SWIR, MWIR and LWIR regions of the electromagnetic spectrum provide mineral abundance and association mapping over entire drill

cores in a variety of geological settings, and yields semi-quantitative data on the distribution of critical raw materials.

We thank AfriTin for access to the Uis drill cores and auxiliary data.

- Ali, S.H., Giurco, D., Arndt, N., Nickless, E., Brown, G., Demetriades, A., Durrheim, R., Enriquez, M.A., Kinnaird, J., Littleboy, A., Meinert, L.D., Oberhänsli, R., Salem, J., Schodde, R., Schneider, G., Vidal, O., and Yakovleva, N., 2017. Mineral supply for sustainable development requires resource governance. *Nature*, 543, 367-372.
- Booyesen, R., Lorenz, S., Thiele, S. T., Fuchsloch, W., Marais, T., Nex, P. A. M. and Gloaguen, R., (submitted). Accurate hyperspectral imaging of mineralized outcrops: An example from lithium-bearing pegmatites at Uis, Namibia. *Remote Sensing of Environment*.
- Contreras Acosta, I.C., Khodadadzadeh, M., Tolosana-Delgado, R., and Gloaguen, R., 2020. Drill-core hyperspectral and geochemical data integration in a superpixel-based machine learning framework: *IEEE Journal of Selected Topics in Applied Earth Observations and Remote Sensing*, 13, 4214-4228.
- Fuchsloch, W.C., Nex, P.A.M., and Kinnaird, J.A., 2018. Classification, mineralogical and geochemical variations in pegmatites of the Cape Cross – Uis pegmatite belt, Namibia. *Lithos*, 296-299, 79-95.
- Thiele, S. T., Lorenz, S., Kirsch, M., Cecilia Contreras Acosta, I., Tusa, L., Herrmann, E., Möckel, R., and Gloaguen, R., 2021. Multi-scale, multi-sensor data integration for automated 3-D geological mapping. *Ore Geology Reviews*, 136, 104252.
- Tusa, L., Khodadadzadeh, M., Contreras, C., Rafiezadeh Shahi, K., Fuchs, M., Gloaguen, R., and Gutzmer, J., 2020. Drill-core mineral abundance estimation using hyperspectral and high-resolution mineralogical data. *Remote Sensing*, 12, 1218-23.

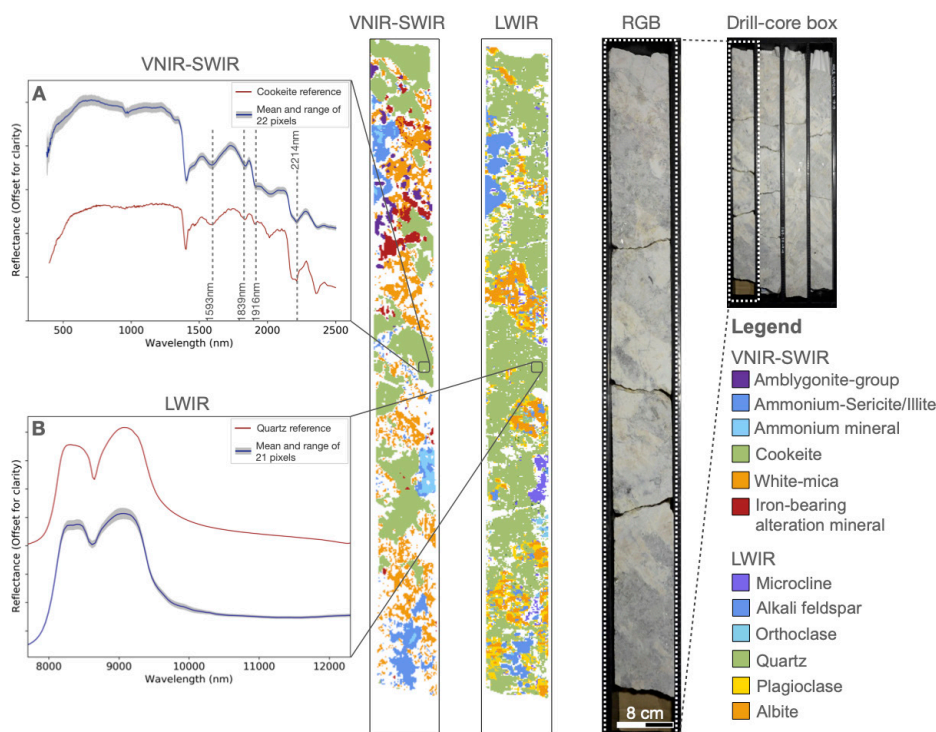


Fig. 2. Mineral maps based on hyperspectral data from a pegmatite drill core from Uis, Namibia. The shown spectra in **a)** and **b)** suggest that Li-bearing cookeite is associated with quartz. Modified from Booysen et al. (submitted).



Ministry of
Energy, Mines and
Low Carbon Innovation

